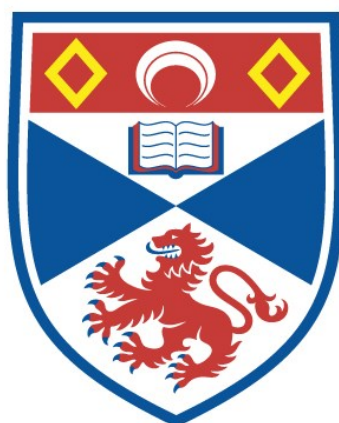


THE GEOLOGY OF THE CAIRNSMORE OF FLEET GRANITE  
AND ITS ENVIRONS, SOUTHWEST SCOTLAND  
VOLUME 1

David R. Cook

A Thesis Submitted for the Degree of PhD  
at the  
University of St Andrews



1976

Full metadata for this item is available in  
St Andrews Research Repository  
at:  
<http://research-repository.st-andrews.ac.uk/>

Please use this identifier to cite or link to this item:  
<http://hdl.handle.net/10023/13352>

This item is protected by original copyright

ProQuest Number: 10171020

All rights reserved

INFORMATION TO ALL USERS

The quality of this reproduction is dependent upon the quality of the copy submitted.

In the unlikely event that the author did not send a complete manuscript and there are missing pages, these will be noted. Also, if material had to be removed, a note will indicate the deletion.



ProQuest 10171020

Published by ProQuest LLC (2017). Copyright of the Dissertation is held by the Author.

All rights reserved.

This work is protected against unauthorized copying under Title 17, United States Code  
Microform Edition © ProQuest LLC.

ProQuest LLC.  
789 East Eisenhower Parkway  
P.O. Box 1346  
Ann Arbor, MI 48106 – 1346

The engine house,

Pibble Mine



THE GEOLOGY OF  
THE CAIRNSMORE OF FLEET GRANITE  
AND ITS ENVIRONS, SOUTHWEST SCOTLAND

by

David R. Cook

A thesis

submitted to the University of St. Andrews in application  
for the Degree of Doctor of Philosophy.

University of St. Andrews

Department of Geology

North Haugh

St. Andrews

Fife.

June 1976.



Th 8829

VOLUME 1

TEXT

## DECLARATION.

I hereby declare that the following thesis is based on work carried out by me, that the thesis is my own composition, and that no part of it has been presented previously for a higher degree.

The research was carried out in the Department of Geology of the University of St. Andrews, under the direction of Dr. P. Bowden and Dr. J.A. Weir.



## CERTIFICATE

We hereby certify that DAVID R. COOK has been engaged in research for nine terms at the University of St. Andrews, that he has fulfilled the conditions of Ordinance No. 16 (St. Andrews) and Resolution of the University Court, 1967, No. 1, and that he is qualified to submit this thesis for the degree of Doctor of Philosophy.

## ACADEMIC RECORD.

I matriculated at the University of St. Andrews in October 1968, and graduated with the degree of Bachelor of Science, First Class Honours, in Geology in June 1972.

In October 1972, I matriculated as a research student at the University of St. Andrews.

## ACKNOWLEDGEMENTS.

I would like to thank all those who helped in any way during my period of research in St. Andrews and the Natural Environment Research Council for a Research Studentship. I am especially indebted to the Landers Family of Craigdistant, who made my summer field seasons extremely enjoyable. My gratitude also goes to my Supervisors and to Dr. W.E. Stephens whose help and constructive criticism have always been appreciated. I also acknowledge the receipt of secondary dispersion data for the Cairnsmore of Fleet area from Rio Tinto Zinc Finance and Exploration, and I thank Dr. A. Smith for making this possible.

Finally my most sincere thanks go to my wife, Diane, who has borne the ups and downs of this research with patience, over the past four years.

## ABSTRACT

The thesis is divided into three parts relating to (i) the sedimentary rocks, (ii) the granite and minor intrusive rocks and (iii) the Fleet orefield.

The sedimentary successions around the Cairnsmore of Fleet pluton are divided into two new formations; the Craignell and Knockeans Formations. The former is subdivided into three facies based upon a geochemical classification of greywackes undertaken using cluster analysis. Facies boundaries within the Craignell Formation and interformational boundaries between this formation and the underlying Moffat Shales and the younger Knockeans Formation are all probably diachronous.

Tectonically derived structures within the sedimentary rocks are correlated with those reported from areas elsewhere within the Southern Uplands. Certain structures are, however, unique to this area and some may be related to the emplacement of the Fleet pluton.

Mineralogical zones within the extensive thermal aureole surrounding the granite are described and correlated with previously published facies of contact metamorphism: albite-epidote hornfels, hornblende hornfels and K-feldspar-cordierite hornfels facies.

Petrological facies within the granite are described and the classification thus produced endorsed geochemically with the aid of cluster analysis. Chemical trends in separated minerals are correlated with bulk chemical variation in the granite which is outlined using

correlation, regression and trend surface analyses. Geochemical and petrological data are compared with published experimental mineralogical studies.

Minor intrusive rocks are similar in composition to those occurring throughout Galloway with two notable exceptions of more basic composition. The chemistry of the minor intrusive suite is compared with that of the granite.

Hydrothermal vein deposits around the western margin of the Fleet pluton are described in detail for the first time. A distinct mineralogical zoning pattern is spatially related to the granite and consists of an inner zone within the pluton and generally close to the contact in the country rocks, containing dominant chalcopyrite, pyrrhotite, pyrite and high temperature ores such as pentlandite and arsenopyrite with a quartzose gangue. Outer zones contain veins of sphalerite and mixed carbonate and quartz gangue, and give way to an outermost zone of galena with carbonate and barytes gangue. Geochemical studies on separated ore minerals has enabled the distinction of ores from particular zones and give an indication of their relative temperatures of formation. Wallrock alteration is described and is generally consistent in its characteristics with the changing mineralogy of the vein deposits.

The ore deposits are related to the geophysically predicted granite batholith beneath the Southern Uplands, but more specifically to the Fleet pluton. The mineralogy and geochemistry of the deposits are consistent with this,

but geochronological studies from other areas suggest that the ores may be at least 40 my younger than the granite. A hypothesis for the origin of the hydrothermal deposits is presented and is based upon data outlined above.

## A B S T R A C T

The thesis is divided into three parts relating to (i) the sedimentary rocks, (ii) the granite and minor intrusive rocks and (iii) the Fleet orefield.

The sedimentary successions around the Cairnsmore of Fleet pluton are divided into two new formations; the Craignell and Knockeans Formations. The former is subdivided into three facies based upon a geochemical classification of greywackes undertaken using cluster analysis. Facies boundaries within the Craignell Formation and interformational boundaries between this formation and the underlying Moffat Shales and the younger Knockeans Formation are all probably diachronous.

Tectonically derived structures within the sedimentary rocks are correlated with those reported from areas elsewhere within the Southern Uplands. Certain structures are, however, unique to this area and some may be related to the emplacement of the Fleet pluton.

Mineralogical zones within the extensive thermal aureole surrounding the granite are described and correlated with previously published facies of contact metamorphism: albite-epidote hornfels, hornblende hornfels and K-feldspar-cordierite hornfels facies.

Petrological facies within the granite are described and the classification thus produced endorsed geochemically with the aid of cluster analysis. Chemical trends in separated minerals are correlated with bulk chemical variation in the granite which is outlined using

correlation, regression and trend surface analyses. Geochemical and petrological data are compared with published experimental mineralogical studies.

Minor intrusive rocks are similar in composition to those occurring throughout Galloway with two notable exceptions of more basic composition. The chemistry of the minor intrusive suite is compared with that of the granite.

Hydrothermal vein deposits around the western margin of the Fleet pluton are described in detail for the first time. A distinct mineralogical zoning pattern is spatially related to the granite and consists of an inner zone within the pluton and generally close to the contact in the country rocks, containing dominant chalcopyrite, pyrrhotite, pyrite and high temperature ores such as pentlandite and arsenopyrite with a quartzose gangue. Outer zones contain veins of sphalerite and mixed carbonate and quartz gangue, and give way to an outermost zone of galena with carbonate and barytes gangue. Geochemical studies on separated ore minerals has enabled the distinction of ores from particular zones and give an indication of their relative temperatures of formation. Wallrock alteration is described and is generally consistent in its characteristics with the changing mineralogy of the vein deposits.

The ore deposits are related to the geophysically predicted granite batholith beneath the Southern Uplands, but more specifically to the Fleet pluton. The mineralogy and geochemistry of the deposits are consistent with this,



but geochronological studies from other areas suggest that the ores may be at least 40 my younger than the granite. A hypothesis for the origin of the hydrothermal deposits is presented and is based upon data outlined above.

C O N T E N T S.

VOLUME 1.

Page No.

Declaration .....	i
Certificate .....	ii
Academic Record .....	iii
Acknowledgements .....	iv
Abstract .....	v
INTRODUCTION .....	1
PART 1, THE SEDIMENTARY ROCKS	
CHAPTER 1, HISTORY OF RESEARCH .....	3
A. The Southern Uplands .....	3
B. The area of study .....	11
CHAPTER 2, PETROGRAPHY AND GEOCHEMISTRY .....	17
A. Introduction .....	17
B. Lithic greywacke group .....	19
(i) Petrography .....	19
(ii) Geochemistry .....	21
a. $TiO_2$ -FeO-MgO .....	22
b. $TiO_2$ -MnO- $Na_2O$ -( $P_2O_5$ )-Sr .....	22
c. $TiO_2$ -Zr-Cr .....	23
d. $Al_2O_3$ - $K_2O$ -(Li)-Rb-Y-(Zn)-(Pb) .....	23
e. $Al_2O_3$ -MgO-Li .....	25
f. $Al_2O_3$ - $P_2O_5$ -(Rb)-(Y)-Zn-Pb .....	25
g. MnO-CaO-Sr .....	25
C. Basic greywacke group .....	26
(i) Petrography .....	26
(ii) Geochemistry .....	27
a. $SiO_2$ - $K_2O$ -Rb-Y-Zr .....	28
b. $TiO_2$ -Cr .....	28
c. $Al_2O_3$ -MnO .....	28
d. $Al_2O_3$ -MgO- $Na_2O$ -Ni .....	29
e. FeO-MgO-Ni-Cr .....	29
f. FeO-Zn .....	29
g. CaO-Y .....	30

D. Feldspathic greywacke group .....	30
(i) Petrography .....	30
(ii) Geochemistry .....	31
a. SiO <sub>2</sub> -Zr .....	32
b. TiO <sub>2</sub> -FeO-MgO-(Zn) .....	32
c. Al <sub>2</sub> O <sub>3</sub> -K <sub>2</sub> O-P <sub>2</sub> O <sub>5</sub> .....	32
d. FeO-MgO-Ni-Cr .....	33
e. MnO-CaO .....	33
f. K <sub>2</sub> O-Rb-Y .....	33
g. K <sub>2</sub> O-Pb .....	34
E. Silicic greywacke group .....	34
(i) Petrography .....	34
(ii) Geochemistry .....	35
a. TiO <sub>2</sub> -Zr .....	36
b. SiO <sub>2</sub> -Zr .....	36
c. Al <sub>2</sub> O <sub>3</sub> -K <sub>2</sub> O-Li-(Rb)-Ni .....	36
d. FeO-Y-(Zn) .....	37
e. MnO-MgO-CaO-Cr-(Ni) .....	37
f. Na <sub>2</sub> O-Li .....	37
g. Rb-Y .....	37
F. Shales .....	38
G. Contaminated samples .....	39
H. Conclusions .....	39
CHAPTER 3, STRATIGRAPHY .....	42
A. Introduction .....	42
B. Moffat Shales .....	42
C. Craignell Formation .....	47
(i) Basic Facies .....	48
(ii) Lithic Facies .....	51
(iii) Silicic Facies .....	53
D. Knockeans Formation .....	54
E. Summary and conclusions .....	55
CHAPTER 4, STRUCTURE .....	58
A. Introduction .....	58
B. Auchinleck-Glenlee Belt .....	60
C. Talnotry Thrust Zone .....	62
(i) Newton Stewart to Loch of the Lowes ...	63
(ii) Loch of the Lowes to Clatteringshaws Loch .....	64
(iii) Knocknairling Burn to Water of Ken ...	67
D. Blackcraig-Ironmacannie Belt .....	68

E. Loch Ken Fault .....	69
F. Blairbuies Thrust Zone .....	71
(i) Blackcraig to Blairbuies Hill .....	71
(ii) Stoan Loch to Bennan Hill .....	74
G. Cairnsmore-Mosssdale Belt .....	75
H. Culcronchie Thrust .....	76
I. Barholm-Drumglass Belt .....	78
J. Pool Ness Thrust .....	80
K. Pibble Thrust .....	82
L. Knockeans-Castramont Belt .....	84
M. Conclusions .....	84
 CHAPTER 5, METAMORPHISM .....	 87
A. Introduction .....	87
B. Regional metamorphism .....	89
C. Contact metamorphism .....	90
(i) The morphology of the aureole .....	90
(ii) Albite-epidote hornfels facies (chlorite-biotite zone) .....	91
(iii) Hornblende hornfels facies .....	92
a. Biotite zone .....	92
b. Hornblende biotite zone .....	93
(iv) K-feldspar-cordierite hornfels facies .	96
(v) Hydrothermal alteration .....	97
 PART 2, THE GRANITE AND MINOR INTRUSIVE ROCKS.	
 CHAPTER 6, INTRODUCTION .....	 99
A. History of previous research .....	99
B. Introduction .....	101
 CHAPTER 7, PETROGRAPHY OF THE GRANITE .....	 104
A. Introduction .....	104
B. Coarse grained biotite granite .....	105
C. Coarse grained biotite-muscovite granite .....	109
D. Coarse grained muscovite-biotite granite .....	113
E. Fine grained biotite-muscovite granite .....	114
F. Fine grained muscovite-biotite granite .....	116
G. Fine grained muscovite granite .....	118
H. Summary and conclusions .....	119

CHAPTER 8, GEOCHEMISTRY OF THE GRANITE .....	126
A. Introduction .....	126
B. Geochemical classification .....	127
C. Geochemistry of separate mineral phases .....	130
(i) Biotite .....	130
(ii) Chlorite .....	134
(iii) Muscovite .....	136
(iv) Feldspar and quartz mixtures .....	138
(v) Conclusions .....	141
D. Areal variations in bulk chemistry and meso- normative minerals .....	142
(i) $\text{SiO}_2$ .....	142
(ii) $\text{TiO}_2$ .....	143
(iii) $\text{Al}_2\text{O}_3$ .....	143
(iv) $\text{FeO}$ .....	144
(v) $\text{MnO}$ .....	144
(vi) $\text{MgO}$ .....	145
(vii) $\text{CaO}$ .....	145
(viii) $\text{Na}_2\text{O}$ .....	145
(ix) $\text{K}_2\text{O}$ .....	145
(x) $\text{P}_2\text{O}_5$ .....	146
(xi) Lithium .....	146
(xii) Rubidium .....	148
(xiii) Beryllium .....	148
(xiv) Strontium .....	149
(xv) Barium .....	150
(xvi) Yttrium .....	150
(xvii) Lanthanum .....	151
(xviii) Cerium .....	151
(xix) Neodymium .....	151
(xx) Zirconium .....	152
(xxi) Nickel .....	152
(xxii) Copper .....	152
(xxiii) Zinc .....	152
(xxiv) Lead .....	153
(xxv) Mesonormative minerals .....	153
(xxvi) Differentiation Index .....	155
E. Variation between geochemical variables and mesonormative minerals .....	156

CHAPTER 9, CRYSTALLIZATION OF THE GRANITE IN RELATION TO EXPERIMENTAL MINERALOGICAL STUDIES .....	161
A. The system $\text{NaAlSi}_3\text{O}_8\text{-KAlSi}_3\text{O}_8\text{-SiO}_2\text{-H}_2\text{O}$ .....	161
B. The system $\text{NaAlSi}_3\text{O}_8\text{-KAlSi}_3\text{O}_8\text{-CaAlSi}_2\text{O}_8\text{-SiO}_2$ ..	161
C. Muscovite .....	163
D. Biotite .....	164
E. Conclusions .....	165
CHAPTER 10, THE MINOR INTRUSIVE SUITE .....	167
A. Introduction .....	167
B. Lamprophyres .....	167
(i) Spessartites .....	167
(ii) Kersantites .....	168
C. Porphyritic microdiorite .....	169
D. Talnotry diorite sill .....	170
E. Clanery Hill ultrabasic intrusion .....	170
F. Geochemistry .....	171
CHAPTER 11, CONCLUSIONS AND INTRUSIVE HISTORY .....	174
PART 3, THE FLEET OREFIELD.	
CHAPTER 12, INTRODUCTION .....	178
A. Introduction and previous research .....	178
B. Spatial relationships between the mineralization and the granite batholith .....	179
CHAPTER 13, THE MINERAL DEPOSITS .....	182
A. Deposits of the copper zone .....	182
(i) Quartz subzone .....	182
a. Orchars vein .....	182
b. Clugie Linn vein .....	184
c. Talnotry vein .....	184
d. Blairbuies vein .....	189
e. Culcronchie veins .....	189
f. Clatteringshaws vein .....	192
g. Drumruck vein .....	193
h. Craignell vein .....	194
i. Craigencallie vein .....	194
j. Kings Laggan vein .....	195
(ii) Quartz-carbonate subzone .....	195
a. Lauchentyre vein .....	196
b. Enrick vein .....	196

B. Deposits of the zinc zone .....	197
(i) Quartz subzone, Dromore area .....	197
a. Dromore vein .....	197
b. Meikle Bennan vein .....	199
c. Pibble Gulch vein .....	200
(ii) Quartz subzone, Wood of Cree area .	200
a. Wood of Cree vein .....	200
b. Coldstream Burn vein .....	203
(iii) Quartz-carbonate subzone .....	204
a. Tonderghie vein .....	204
b. Chain Burn vein .....	205
C. Deposits of the lead zone .....	206
(i) Carbonate-quartz subzone .....	207
a. Pibble vein .....	207
b. Bargaly veins .....	210
(ii) Carbonate subzone .....	211
a. Blackcraig veins .....	211
b. Cairnsmore veins .....	213
c. Palnure vein .....	213
d. Silver Rig vein .....	214
e. Dallash vein .....	215
f. Balloch (Englishman's) Burn vein	216
g. Pool Ness vein .....	216
D. Conclusions .....	216
CHAPTER 14, GEOCHEMISTRY OF THE ORE MINERALS .....	219
A. Introduction .....	219
B. Sphalerite .....	219
(i) Iron .....	221
(ii) Cadmium .....	222
(iii) Manganese .....	223
(iv) Nickel .....	223
(v) Cobalt .....	223
(vi) Silver .....	224
(vii) Lead and copper .....	225
(viii) Arsenic .....	225
(ix) Conclusions .....	225
C. Galena .....	225
(i) Silver .....	226
(ii) Zinc/cadmium ratios .....	227
(iii) Zinc/iron ratios .....	227
(iv) Conclusions .....	228

D. Chalcopyrite .....	228
(i) Nickel and cobalt .....	229
(ii) Silver .....	229
(iii) Arsenic .....	229
(iv) Manganese .....	230
(v) Zinc/cadmium ratios .....	230
(vi) Conclusions .....	230
E. Pyrrhotite and Arsenopyrite .....	231
(i) Pyrrhotite .....	231
(ii) Arsenopyrite .....	231
F. Crude ores .....	231
(i) Orchars vein .....	231
(ii) Talnotry vein .....	233
(iii) Culcronchie vein .....	234
(iv) Tonderghie vein .....	235
(v) Pibble vein .....	236
G. Secondary dispersion .....	237
H. Summary and conclusions .....	238
CHAPTER 15, WALLROCK ALTERATION .....	241
(i) Orchars vein .....	241
(ii) Culcronchie vein .....	243
(iii) Wood of Cree vein .....	244
(iv) Bargaly vein .....	244
(v) Dallash vein .....	245
(vi) Conclusions .....	245
CHAPTER 16, CONCLUSIONS .....	247
A. Temperature of formation .....	247
B. Origin of the ores .....	248
C. The area of study in relation to the rest of the Southern Uplands .....	252



## VOLUME 2.

Page No.

APPENDIX 1, Sample preparation and methods of chemical analysis of silicates and sulphides, and staining of carbonates	1
A. SAMPLE PREPARATION .....	1
(i) Sample collection .....	1
(ii) Crushing .....	1
(iii) Mineral separation .....	2
B. CHEMICAL ANALYSIS .....	4
(i) Major element analysis of silicate rocks and minerals ....	4
(ii) Minor and trace element analysis of silicate rocks and minerals .	5
(iii) Determination of $\text{FeO}$ , $\text{P}_2\text{O}_5$ , $\text{H}_2\text{O}^{\text{m}}$ , $\text{H}_2\text{O}^{\text{f}}$ and loss on ignition.....	5
(iv) X-ray fluorescence analysis of Rb, Sr, Y, Zr, Cu, Pb, Zn .....	6
(v) Energy dispersive analysis of Ba, La, Ce, Nd .....	7
(vi) Sulphide analysis .....	7
(vii) Staining techniques for carbonate minerals .....	8
APPENDIX 2, Techniques of statistical analysis ...	9
(i) Correlation and regression analysis .....	9
(ii) Trend surface analysis .....	9
(iii) Cluster analysis .....	10
APPENDIX 3, Chemical analyses of the sedimentary rock samples .....	12
APPENDIX 4, Chemical analyses of the granite samples .....	31
APPENDIX 5, CIPW- and Mesonormative analysis of the granite samples .....	45
APPENDIX 6, Chemical and normative analyses of the minor intrusive suite .....	62
APPENDIX 7, Chemical analyses and numbers of ions per formula unit of separated minerals	67
APPENDIX 8, Chemical analyses of sulphides and crude ores .....	81
APPENDIX 9, Chemical analyses of wallrocks adjacent to hydrothermal vein deposits	90
APPENDIX 10. Localities of samples used in petrological and geochemical analysis.....	93

TABLES 1-24 .....	100
FIGURES 1-8 .....	128
FIGURES 9-14 .....	129
FIGURES 15-19 .....	130
FIGURES 20-26 .....	131
FIGURES 27-30 .....	132
FIGURES 31-36 .....	133
FIGURES 37-42 .....	134
FIGURES 43-46 .....	135
FIGURES 47-74 .....	136
FIGURES 75-86 .....	137
FIGURES 87-89 .....	138
FIGURES 90-97 .....	139
FIGURES 98-104 .....	140
FIGURES 105-109 .....	141
PLATES 1-4 .....	143
PLATES 5-8 .....	144
PLATES 9-11 .....	145
PLATES 12-16 .....	146
PLATES 17-21 .....	147
PLATES 22-26 .....	148
PLATES 27-29 .....	149
PLATES 30-33 .....	150
PLATES 34-37 .....	151
BIBLIOGRAPHY .....	152
MAPS 1-9 .....	inside back pocket.

I N T R O D U C T I O N

The area of study is situated in the Western half of Kirkcudbrightshire in the region of Galloway, South West Scotland (Fig. 1). It is elongated parallel to the strike of the Lower Palaeozoic strata surrounding the outcrop of the Cairnsmore of Fleet granite, between the southeasterly trending valleys of the River Cree in the west and Water of Ken in the east. Map coverage is by Ordnance Survey 1 inch sheet 73 and 6 inch sheets: NX45NE; NX55NW; NX46NW, NE, SW, SE; NX56NW, NE, SW, SE; NX66NW, NE, SW; NX47NE, SE; NX57NW, NE, SW, SE; NX67NW, NE, SW, SE; NX58 SE; NX68SW.

Areas of highest topography occur over the granite and are dominated by Cairnsmore of Fleet (2331 feet), Craignelder (1971 feet), Black Craig of Dee (1616 feet) and Fell of Fleet (1544 feet). The granite hills are rounded in contrast to the more rugged area to the northwest, where hills such as Curlywee (2212 feet), Millfore (2152 feet), and Craignell (1550 feet) are composed of greywackes and shales. To the south of the granite a region of rolling topography with poor exposure never attains heights in excess of 1500 feet.

Drainage is effected in the west by Penkiln, Painure and Moneypool Burns, all of which flow southwest into the River Cree. Most of the central and southerly parts of the area are drained by the Big and Little Waters of Fleet which together reach Wigtown Bay at Gatehouse of Fleet. The catchment areas of the Black Water of Dee and Water of Ken cover the north and east and water is

taken out to the Solway Firth via the River Dee at Kirkcudbright.

In the last century most of the upland areas were used as sheep pasture and the valley floors and coastal region for cattle. However recently an ever increasing amount of the hill land is being afforested and reduced to a desert of pine trees. In the foreseeable future existing exposures of rock will be unobtainable or covered by vegetation.

Map references of localities are given in an eight figure format enclosed by brackets. The first and fifth numbers, 2 and 5 respectively refer to 100 kilometer grid intersections and replace the reference letters NX. Geological maps on the scale of six inches to one mile are provided in the back pocket.

PART 1.

THE SEDIMENTARY ROCKS.

CHAPTER 1  
HISTORY OF RESEARCH

A. The Southern Uplands

The geological structure of the Southern Uplands had received little attention until mid-way through last century when a number of papers were presented on the subject. Harkness (1851) recognised three distinct bands of black shale; those exposed at Hartfell, Dobb's Linn and Selcouth Burn. He interpreted these "anthracite beds and graptolite shales" as being exposures of the same band repeated across country by strike faults with NNW. downthrows. The crushed and contorted nature of the shales lead him to believe that some of the faults passed through shale inliers, whilst slickensided and polished greywacke surfaces, to him, furnished further proof of faulting. He proposed that an anticlinal axis passing across the southern area of the Silurian outcrop was a result of the intrusion of the Criffel pluton.

His classification of the Silurian (now Ordovician and Silurian) was as follows:

3. WENLOCK. Balmae Beds with a dip to the south.
2. CARADOC. Greywackes and shales with dips to the NNW.
1. LLANDEILO. Graptolite and trilobite beds of Peebleshire.

Later in the same year, Murchison (1851) presented a paper to the Geological Society of London in which he discussed the problems in determining direction of younging in formations within the Southern Uplands, owing to lack

of palaeontological control. He believed that the same strata were repeated by faulting and folding parallel to the strike and placed the greywackes and shales below the Llandeilo.

Geikie (1871) observed that the Lower Silurian (Ordovician) belt was highly folded and suggested that the overall structure was one of a "long arch" the axis of which ran parallel to the length of the Southern Uplands. The fact that this theoretical structure did not agree with observations in all areas was recognised, and an order of succession was presented in which the black shale beds and associated greywackes were classified as Llandeilo.

The hypothesis of a southern anticlinal structure was endorsed by Lapworth (1874), and a proposal that strata of Cambrian and Lower Silurian (Ordovician) age were exposed within it was put forward. To the north he suggested the presence of an undulating belt of Llandeilo and Llandovery strata. Reappearance of black shale inliers was attributed to the effects of folding. Lapworth agreed with Harkness (1851) that the shales were the same repeated band and divided them into the Lower, Middle and Upper Anthracite. These groups he separated into zones according to their palaeontology and observed that the Middle and Upper Anthracites were absent in the north of the belt, the only complete succession being found in the central area. Lapworth's (1874) classification of the Lower Palaeozoic rocks of the Southern Uplands was as follows:

3. UPPER SILURIAN. Balmae and Riccarton Beds,  
(Wenlock and Lower Ludlow).
2. MIDDLE SILURIAN. 2. Gala Group, Girvan Series,  
Duntercleugh Beds and Wrae Beds,  
(Upper and Lower Llandovery and  
Upper Caradoc).  
  
1. Moffat Shale or Anthracite,  
(Llandeilo and Lower Caradoc).
1. LOWER SILURIAN. Hawick and Selkirk Rocks,  
(Cambrian).

Two years later Lapworth (1876) modified his earlier interpretations of the succession, placing the graptolitic shales at the base and stating that the Riccarton or Balmae Beds were uppermost, lying unconformably upon Hawick Rocks.

Lapworth (1878) in his classic paper on the "Moffat Series" gave the greywackes above the black shales a Llandovery age. He suggested that in the south the dip of these rocks gradually changed from a northerly to a southerly direction and passed upwards conformably into Wenlock strata. He also observed that to the northwest and southeast of Moffatdale the Moffat Series diminished in thickness as shales were replaced by greywacke.

In 1889 Lapworth presented a hypothesis which remained the basic structural concept of the Southern Uplands for the next eighty years. The Moffat Series was envisaged as rising to the surface in the cores of anticlines which were inverted or overfolded. These folds in turn were related to two broad structural features. The northern of these named the Leadhills Line was the axis of a "pseudo-synclinal" or endocline. Basically this is an



anticlinorium in which all the fold axes dip inwards towards the major axis. To the south, the Hawick Line was proposed to be the axis of a "pseudo-anticlinal" or exocline, which is a synclinorium in which all the fold axes dip outwards from the axis.

Lapworth (1889) also divided the rocks of the Southern Uplands into two "grand lithological terranes". The Lower or Moffat Terrane contained strata ranging from Upper Llandeilo to Upper Llandovery and included Glenkiln, Hartfell and Birkhill Shales. The Upper, Gala or Queensberry Terrane embodied rocks of Tarannon (Lower Llandovery) age and included the Gala or Queensberry Grits and the Riccarton Beds. He revived previous ideas (Harkness, 1851) that exposures of Moffat Shales were also related to large strike faults which removed Gala rocks from the crests of anticlines, thus exposing cores of Moffat Shale.

Peach and Horne (1899) accepted Lapworth's (1889) interpretation of the structure of the Southern Uplands but stated that reverse faults associated with the Moffat Shale inliers did not show any evidence of large scale horizontal displacement compared with those of the Northwest Highlands. The Lower Palaeozoic rocks were divided into three belts. The northern included highly folded Arenig, Glenkiln and Hartfell rocks; the central was dominated by Llandovery greywackes and shales in which Ordovician strata occurred along the axes of complex anticlines, whereas isoclinally folded Wenlock strata were characteristic of the southern belt. A detailed account of the zoning and lithology of the Moffat Series based on the work of Lapworth and a classification of the

greywackes and shales, which was similar to those already formulated, was also presented by Peach and Horne (1899). The work is the first and only complete account of the Ordovician and Silurian rocks of the Southern Uplands.

Pringle (1935) accepted the structure proposed by Lapworth and compared it with the Jura Mountains. Subdivisions of the Ordovician and Silurian from Lapworth (1876, 1889) and Peach and Horne (1899) were retained.

New facts and theories appertaining to the structure of the Southern Uplands were brought forward by Craig and Walton (1959) after successfully determining the direction of younging in greywacke beds using sedimentary structures. Two important proposals were made in this work. The first was that although the Riccarton Beds normally dip southwards they appear to young to the north and secondly, in the Southern Belt, folding is of <sup>m</sup>asymmetrical double fold flexures rather than isoclines. Two major types of structure were also recognised from the Kirkcudbrightshire area; belts of steeply dipping or inverted beds with few folds and flat lying belts in which relatively small thicknesses of rock are repeated many times by folding. A line joining the crests of the folds (i.e. faltenspiegel) is approximately horizontal. Craig and Walton (ibid) rejected the concept of a synclinorium to explain the structure of the Kirkcudbright area. They proposed that the general structure of the Southern Uplands was one of a series of large compound monoclinial structures facing and descending towards the northwest. These were envisaged as being cut

by northerly dipping thrusts or reverse faults with a southerly translation. It was proposed that this faulting was such that it would more than cancel the effect of the folding, so that even though the rocks generally younged to the north, each successive fault-bounded block was younger in a southerly direction. They concluded that the Raeberry Castle Beds were older than the Riccarton Beds but were still probably Wenlock in age and that the Hawick Rocks might possibly be of Ludlow age. This contrasts with Lapworth (1876) who placed the Hawick Rocks unconformably below the Riccarton Beds.

Similar ideas were presented by Kelling (1961), Walton (1961) and Gordon (1962) who showed that structures in rocks in the Rhinns of Galloway and around Glenluce (Wigtownshire) were in accordance with these proposals.

Rust (1965) demonstrated that each successive formation in the Whithorn (Wigtownshire) area was fault-bounded and successively younger in a southerly direction. The Hawick Rocks were placed, on palaeontological evidence, below the Riccarton Beds. A stratigraphical succession based on his own work and that of Gordon (1962) and Peach and Horne (1899) was set up.

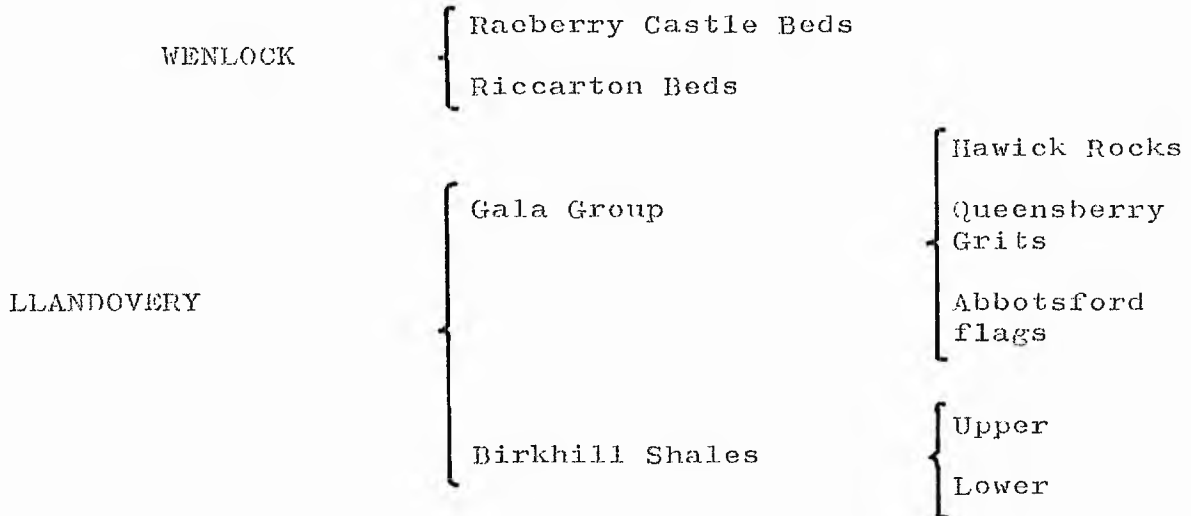
FORMATION	ZONE	SERIES
Riccarton Beds	<u>Cyrtograptus murchisoni</u>	L. Wenlock
Fault		
	<u>Monograptus crenulatus</u>	} U. Gala (Llandovery)
Hawick Rocks	<u>Monograptus griestoniensis</u>	
Fault		U. Llandovery
	<u>Monograptus crispus</u>	} L. Gala (Llandovery)
Garheugh Formation	<u>Monograptus turriculatus</u>	
Fault		
	<u>Monograptus gregarius</u>	} L. Llandovery
Kilfillan Formation	<u>Diplograptus vesiculous</u>	
	<u>Diplograptus acuminatus</u>	

The boundary faults were described as steep slip strike faults with associated zones of tectonic slicing.

The importance of faulting in the structure of the Southern Uplands was stressed by Toghil (1970). The southeast limit of the Moffat Shale inliers was described as being a "major dislocation". It was proposed that a fault, the Ettrick Valley Fault, thrust tightly-folded greywacke and black shale successions over younger (northerly dipping) greywackes to the southeast. The structure of the upper Ettrick Valley was shown to be of imbricate type produced by the "shearing out of the inverted limbs of isoclines". This latter idea is reminiscent of proposals put forward by Lapworth (1889). Toghil (ibid) suggested that faulting and folding was the cause of repetitions in the outcrop of the Moffat Series across strike. The structural concept of Craig and

Walton (1959) was endorsed in this work.

Greig (1971) following Lapworth (1889), Peach and Horne (1899) and Rust (1965) subdivided the Silurian as follows:



Weir (1974a) suggested that crustal segmentation was the major characteristic structure within the Southern Uplands. Upthrust wedges with a horizontal displacement were proposed as being dominant features. The imbricate structure associated with the Ettrick Valley Thrust was compared with similar structures associated with major thrusts in the Northwest Highlands and a décollement along the base of the Moffat Shales proposed. Outcrops of Moffat Shales at Dobb's Linn and Hartfell were envisaged as being associated with faults of lesser magnitude possibly connected at depth with this décollement. The greywacke terrane between the faults was compared with the fault-bounded monoclinial fold belts of Kirkcudbrightshire (Craig and Walton, 1959). Thrust wedges with a northwesterly translation in the Girvan

area were contrasted and the whole structure interpreted as a 'double-nappe'.

Fyfe and Weir (in press) have recognised a belt of Schuppen related to the Ettrick Valley Thrust at Selcouth Burn, southeast of Moffatdale, and it is proposed that this demonstrates the importance of the fault. They observed that the Ettrick Valley Thrust separates a belt with dominantly southeasterly translation to the north from one of northwesterly translation to the south.

Mitchell and McKerrow (1975) and Weir (in prep.) have independently proposed a tectonic model explaining the structures in the Lower Palaeozoic rocks of the Southern Uplands. Both theories require that horizontal movement has taken place along thrusts or reverse strike faults. Mitchell and McKerrow (ibid) envisage continuous thrusting during the Ordovician and Silurian as a result of turbidite sequences being scraped off a descending oceanic plate at the point of subduction, thus explaining the southeasterly younging between greywacke belts. Weir (in prep.) however interprets the major structure as being developed by one event at the Caledonian climax in the late Silurian.

#### B. The area of study

The first systematic survey of the area was carried out in the second half of last century by the Geological Survey (Irvine, 1878). The Lower Silurian (Ordovician) was subdivided as follows:

LLANDEILO	}	3. Queensberry Grits
		2. Lower or Moffat Black Shale Group
		1. Ardwell Group

The Ardwell Group was described as occupying the tract of ground south of the Pibble black shale belt (Fig. 1) and consisted of brown-crusted, red, blue and grey jointed sandy greywackes with purple shales and bluish or yellow siltstones. Rocks of this group were also said to occur in the cores of anticlines within the black shale inliers further north. The Lower or Moffat Black Shale Group was described as being exposed in anticlines within the upper greywacke group between the Pibble and Talnotry black shale belts. Massive grits with occasional zones of grey-blue shales of the Queensberry Grits series covered the whole of the greywacke tract north of the Pibble black shales.

It was observed (Irvine, 1878) that all strata dipped to the northwest and the beds were presumed to young in that direction. The apparent thickness and recurrence of black shales within the greywackes was explained as being the result of inverted folding producing limbs dipping in similar directions, following proposals made by Murchison (1851), Geikie (1871) and Lapworth (1874, 1876).

Two black shale groups were recognised by the Geological Survey at this time; the Lower or Moffat Black Shale and the Upper or Leadhills Black Shale. Irvine

(1878) observed that they were very similar in appearance and would be inseparable if it were not for the apparent superposition of the upper group and the 6000+ feet of intervening greywackes. This idea was rejected by Lapworth (1889) who demonstrated that all the black shales were exposures of the same band.

The publication of the Explanation to Sheet 5 (Horne, 1896), which covers most of the eastern part of the area, was delayed until 1896 so that the ground could be resurveyed in the light of Lapworth's work. In this publication the Silurian (Ordovician and Silurian) was classified thus:

- |                      |   |  |
|----------------------|---|--|
| LLANDOVERY           | } | 4. Hawick Rocks,<br>brown crusted greywackes,<br>flags and shales.                   |
|                      | } | 3. Queensberry Grits,<br>massive grits, greywackes and<br>shales.                    |
|                      | } | 2. Flags and shales with greywacke.  |
|                      | } | 1. Birkhill Shales,<br>black shales alternating with<br>grey shales in higher zones. |
| CARADOC              | } | Barren Mudstones,<br>shales and mudstone.  |
|                      | } | Hartfell Shales,<br>black shales.  |
|                      | } | Glenkiln Shales,<br>black shales.  |
| LLANDEILO and ARENIG | } | Radiolarian cherts, mudstones<br>and shales associated with<br>fine volcanic tuffs.  |



The Laurieston and Hensol black shale exposures (Fig. 1) were described as dominantly Birkhill, but with some volcanic tuffs and radiolarian chert associated with Hartfell Shales at the former locality. Neither of these bands has been investigated in the present survey but they are correlated with those at Castramont and Slogarie (Fig. 1). These latter localities were given cursory mention by Horne (1896) and he proposed that they came to the surface in cores of isoclinal folds.

The Queensberry Grits of Horne (1896) were the equivalent of those described by Irvine (1878) except that they were reclassified as Llandoverly. Some of the Ardwell Beds (Irvine, 1878) became Queensberry Grits and the rest were made equivalent to the Hawick Rocks. Horne failed to describe the locality or the nature of the contact between the Queensberry Grits and the Hawick Rocks.

The last detailed account to be published on the geology of the area was by Peach and Horne (1899). They observed that Birkhill Shales occur only up to the gregarius Zone in the Hensol, Barend and Laurieston inliers and that greywackes immediately succeed the shales in the first and second localities. The Hensol band was described as being in the core of a normal fold, the Barren Mudstones succeeded on both limbs by Lower Birkhill Shales. They also stated that Glenkiln Shales occur in the black shale exposures at Laurieston.

Other black shale bands around the southwestern margin of the Cairnsmore of Fleet granite were noted and at Palnure graptolites were recognised but in too poor a state of preservation for identification.

A Glenkiln-Hartfell locality was described one mile north of the Bridge of Cree (Map 1) on the River Cree. Here Diplograptus foliaceus (Murchison) and Climacograptus were identified, and further north the linearis Zone was exposed containing Diplograptus quadrimucronatus (Hall), Dicellograptus morrisoni (Hopkinson) and Climacograptus. A similar lithology was described as occurring one mile up the Penkiln Burn yielding poorly preserved fragments of a similar fauna.

The classification of the Tarranon or Llandoverly greywackes by Horne (1896) was retained, and they noted that flags and shales at the base of the succession contained a turriculatus Zone fauna.

More recently Gordan (1962) studied the succession southwest and along strike from this area, in the region of Glenluce. Silurian greywackes were subdivided into two petrologically and structurally distinct units; the Kilfillan and Garheugh Formations. Kilfillan greywackes were described as dark greenish-grey, coarse to medium grained, occasionally pebbly greywackes interbedded with blue-black siltstones, mudstones and dark grey to black shales. The arenites of the Garheugh formation were distinguished only with difficulty from those of the Kilfillan formation, being greenish-grey in colour and interbedded with siltstones and shales.

A Birkhill fauna was found in shales of the Kilfillan formation and claimed to be the northerly equivalent of the Birkhill Shales. Correlation was made between Gala rocks and the Garheugh Formation on grey-

wacke composition and the presence of red shale beds. It was concluded that the Garheugh Formation may be conformable upon Birkhill Shales and therefore younger than the Kilfillan formation. But Greig (1971) observed that intraformational boundaries are obscure in the Glenluce area.

Rust (1965) continued Gordon's work as far south as Burrow Head (see above). Greywackes outcropping on the coast between Creetown and Gatehouse of Fleet across Wigtown Bay were correlated by Weir (1968) with the Cardhigdown Beds of the Whithorn area, (Rust, 1965) and are therefore equivalent to the Hawick Rocks (? Telychian in age).

## CHAPTER 2.

## PETROGRAPHY AND GEOCHEMISTRY.

A. Introduction.

In order to study the stratigraphy of the complete sedimentary sequence it is necessary to classify the greywackes. The use of a geochemical classification is favoured because of the large proportion of the area covered by the thermal aureole of the Fleet granite. Mineralogical reactions taking place during metamorphism are assumed to have done so in a closed system, as addition or removal of elements is not evident. Besides the metamorphic effects (Chapter 5), absence of fossils and distinctive lithological marker horizons make a classification of this type inevitable.

Samples of greywacke and shale were obtained objectively from grid line intersections (Fig. 2) and analysed petrographically and geochemically by the techniques outlined in appendix 1. Classification of the chemical data was undertaken by computerized cluster analysis (appendix 2). Six significant clusters emerge (Fig. 3) from which non-metamorphosed samples of greywacke were studied petrographically for differences in mineralogy and texture. The groups are named accordingly:

1. Lithic greywacke group.
2. Basic greywacke group.
3. Feldspathic greywacke group.
4. Silicic greywacke group.
5. Shales.
6. Contaminated samples.

As may be anticipated the largest differences in chemistry occur between the four greywacke groups and the shales and consequently fusion occurs at a high coefficient (Fig. 3). The coefficient labelled error sum on the dendrogram is in fact twice the increase in error sum caused by fusion. The point at which clusters become significant is taken as the level at which fusion of another cluster produces a larger than normal increase in the error sum. This is labelled "cut-off" on the small insert graph on Figure 3.

Each greywacke group was subsequently analysed for significant correlations in major and trace element chemistry (Figs. 4-8). Systems with mutually positive correlations are related to the input of different rock and mineral assemblages. Further analysis of the groups using ternary variation diagrams was attempted (Fig. 9) but found to be inadequate due to the complicated nature of the data. Major differences in chemistry are in absolute rather than relative amounts.

The lithic and feldspathic greywacke groups fall into the equivalent petrological subdivisions of Pettijohn (1957, p. 291), rock fragments and feldspar clasts being dominant respectively. The basic greywacke group is regarded as a variety of lithic greywacke (*ibid*) and is chemically more closely related to the lithic greywacke group (Fig. 3). Greywackes of the silicic group are equivalent to quartz wacke of Krumbein and Sloss (1963, p. 172) and subgreywacke of Pettijohn (1949).

B. Lithic greywacke group.(i) Petrography

A low lutite content and high proportion of rock and mineral clasts of all types is characteristic of rocks in the lithic greywacke group (plates 1A and B). In hand specimen they are usually greenish-grey but become bluish-grey when close to the thermal aureole. Samples for analysis were taken from beds which appeared in the field to represent the modal grain size rather than extremely coarse or fine grained variants. The average maximum grain size of lithic group greywackes collected in this way is 2 mm and the modal grain size 0.1 mm.

Monocrystalline grains of quartz, many of which display undulose extinction, are the dominant type of mineral clast. Primary inclusions in these are common and all four types, i.e. regular, irregular, globular and acicular (Keller and Littlefield, 1950) occur. Quartz grains containing both globular and irregular inclusions are present in greater numbers than those containing the other categories, indicating a dominant primary igneous source. Feldspar content may equal but rarely exceeds that of quartz. Orthoclase is kaolinised and often contains flakes of sericite and appears to be derived from the same source as granitic clasts also present in large quantities. Unaltered microcline, recognised by its distinctive cross-hatched twinning, occurs sporadically as monocrystalline grains, but has not been observed in rock fragments. Small grains of albitic plagioclase are also

fresh and unaltered, whereas larger more anorthitic clasts tend to be corroded and covered with small flakes of white mica. The latter also occur in coexisting granitic clasts. Ragged flakes of muscovite and biotite are common and may have an igneous or metamorphic source, whereas small globular grains of zircon may be derived from these and pre-existing sedimentary rocks. Biotite is invariably altered to a chlorite with typically anomalous blue interference colours. Small clasts of pyroxene (probably augite) are derived from rocks not represented in the clastic suite, but probably reflect a basic igneous input (see section B(ii) below). Sparsely occurring minerals include amphibole, tourmaline and sphene.

The proportion of rock to mineral clasts is high and fragments with an igneous source occur in large numbers. The plutonic igneous suite is dominated by granitic fragments including types with graphic and granophyric intergrowths. Ferromagnesian minerals in these clasts are chloritized and muscovite is absent. Numerous volcanic fragments mainly of spilitic or basaltic composition are present, the former being distinguishable by their albitic plagioclase laths set in a groundmass of chlorite and magnetite. Owing to heavy alteration other basic igneous fragments cannot be classified further. Polycrystalline aggregates of vein quartz are common showing straight crystal interfaces and slightly undulose extinction.

Clasts of metaquartzite exceed numbers of all other metamorphic rocks. Within these, quartz crystals have a

high length to breadth ratio, extremely undulose extinction and sutured crystal interfaces, typical of quartz recrystallized under stress. The only other metamorphic clasts are polycrystalline micaceous aggregates of schist, although garnet has been observed at one locality.

Fragments of sedimentary rock are restricted to intraformational mudstone and copious quantities of chert occurring as well-rounded, felted masses of cryptocrystalline silica.

Phyllosilicates and fine grained detrital quartz and feldspar make up the bulk of the matrix. Minor quantities of carbonate (calcite, dolomite or ankerite) of probable diagenetic origin also occur. Illite, sericite and paragonite are difficult to distinguish in such a finely divided state, although illite has been detected in greywackes to the south between Creetown and Gatehouse of Fleet (Weir, 1974b). Matrix chlorite is occasionally present as fibrous masses showing faint green pleochroism and anomalous blue interference colours, but usually only in rocks close to the metamorphic aureole.

(ii) Geochemistry

Nearly half of the greywackes (43) fall within this group and their chemical means are closely comparable with those of the total sample set (tables 1 and 2). Significant differences occur only in  $Al_2O_3$  and  $K_2O$  which are lower and higher respectively. Compared to the average Silurian greywacke from the Southern Uplands (Alsayegh, 1971),  $SiO_2$  and Sr are enriched but MgO and CaO are depleted. Trace element averages contrast highly with world-wide data (Taylor, 1965), higher values are obtained for Li,



Zr and Ni and lower for Rb, Sr, Y and Cu. Wide variations are expected because composition depends upon source rocks and conditions of sedimentation.

Numerous correlations above the 97.5% confidence level occur (Fig. 4). Systems of major oxides and trace elements having mutual and positive correlations are described below with reference to input of particular source materials, (Elements or oxides in brackets correlate significantly with most but not all other variables in the system).

a. TiO<sub>2</sub>-FeO-MgO.

Correlation between these variables (Fig. 12) reflects an input of ferromagnesian minerals and basic igneous clasts such as spilite, pyroxene, amphibole, biotite, and tourmaline. Chlorite within altered basic fragments and matrix will also be an important contributor.

b. TiO<sub>2</sub>-MnO-Na<sub>2</sub>O-(P<sub>2</sub>O<sub>5</sub>)-Sr

Deposition of Na-rich and probably basic extrusive igneous rocks such as spilite (or keratophyre) is held responsible for this system. TiO<sub>2</sub> occurs in all ferromagnesian rocks and links these with MgO and FeO (above), but absence of the latter oxides indicates that there is more than one source of ferromagnesian detritus. MnO and Sr will be associated with plagioclase (Taylor, 1965; Deer, Howie and Zussman, 1966), but CaO is not present owing to its additional occurrence in calcite, apatite, pyroxene, etc., although diagenetic breakdown of plagioclase will have undoubtedly provided much of the calcite present. P<sub>2</sub>O<sub>5</sub> does not correlate highly with Na<sub>2</sub>O and may indicate

the additional source of apatite in granites described later. A strong correlation exists between  $P_2O_5$  and Sr owing to  $Sr^{2+}$  replacement of  $Ca^{2+}$  sites in the apatite lattice (Taylor, 1965).

c.  $TiO_2$ -Zr-Cr

Resistate minerals such as zircon, rutile, spinel and sphene are probably responsible for these correlations (Figs. 12 and 13). Spinel may contain up to 60%  $Cr_2O_3$  and 20%  $TiO_2$  (Deer, Howie and Zussman, 1966). The mean Ti/Cr value for the lithic greywacke group is 26 compared to 0.15 and 45 for ultramafic and basic igneous rocks (data computed from Krauskopf, 1967), which possibly indicates a source of the latter. Besides Cr and  $TiO_2$ , Zr has a positive correlation with  $SiO_2$  and is undoubtedly related to an input of zircon-bearing ortho- and metaquartzite detritus. Similar heavy mineral-bearing arenites may contribute other resistates, but lack of significant correlation between  $TiO_2$ , Cr and  $SiO_2$  may be the result of the presence of basic igneous material.

d.  $Al_2O_3$ - $K_2O$ -(Li)-Rb-Y-(Zn)-(Pb).

This system is the result of the presence of granitic clasts and such minerals as potash feldspar, biotite (and derived chlorite) and muscovite (Fig. 10). Li-Rb, Zn- $K_2O$  and Pb- $K_2O$  correlations have a significance lower than 97.5%.

$K_2O$  and  $Al_2O_3$  are major oxides in potash feldspar, biotite and muscovite whereas Rb is a minor element and occurs within range of 250 to 850 ppm, 120 to 2500 ppm and

70 to 1000 ppm respectively (Wedepohl et al., 1970). Rb<sup>+</sup> substitutes for K<sup>+</sup> in micas in preference to feldspars, but the bulk of Rb occurs in feldspar lattices (Taylor, 1965). The mean K/Rb ratio is 238, close to the average continental value of 230 (Taylor, 1965; Erlank, 1968; Wedepohl et al. 1969). Granites have lower K/Rb values and basalts higher in the range 150 to 300, therefore a mixed or intermediate source may be proposed. According to Alseyegh (1971) removal of biotite from the granitic system in the course of weathering will tend to increase the K/Rb ratio, although inclusion of these elements in clay minerals will counteract this.

Li is highly concentrated in late stage ferromagnesian minerals and substitutes for Mg in granitic biotites and muscovites (Taylor, 1965). Its presence in this system will be the result of the above effect. Because the bulk of Rb is held in feldspars and Li in micas, a poor correlation exists between them.

Variation in the absolute concentration of Y between basalts (32 ppm) and granites (38 ppm) is not very significant (Wedepohl et al., 1969), although it is known to substitute for Ca<sup>2+</sup> in granitic apatite and sphene. Inclusion in the granitic system indicates its enrichment in these rocks.

Zn replaces Fe in biotites, chlorites and muscovites, but has an insignificant correlation with K<sub>2</sub>O because it occurs in very small quantities in potash feldspar.

Pb is expected to occur in the K<sup>+</sup> site of feldspars and micas, and in the Ca<sup>2+</sup> site of granitic apatite

(Taylor, 1965). Poor correlation with  $K_2O$  may be an effect of the latter process.

e.  $Al_2O_3$ -MgO-Li

Correlation of these elements probably represent biotite, chlorite and muscovite and are associated through  $Al_2O_3$  with the major granitic system above (Fig. 10). The presence of Li indicates a granitic rather than metamorphic source.

f.  $Al_2O_3$ - $P_2O_5$ -(Rb)-(Y)-Zn-Pb

$P_2O_5$  in this system shows that apatite has a granitic source (Fig. 10) and it is this that promotes its low correlation with  $Na_2O$  in the extrusive igneous system. Correlations between Y, Pb and  $P_2O_5$  probably represent replacement of  $Ca^{2+}$  in apatite, but low correlation between Y and Pb indicate that their presence in this mineral is unrelated.

g. MnO-CaO-Sr

These elements occur in plagioclase feldspar and calcite, although the latter mineral is uncommon in the lithic greywacke group (Fig. 13). Inclusion of MnO and Sr in the basic igneous system shows that plagioclase is related to this source however much CaO is derived from other minerals and sources.

There are few negative correlations between the major associations and the implication of this is that increased input from one source did not take place at the expense of others.  $SiO_2$  has negative correlations with most of the major oxides but more important are the

negative correlations with Li, Sr and Zn (Fig. 14). These may indicate that deposition of siliceous fragments may have occurred to the detriment of material from other sources.

### C. Basic greywacke group.

#### (i) Petrography

This group comprises ~~of~~ nineteen grey to greenish-grey medium grained greywackes which are occasionally pelitic (plates 2A and B). Their modal grain size is between 0.2 mm and 0.25 mm and mean maximum clast size 1.5 mm. Lutite content tends to be higher than the lithic group but petrographically they fall into the lithic greywacke category of Pettijohn (1957) and are separated from the lithic group by differences in geochemistry and mineralogy.

Total quantities of monocrystalline quartz clasts vary considerably but feldspar is usually subordinate. Much of the quartz shows strained extinction and although irregular primary inclusions predominate, globular, acicular and regular types also occur (Keller and Littlefield, 1950). Both orthoclase and plagioclase are heavily altered and contain secondary white mica, although albitic plagioclase remains relatively fresh. Clasts of microcline are far less common than in the lithic group which may indicate a more restricted source of microcline-bearing granite. Small pyroxene fragments characteristically occur in greater quantities than in the lithic group, presumably as a result of a greater basic igneous influence at the source.

Resistant minerals such as zircon and sphene are of widespread but minor occurrence. Small amounts of biotite and muscovite are present and in common with the lithic group tourmaline is rare and localised in occurrence.

The ratio of rock to mineral clasts is high and similar to the lithic group. Numerous igneous fragments occur, granite being the major plutonic type. These occasionally show myrmekitic or graphic intergrowths and have provided some of the monocrystalline quartz and feldspar detritus. Highly altered, rounded chloritic clasts are difficult to identify with certainty, but probably are of fine grained basic igneous origin. Large numbers of spilite fragments are present and the overall basic igneous content is higher than the lithic group. Polycrystalline aggregates of vein quartz are however less abundant.

Clasts of metamorphic origin are again dominated by metaquartzite with schist occurring only rarely. However metamorphic detritus is more restricted in quantity than the lithic group and consequently quartz containing acicular and regular primary inclusions is reduced in amount.

Sedimentary rock clasts and matrix are similar in composition and quantity to the lithic group and the reader is referred to the relevant section (2B(i)).

(ii) Geochemistry

Means of the analyses of basic group greywackes compare neither with Kilfillan or Garheugh greywackes (tables 1 and 2, and Alsayegh, 1971) although the trace

element assemblage of the latter is similar.  $\text{SiO}_2$ ,  $\text{MgO}$  and  $\text{Cr}$  are enriched and  $\text{Al}_2\text{O}_3$ ,  $\text{Na}_2\text{O}$ ,  $\text{K}_2\text{O}$  and  $\text{Sr}$  depleted relative to the means of the total data set. This may be the result of increased quantities of siliceous and basic igneous or ferromagnesian fragments over granitic or feldspathic detritus.

A matrix of significant correlations between chemical variables is provided on Figure 5.

a.  $\text{SiO}_2$ - $\text{K}_2\text{O}$ - $\text{Rb}$ - $\text{Y}$ - $\text{Zr}$

The inclusion of  $\text{SiO}_2$  and  $\text{Zr}$  in a system essentially comparable to the granite system of the lithic group (Figs. 10 and 13) may indicate that both granitic and siliceous (heavy mineral-bearing quartzite or chert) detritus has the same provenance. A more mixed source of feldspathic detritus may account for the absence of  $\text{Al}_2\text{O}_3$ .

The average  $\text{K/Rb}$  ratio (216) is slightly lower than the lithic group owing to increased acidity of the granitic source or an overall increase in amounts of granitic detritus. The latter however seems unlikely on petrological and geochemical evidence presented above.

b.  $\text{TiO}_2$ - $\text{Cr}$

Correlation of these variables is only significant at the 97.5% level (Fig. 12) and  $\text{TiO}_2$  correlates with  $\text{FeO}$  and  $\text{MgO}$  at a lower value. The average  $\text{Ti/Cr}$  ratio (13) is lower than the lithic group reflecting the greater importance of a basic igneous, ferromagnesian-bearing source.

c.  $\text{Al}_2\text{O}_3$ - $\text{MnO}$

These oxides probably represent plagioclase feldspar detritus. Positive correlations exist with  $\text{Sr}$  but

both at a confidence level less than 97.5%. CaO does not appear in the system owing to complications arising from its presence in many other mineral phases.

d. Al<sub>2</sub>O<sub>3</sub>-MgO-Na<sub>2</sub>O-Ni

It is proposed that this system is a result of basic igneous, mainly spilitic fragments (Fig. 12). The presence of Al<sub>2</sub>O<sub>3</sub> emphasises the dominant role of albitic plagioclase in this material. MgO and Ni are contained within ferromagnesian minerals and derived alteration products. The Mg/Ni ratio is 280, as compared to 250 and 450 for gabbroic and dioritic rocks respectively (computed data from Nockolds and Mitchell, 1946).

e. FeO-MgO-Ni-Cr

The main sources of these variables are ferromagnesian and derived clay minerals and input is linked through MgO and Ni to the basic igneous system above (Fig. 12). Separation has taken place as a result of additional sources of ferromagnesian and chloritic detritus. Fe/Cr ratios average 110 and are between those for ultrabasic (35) and basic igneous (190) rocks (calculated from Nockolds and Mitchell, 1946).

Low Mg/Ni and Fe/Cr ratios emphasise the importance of basic igneous detritus in the basic greywacke group.

f. FeO-Zn

Zn correlates well with FeO because it substitutes for Fe<sup>2+</sup> sites in late crystallizing ferromagnesian phases, notably biotite (Taylor, 1965). Basaltic pyroxene has an average Zn-content of 50 ppm and spilite, 100 ppm (Wedepohl et al., 1969). Granitic biotites and chlorites



contain much more, with average analyses from the Fleet granite yielding 650 ppm and 925 ppm Zn respectively (appendix 7).

g. CaO-Y

Correlation of these variables is related to apatite, sphene or calcite, and they are linked through Y to the granitic system (above). Although correlations of  $P_2O_5$  with both are poor, apatite of granitic origin cannot be discounted as a source. A mixed origin may be inferred.

Negative correlations are significant between most elements of the two major systems, i.e.  $SiO_2-K_2O-Rb-Y-Zr$  and  $FeO-MgO-Na_2O-Ni-(Cr)$ . This is a result of deposition from currents with two contrasting sources and differing geographical locations. Increased input of detritus with a granitic and siliceous provenance results in a depletion of basic igneous and ferromagnesian material and vice versa. This contrasts with the lithic group where the siliceous source appears to be independent of all others.

D. Feldspathic greywacke group.

(i) Petrography

Greywackes of the feldspathic group are pale green to greyish-green in colour and have a variable grain size (plates 3A and B). Their mean maximum clast size is 1 mm and modal grain size 0.1 mm. Overall clastic content is lower than the basic or lithic groups, and as the total amount of feldspars usually exceeds that of rock fragments they are classified within the feldspathic greywacke category of Pettijohn (1957).

Monocrystalline grains of quartz occur less extensively than in the previous groups and the few regular and acicular inclusions in these (Keller and Littlefield, 1950) indicate a mixed igneous and metamorphic source. Large quantities of orthoclase, plagioclase and microcline are in various stages of alteration to clay minerals, and occasionally exceed quartz in total quantity. Small fresh fragments of albitic plagioclase are less common and microcline more common than in the previous groups. Fewer ferromagnesian minerals and clasts of sphene occur, but globular grains of zircon are more widespread.

In contrast to the lithic and basic groups the proportion of rock to mineral clasts is low. However granitic fragments still dominate the plutonic igneous suite and include types with granophyric, graphic and myrmekitic intergrowths. Feldspars within these match coexisting monocrystalline clasts. Polycrystalline aggregates of vein quartz exceed all other igneous rocks which include chloritized basic clasts and rare fragments of spilite.

Metaquartzite and schist are less frequent in their occurrence whereas copious quantities of chert are present. Mudstone clasts are again relatively minor.

Matrix and cement resemble that of the previous two groups except that the proportion of clay minerals and carbonate is usually higher, owing to the higher feldspar content.

(ii) Geochemistry

Thirteen greywackes are classified within this

group (Fig. 3) and few comparisons exist between the chemistry of these and greywackes of the Garheugh or Kilfillan formations (Alsayegh, 1971; tables 1 and 3).  $Al_2O_3$ , CaO,  $Na_2O$ ,  $K_2O$ ,  $P_2O_5$  and Sr are significantly higher and  $SiO_2$  and Cr lower than the means for the total population. Such differences are the result of larger quantities of feldspar occurring at the expense of siliceous, basic igneous and ferromagnesian detritus. The mean  $Na_2O/K_2O$  ratio is 1.45 compared with 1.02 and 1.05 for the lithic and basic groups respectively, indicating relatively higher amounts of plagioclase over potash feldspar and/or a reduction in biotite and muscovite. The latter seems more probable in the light of microscopical evidence. A correlation matrix of significant correlations is provided on Figure 6.

a.  $SiO_2$ -Zr.

Correlation between these variables occurs as a separate system, which compares with the lithic group and represents material from zircon-bearing quartzite successions (Fig. 13).

b.  $TiO_2$ -FeO-MgO-(Zn)

This association is related to ferromagnesian and derived clay minerals (Fig. 12). The presence of Zn may be a result of relatively large amounts of biotite compared with other ferromagnesian or basic igneous clasts.  $Na_2O$  is notably absent owing to a decline in emphasis of spilitic detritus.

c.  $Al_2O_3$ - $K_2O$ - $P_2O_5$

The granitic system contains a reduced number of correlatable components because of a reduction in the

number of granitic clasts. In the feldspathic group chemical systems represent individual minerals or pairs of minerals which may be related through one or more variables to rock associations.

Correlations between  $\text{Al}_2\text{O}_3$ ,  $\text{K}_2\text{O}$  and  $\text{P}_2\text{O}_5$  represent potash feldspar and apatite derived from the same granitic source (Fig. 10). Break-up of the major granitic system is undoubtedly a consequence of the increased quantity of monocrystalline grains of granitic affinity observed in thin section.

d. FeO-MgO-Ni-Cr

These variables are related to the ferromagnesian system above but more specifically refer to those with a more basic igneous source, hence the inclusion of Ni and Cr (Fig. 12). Mg/Ni and Fe/Cr ratios are 330 and 280 compared with 280 and 110 for the basic group. The inference of this is a restricted basic igneous source or a change in emphasis to rocks of intermediate composition. The small quantities of ferromagnesians and basic igneous fragments observed in thin section tend to support a reduced basic igneous provenance.

e. MnO-CaO

Correlation of these oxides is a result of plagioclase feldspar detritus and to a lesser extent diagenetic calcite (Fig. 13). The MnO content of plagioclase from igneous rocks varies between 40 and 400 ppm (Nockolds and Mitchell, 1946).

f.  $\text{K}_2\text{O}$ -Rb-Y

These variables are related to the potash feldspar/apatite system (above) and represent biotite and muscovite

derived from granitic sources (Fig. 10). Both Rb and Y are enriched in granitic micas (see chapter 8 and appendix 7). The average K/Rb ratio is 266 compared with 238 and 216 for the lithic and basic groups respectively. This endorses chemically the observed enhancement of potash feldspar over biotite.

g. K<sub>2</sub>O-Pb

Pb<sup>2+</sup> substitutes for K<sup>+</sup> in potash feldspars and micas of granites and is here probably related to the large amounts of potash feldspar present and therefore associated with the granitic system (above, see chapter 8 and appendix 7).

No significant negative correlations occur between any of these systems, therefore a relatively constant input from all sources is proposed.

E. Silicic greywacke group

(i) Petrography

Pale greenish grey greywackes with a characteristically high lutite content are diagnostic of this group (plates 4A and B). Their mean maximum grain size is 0.5 mm and modal grain size 0.1 mm. Sorting is moderate and better than in any of the previous groups. The abundance of quartz clasts allows these rocks to be classified as subgreywacke (Pettijohn, 1949) or quartzwacke (Krumbein and Sloss, 1963, p. 173).

The bulk of the mineral clast population is composed of monocrystalline grains of quartz, many of which show undulatory extinction. Within these, primary inclusions are predominantly of the globular, regular and acicular types, irregular inclusions occurring less

frequently. Both plagioclase and orthoclase feldspars show signs of alteration to clay minerals and appear turbid in thin section. Microcline has been observed at only two localities. Ragged and often orientated flakes of muscovite occur in greater quantities than in other groups (above). Rounded grains of zircon and chloritized flakes of biotite are found frequently whereas sphene, tourmaline and pyroxene clasts are rare.

The proportion of rock to mineral clasts is low compared with the lithic and basic greywacke groups and siliceous types predominate. Few plutonic igneous fragments are observed and most of these are granitic. Spilite and altered basic igneous rocks occur infrequently. Polycrystalline aggregates of vein quartz are the most abundant igneous clasts.

Metaquartzite fragments are present in greater quantities than schist, although breakdown of the latter rock may have provided the large amounts of detrital muscovite.

In common with the other groups (above) the major sedimentary clast is chert with subordinate mudstone.

Large quantities of matrix are characteristic of this group. Phyllosilicates such as chlorite, sericite and illite and rock flour composed of very fine-grained quartz and feldspar are abundant. Diagenetic calcite occurs in greater amounts than in the other groups and powdered samples effervesce readily in acid.

#### (ii) Geochemistry

Thirteen of the greywacke samples fall into this

group (Fig. 3) and again do not compare chemically with Kilfillan or Garheugh rocks (Alsayegh, 1971; Tables 1 and 3). Relative to the total sample set they are enriched in  $\text{SiO}_2$  and CaO and depleted in  $\text{Al}_2\text{O}_3$ , FeO, MgO,  $\text{K}_2\text{O}$ , Li, Rb, Sr, Ni, Zn and Cr. This reflects the scarcity of rock and mineral clasts, other than quartz, observed in thin section. A matrix of significant correlations between chemical variables is provided on Figure 7.

a.  $\text{TiO}_2$ -Zr

This correlation is comparable with the resistate ( $\text{TiO}_2$ -Zr-Cr) system of the lithic group. Exclusion of Cr is undoubtedly the result of a less basic provenance (Fig. 13).

b.  $\text{SiO}_2$ -Zr

Associated with the correlation above these elements reflect the presence of zircon-bearing quartzite fragments and are similar in this respect to the lithic and feldspathic groups (Fig. 13).  $\text{TiO}_2$ ,  $\text{SiO}_2$  and Zr do not form a complete system owing to additional sources of Ti-bearing minerals.

c.  $\text{Al}_2\text{O}_3$ - $\text{K}_2\text{O}$ -Li-(Rb)-Ni

These variables again form a granitic system, although correlation between Rb and  $\text{Al}_2\text{O}_3$  is less than the 97.5% confidence level (Fig. 10). The presence of Ni indicates that a substantial amount of this element must be associated with granitic ferromagnesian e.g. biotite (chapter 8 and appendix 7). The average K/Rb ratio (212) is lower than any of the other groups, reflecting an input of greater amounts of granitic detritus relative to other rocks, or greater amounts of biotite and muscovite relative

to potash feldspar. The large amounts of muscovite from a ?metamorphic source may account for this.

d. FeO-Y-(Zn)

A comparable correlation exists in the basic greywacke group (above) although it does not contain Y. This may be the result of increased importance of granitic ferromagnesian Y-bearing detritus (Fig. 12). Biotites from the Fleet granite often contain over 300 ppm Y (chapter 8 and appendix 7).

e. MnO-MgO-CaO-Cr-(Ni)

Correlation of these elements is the result of input of ferromagnesian minerals and anorthitic plagioclase. The Mg/Ni ratio (395) is high and absolute concentrations of Ni and Cr low compared with other groups (tables 2 and 3, figs. 12 and 13). This is evidence for a reduced basic igneous source which is endorsed by the scarcity of spilite, pyroxene and amphibole clasts in thin section.

f. Na<sub>2</sub>O-Li

The inference from this correlation is that the bulk of Na<sub>2</sub>O has a granitic rather than spilitic source. Li is concentrated in highly fractionated granites and is accompanied in the Fleet pluton by a late stage Na-enrichment (see part 3). It is also possible that some of the granitic fragments are alkaline in origin.

g. Rb-Y

Significant correlation between these elements links the two granite systems (above) together. Chemical systems are fragmented in a similar fashion to the feldspathic greywacke group owing to the predominance of monomineralic



grains.

$\text{SiO}_2$ ,  $\text{TiO}_2$  and Zr have fairly strong negative correlations with MnO, MgO, CaO, Cr and Ni although some are below the 97.5% confidence level. This demonstrates that input of the quartzitic-resistate assemblage is somewhat inversely proportional to that of ferromagnesian or more basic igneous material. Deposition of granitic detritus appears to have been fairly constant. The existence of two fairly distinct provenances may explain these relationships. Granite must have been exposed in both but one must have contained more basic igneous material and less quartzitic material. The greater maturity of these greywackes may also indicate that erosion of uplifted sedimentary rocks, perhaps greywacke in composition, was providing detritus.

#### F. Shales.

The geochemical classification includes this group of twelve samples of shale and pelitic hornfels (Fig. 3). Those unaffected by thermal metamorphism are well laminated by bands of arenaceous and argillaceous material, which are invariably puckered or microfolded. An incipient strain-slip cleavage is occasionally associated with this rucking. Major micaceous and clay minerals observed are chlorite and sericite although illite undoubtedly occurs. Fine grained detrital quartz and feldspar are abundant and a few grains of albitic plagioclase have been identified. Other detrital minerals are Fe-Ti oxides, muscovite, zircon and rare tourmaline. Many of the shales are black and contain laminae of carbonaceous material.

Table 4 gives a comparison of the average chemistry of the shales with average world-wide analyses. The abundance of clay minerals in shales compared with greywackes is reflected by a higher content of  $Al_2O_3$ , FeO, MgO,  $K_2O$ , Li, Rb, Ni and Zn. Significantly lower values of  $SiO_2$  and Zr indicate a lower detrital input (tables 2 and 4). The mean Cr content is 183 ppm compared with 181 ppm for the greywackes and 100 ppm from world-wide shale analyses (Taylor, 1965). This enrichment is evidence for an important basic igneous provenance which is also found in the basic and lithic greywacke groups. Higher than average amounts of Ni endorse this concept (tables 1, 2 and 4).

#### G. Contaminated samples

A greywacke and a shale sample are classified in an independent group because they are contaminated with base metal sulphides (Fig. 3). High values of Pb and Zn indicate the presence of galena and sphalerite, which have been occasionally observed with calcite, infilling joints.

#### H. Conclusions.

The separate groups of greywacke which have been classified and described using geochemical and petrological data are members of a continuously evolving sedimentary pile. Differences in lithology arise from differing conditions at their source and during transport and sedimentation. Geochemical and petrological trends emerge when the four greywacke groups are compared and evolve from the basic through the lithic and feldspathic to the silicic group. This, very generally, is their order of

superposition, but further details are provided in chapter 3.

From the basic group to the silicic group the mean maximum clast size decreases whilst the modal grain size stays reasonably constant, owing to the increase in sorting observed in thin section. Intensity of erosion at the sources may have lowered or pre-existing sediments may have been uplifted to provide texturally more mature clasts. Sedimentation and/or lack of tectonic activity may have reduced the gradient of the ocean floor, and thereby reduced the potential energy and therefore power of transport of turbidity currents. All these factors would promote sorting of detritus before and during transport. Reduction in quantities of unstable minerals such as ferromagnesian and feldspars, and arenite to lutite and rock to mineral clast ratios endorse these concepts.

The sources of detritus and their relative importance change from group to group. Basic group greywackes are dominated by a granitic igneous and quartzitic province but a distinct basic igneous province also occurs. They are probably separated geographically and fragments have been transported from each by turbidity currents with differing directions. The significance of the basic igneous area wanes either as a result of its complete denudation or a change in direction of currents. Fragments with an acid igneous and quartzitic source are dominant in lithic and feldspathic group greywackes.

*order 20 ?*

Finally in the silicic group clastic basic igneous material has almost disappeared and acid igneous fragments are depleted in response to an increased input of siliceous material both of sedimentary and metamorphic origin.

Some of the differences in trace element chemistry of the greywacke groups are outlined in ternary diagrams on Figure 9. The importance of a basic igneous source in the basic group is demonstrated by its position near to and trending towards the Ni, Cr apex. In both diagrams the lithic group takes a more median position, representing a more "average" type.

The Sr enrichment in feldspathic group greywackes is indicated by their position near to the Sr apex in the upper diagram. A trend towards the Zr apex in the lower diagram is a result of increased detrital resistate input in the silicic group. A relative increase in granitic detritus from the basic to lithic and feldspathic groups followed by a decline in the silicic group is illustrated on the lower diagram by an initial trend towards and subsequently away from the Rb, Li apex.

CHAPTER 3  
STRATIGRAPHY

A. Introduction.

The Lower Palaeozoic succession is divided into three units based upon lithological, geochemical and very sparse palaeontological evidence:

3. Knockeans Formation.
2. Cragneill Formation.
1. Moffat Shales (Birkhill and Hartfell Shales)

The areal disposition of these stratigraphical units and the distribution of chemically classified samples are given on Figures 1 and 15. The relative proportion of each greywacke class in each structural belt (Fig. 15) is represented by pie diagrams on Figure 16. The Cragneill turbidites are dominated by lithic and basic group greywackes whereas those of the silicic group predominate in the Knockeans succession.

The structure of the region, which will be described in detail in chapter 4, is governed by four major strike faults and associated zones of Schuppenstruktur. These divide the sedimentary rocks into five belts (A to E, Fig. 15) across which lithological correlation is attempted (Figs. 17 to 21).

B. Moffat Shales.

The basal Moffat Shale sequence comprises black carbonaceous and grey/green shales which are only exposed in the zones of strike faulting (Fig. 1). Thermal metamorphism and shearing associated with this faulting have

reduced graptolite remains within the shales to unidentifiable and often pyritised fragments. In the present survey fossils were found which could be classified with a useful degree of confidence at only two localities. However Peach and Horne (1899) describe other fossiliferous localities outside the thermal aureole which may be correlated with those closer to the granite. Otherwise lithological comparison with Dobb's Linn and other described sections of the Moffat Shales has been employed to correlate these rocks.

The thickest and apparently lithologically most complete succession of Moffat Shales is exposed within Schuppen of the northerly zone of strike faulting, the Talnoy thrust zone (maps 1 to 4, tables 5 and 6). It is considered that these may represent sedimentation on the "axial" zone of the geosyncline proposed by Lapworth (1878), Peach and Horne (1899) and Walton (1963, 1965.). A four fold lithological subdivision of the succession is apparent and is compared with the Dobb's Linn section (table 8).

#### CRAIGNELL FORMATION

--- conformable contact ---

4. Upper Birkhill Mudstones:- dark and light grey thinly laminated mudstones with interbedded thin black shale horizons.
3. Lower Birkhill Mudstones:- dark grey to black mudstones, often hard and blocky or highly cleaved.
2. Upper Hartfell Mudstones:- pale green, olive to brown weathering mudstones and subordinate black shale bands.

1. Lower Hartfell Mudstones:- sooty black, rusty weathering mudstones and fissile shales, sometimes highly pyritous and merging at the base with Glenkiln black shales.

Not all outcrops, especially those of black shale alone, are distinctive enough to be classified according to these subdivisions. Those that are distinctive are marked B and II on the maps (Birkhill Mudstones and Hartfell Mudstones respectively).

Thickness of the succession is difficult to estimate owing to repetition of bands by strike faulting and absence of exposures showing the complete succession.

The Talnotry thrust zone is the only locality in the area where all four lithological divisions of the Moffat Shales are exposed. A basal Hartfell-Glenkiln horizon has been recognised in black mudstones exposed by the Penkiln Burn northwest of Glenhoise (24275683). Here poorly preserved specimens of Orthograptus cf. calcaratus (Lapworth) and Climacograptids occur in sooty black pyritous mudstones. Glenkiln-Hartfell Shales have been described from the River Cree north of Newton Stewart (24005670) and where the same band crosses Penkiln Burn near Cumloden (24165677, map 1; Peach and Horne, 1899). Grey-green shales of Upper Hartfell barren grey mudstone lithology (Table 8) are exposed immediately above the Talnotry basal thrust by the Grey Mare's Tail Burn (table 6, map 2, 24915722) and at the roadside 750 metres southwest of Talnotry (plates 5B and 6B, locality 868, 24785707, map 2). Many exposures of black mudstones with a comparable lithology to the Lower Birkhill Shales occur but unfortunately palaeontological evidence confirming

particular horizons is lacking. In the bed of the Penkiln Burn north of Minnigaff (grid squares 241, 566 and 241, 567; map 1) dark and light grey laminated mudstones with thin subordinate black bands of a type similar to Upper Birkhill Shales pass unconformably into basal turbidites of the Craignell Formation. This contact is repeated a number of times along the stream section, as a result of strike faulting, further upstream (24305087) these shales supercede with apparent conformity black pyritous mudstones of Lower Birkhill type (table 5, map 1).

Four kilometres to the southwest in the Blairbuies thrust zone (maps 1, 5 and 9) there is a notable change in the Moffat Shales. Exposures of both green, and dark and light grey laminated mudstones are subordinate to those of black mudstone. Lower Hartfell and Lower Birkhill black mudstones occur extensively especially in the area between Blairbuies and Ardwell Hills (map 1, grid square 247, 566), and contain pyritized casts of unidentifiable graptolites. Black mudstone sequences of Lower Birkhill lithology are observed at two localities to pass upwards into graded turbidites of the Craignell Formation. Grey-black laminated mudstones which are prevalent in the Talnoy thrust zone are attenuated or absent and may be represented stratigraphically by basal beds of the Craignell Formation.

Exposures of black mudstone to the east between Loch Ken and the granite contact (map 5, grid squares 265, 571; 265, 572) are correlated with outcrops at



Barend (Fig. 1, 26955730). The youngest fossiliferous horizons at this locality are interbedded black and grey Lower Birkhill mudstones of the gregarius Zone (table 8) which lie conformably below deposits of greywacke (Peach and Horne, 1899, p. 161). From the apparent lithological continuity observed in the Moffat Shales elsewhere within the Southern Uplands it seems likely that most if not all of the Upper Birkhill succession observed in the Talnothy thrust zone has been replaced by greywacke in the Blairbuires thrust zone.

Further south black mudstones of Birkhill affinity are associated with the Culcronchie Thrust. At Slogarie (Fig. 1, 26525689) the contact between these and the Cragneill formation is marked by a thick intraformational black mudflake pseudoconglomerate. Turbidity currents depositing Cragneill arenites must have been sufficiently powerful to tear up fragments of the pre-existing cohesive mud. Exposures of Moffat Shale at Hensol (Fig. 1, 26785690) are correlated with these, and here a fossiliferous succession of Lower and Upper Hartfell and Lower Birkhill mudstones is exposed (Peach and Horne, 1899, p. 170). Upper Birkhill mudstones do not occur and greywackes conformably supercede beds containing a gregarius Zone fauna.

Exposures along the two southerly strike faults, the Pool Ness and Pibble Thrusts, also contain mudstones comparable to the Lower Birkhill of Dobb's Linn and pass upwards conformably into Cragneill arenites. The uppermost beds exposed at Pool Ness (locality 1169, 25665623, plates 10 and 11) are dark grey or black in colour and

finely laminated. Outcrops associated with the Pibble Thrust are correlated with inliers of Moffat Shale at Laurieston (Fig. 1), where beds up to the gregarius Zone again occur.

To summarise, investigations into Moffat Shale sequences show that Upper Birkhill mudstones are replaced in a southerly direction by basal Craignell turbidites between the Talnoy and Blairbuies thrust zones. Further south the contact appears to be more constant in age at the gregarius Zone. This variation may be the result of deposition in areas to the south of the axial rise proposed by Lapworth (1878) and endorsed by Peach and Horne (1899) and Walton (1963, 1965).

Sedimentation of black mudstone took place continuously from Glenkiln to the top of the Lower Birkhill when it was superceded by turbidites in localities as far away as Crossmichael (27505680) and Luce Bay (23005510). However towards the north deposition of Moffat Shales may have continued in response to deposition on an axial rise away from the environment of turbidity currents. Overstep by Craignell arenites probably took place from south to north and resulted in overall turbidite deposition by the middle of the Fronian stage (table 8). Until palaeontological evidence is forthcoming and the age of the base of the Craignell Formation determined accurately, this latter concept should be viewed with caution.

### C. Craignell Formation.

The Craignell Formation occupies the tract of

land north of the Pibble Thrust and occurs both in Schuppen associated with large strike faults and in wide belts bounded by these faults (Fig. 1; belts A, B, C and D, Figs. 15 and 23). The arenites are divided into three lithostratigraphical units based on differences in lithology and geochemistry:

1. Basic Facies.
2. Lithic Facies.
3. Silicic Facies.

The proposed disposition of the four geochemical and petrological types of greywacke in the Craignell Formation is given on Figure 17. This block diagram has been constructed using data from correlation diagrams (Figs. 18 to 21) and additional field observations. The strata of each fault-bounded block have been rotated back to the horizontal and lithological and geochemical correlation has been attempted between them. The horizontal scale is correct for distances measured parallel to the strike (i.e. parallel to the scale bar), but across-strike variations are based upon distances between beds at their present structural position and consequently may bear little relationship to actual distances during sedimentation. Contacts between the various facies are labelled by arrows.

(1) Basic Facies.

Greywackes classified (chapter 2) within the basic group on geochemical and petrological grounds are incorporated into the Basic Facies of the Craignell Formation, although small parts of the succession may be

occupied by silicic and feldspathic types (Fig. 17). They occur at the base of the Craignell Formation in the northwest where they rest conformably upon Moffat Shales. Towards the east and south the facies thins forming a sedimentary wedge, and in the north it occurs as tongues in surrounding lithic group greywackes (Fig. 17).

Its greatest development lies towards the northwest where the base is probably Fronian in age (table 8). However the contact with the underlying Moffat Shales appears to be diachronous and occurs in the gregarius Zone (Idwian) further south.

Two thick shale sequences are interbedded with turbidites of the Basic Facies in the north and west and may represent time stratigraphic horizons. Both of these thin towards the south and east and cut across the contact between Basic and Lithic Facies, indicating its diachronous nature. Increase in thickness of this facies probably relates to a source of detritus towards the northwest, the true nature of which is discussed below.

Graded units have frequently been observed in turbidites away from the metamorphic aureole and are invariably less than 200 mm thick. Thick sequences of interbedded arenite and pelite occasionally occur. Beds in these are usually of equal thickness (ca. 100 mm) and are not mutually graded. Few sole markings have been observed and the occasional drag mark indicates current directions running approximately parallel to the strike (ENE.-WSW), in accordance with observations from elsewhere within the Southern Uplands (Walton, 1955; Gordon, 1960).

Similarities exist between turbidites of this facies and the Pyroxenous Group of the Peebles area (Walton, 1955) and Kilfillan Formation south of Glenluce (Gordon, 1960). Both these latter units have been classified on their graptolite faunas as Lower Llandovery, and represent the arenitic northern lateral equivalents of the Birkhill Shales. Their upper boundaries have not been described in detail and in fact the relationship between the Kilfillan and younger Garheugh Formation (Gordon, 1960; Rust, 1965) is unknown. Basal beds of the Basic Facies rest conformably upon gregarius Zone mudstones in the south and therefore represent some of the Lower Llandovery.

All three groups contain abundant basic igneous fragments and are poorly sorted (Walton, 1955; Gordon, 1960). Amounts of detrital pyroxene appear to increase towards the northeast from Glenluce to Peebles. Detrital ferromagnesian are uncommon in the Kilfillan Formation (Gordon, 1960), fairly widespread in the Basic Facies of the Craginell Formation and abundant in the Pyroxenous Group (Walton, 1955). Large quantities of monocrystalline quartz and feldspar fragments are common to all, but the Basic facies contains more granitic clasts. Gordon (1960) observed an increase in granitic fragments at the expense of feldspar in Kilfillan arenites towards the northwest of the Glenluce area. The source of granitic detritus in these sediments is probably closer to the Fleet area. Bivariate analysis (chapter 2) of the geochemistry of basic group greywackes endorses the concept of two fairly distinct provenances, one of basic the other of granitic

igneous material.

The Basic Facies of the Craignell Formation has not been set up as a formation because of the lithological similarities both in the field and under the microscope that exist with greywackes of the Lithic Facies. It is proposed, however that this succession is the equivalent of the upper parts of both the Kilfillan Formation and the Pyroxenous Group, and is a transition both in time and space between these and succeeding deposits.

A continental massif containing large areas of granitic and ophiolitic rocks provided the detritus for these deposits. The presence of chert fragments is the result of erosion of a pre-existing sedimentary pile. The north-westward thickening of the facies and the ophiolitic clast assemblage together suggest the Ballantrae Igneous Complex or equivalent rocks as a possible source, within the landmass designated as Cockburnland (Walton, 1963). During Lower Birkhill times (Idwian, Fig. 22) this appears to have been an area of very positive topography, undergoing rapid mechanical erosion, as indicated by the immaturity of the derived detritus.

#### (ii) Lithic Facies

The Lithic Facies contains most of the lithic group greywackes and a few of the feldspathic group, described above (chapter 2). It forms the bulk of the Craignell Formation and generally supercedes deposits of the Basic Facies except in the north (Fig. 17). The contact between these facies is diachronous and turbidites of the Lithic Facies lie conformably above gregarius Zone

mudstones in the southeast. To the northwest the upper contact with the Silicic Facies is marked by a thick grey shale horizon. Like those below, it appears to thin rapidly to the south and east and may be the result of continued reduced sedimentation in the axial region of the geosyncline.

Coarse to medium grained arenites with a characteristic wide range in clastic composition and high arenite to lutite ratio are typical. Granitic clasts are still predominant, but fewer are of basic igneous and ferromagnesian composition compared with the Basic Facies. Graded bedding commonly occurs in units between 100 and 200 mm in thickness, but to the east of Loch Ken the beds are massive and not obviously graded. They are equated with the Intermediate Group (Walton, 1955) of Peebles and the Garheugh Formation (Gordon, 1962) of Glenluce, but contain fewer clasts of basic igneous derivation. Sedimentation has been dominated by the continued proximity of a source of granitic detritus, and geochemical investigations (chapter 2) have indicated a more homogeneous source compared with the Basic Facies.

Sedimentation of both Basic and Lithic facies undoubtedly took place simultaneously for much of the upper part of the Idwian stage. Differences between them are probably a result of their differing proximity to the sources of detritus. Turbidites of the Basic facies in this area were replaced completely by those of the Lithic Facies, owing to a reduction in the input of basic igneous material, probably during the Fronian stage.

Cockburnland (Walton, 1963) to the north is again proposed as a major source of clastic material. From this landmass predominantly granitic and metamorphic detritus was provided from a northerly or northeasterly source as indicated by thickening of the facies in this direction (Fig. 17).

(iii) Silicic Facies

This facies is well developed in exposures along the southerly structural belt of the Craignell Formation (Figs. 17, 21 and 23), and is also thinly represented in the upper parts of the sequence in the north-west (Fig. 18). Turbidites are lithologically less constant especially to the south where lithic, feldspathic and silicic types occur. They are generally finer grained and have a higher lutite content than rocks of the Basic and Lithic Facies. Graded bedding usually occurs in units less than 100 mm in thickness and has more frequently been observed in the southern exposures. Sole markings in arenites north of Culreoch (25835628) indicate ENE. or WSW. current directions.

The Silicic Facies in the northwest between Poultrybuie and Craignell (Figs. 1 and 18) comprises fine grained silicic group greywackes interbedded with two conglomeratic horizons (map 2), above a thick band of grey shale. Clasts in the conglomerate are predominantly siliceous. Exposures further northwest i.e. higher in the succession were not studied, therefore it is not possible to state whether these rocks represent a transition to a more siliceous formation or a relatively thin localised sequence within a succession of lithic greywacke.



The presence of more mature siliceous sediments interbedded with conglomerates may indicate shallow water sedimentation in response to uplift of the southern margin of Cockburnland.

Turbidites of the Silicic Facies contain large amounts of siliceous detritus such as chert, metaquartzite and vein quartz, although granitic fragments are still fairly common. They probably represent a transitional sequence between the relatively coarse grained immature lithic greywacke forming the bulk of the Craignell Formation and the younger finer grained more mature greywackes of the Knockeans Formation.

#### D. Knockeans Formation.

Sediments of the Knockeans Formation occupy the ground to the south of the Pibble Thrust (Fig. 1). Turbidites are characteristically fine grained, with a high lutite content and are predominantly of the silicic group (chapter 2). Thick sequences of ungraded interbedded arenitic and pelitic bands occur. Rocks are pale green and weather, often deeply, to brown limonitic secondary minerals.

This formation is correlated with the Hawick Rocks of Whithorn (Rust, 1965a, 1965b) on clastic composition, texture and the presence of large quantities of secondary calcite. Similar turbidites a few kilometers south of Creetown have been correlated (Weir, 1968) with the Carghidown Beds which represent the lower part of the Hawick Rocks succession in Wigtonshire (Rust, 1965). All

these sequences contain fine grained greywackes with a restricted clastic composition.

Compared with Craignell arenites these rocks show better sorting, contain more quartz and a very restricted igneous clast assemblage. Metaquartzite and chert fragments are very common. Deposition must have been rapid enough to prevent winnowing of the lutite fraction by bottom currents. Cockburnland has been proposed (Weir, 1974b) as a source of detritus in turbidites further south, in which sedimentary structures indicate ENE. or WSW. transport directions. This landmass must have been composed of metasedimentary rocks (probably Dalradian) intruded by soda granites with an additional but very restricted exposure of ophiolites (ibid). The geochemistry and petrology of Knockeans turbidites are in agreement with these conditions (chapter 2). Statistical analysis of the geochemical data suggests that source areas of the ophiolite and metasedimentary detritus may be widely separated.

In accordance with palaeontological evidence from the Whithorn area (Rust, 1965a) these rocks are placed in the uppermost zones of the Llandovery (Telychian stage). They are the result of continued degradation of Cockburnland to the north, and their increased maturity may indicate that pre-existing Lower Palaeozoic turbidites were uplifted and contributing to the detritus by this time.

#### E. Summary and conclusions

Deposition of the Moffat Shale sequence took place

continuously from the gracilis Zone in the Ordovician to the gregarius Zone (Iwdian, Fig. 22) in the Llandovery. At this time the basal shales were succeeded in south and central parts of the area by turbidites of the Lithic and Basic Facies of the Craignell formation. Further north along the axial rise of the geosyncline sedimentation of Moffat Shales continued probably into the early Fronian (Fig. 22) when they were replaced by Basic Facies greywackes of the Craignell formation in the northwest of the area. To the east and south Lithic Facies greywackes were also gradually replacing those of the Basic Facies in a northwesterly direction. By the end of the Fronian (Fig. 22) owing to depletion of the source of basic igneous (ophiolitic) clasts, the area of deposition of the Basic Facies was greatly reduced.

With continued deposition of the Craignell Formation, turbidites become more mature and are represented by the Silicic Facies. The southern margin of Cockburnland at this time may have encroached into original areas of turbidite deposition, as a result of uplift of newly formed sedimentary rocks. This may be in consequence of back-thrusting of turbidite successions off an oceanic plate at its point of subduction i.e. the top of a Benioff Zone, as envisaged by Mitchell and McKerrow (1975). They propose continual accretion of the southern margin of Cockburnland as a result of this process.

The nature of the boundary between the Craignell and Knockeans Formations is unknown but is probably

transitional. Deposition of the more mature Knockeans sediments probably continued until the end of the Llandovery (Telychian, Fig. 22).

## CHAPTER 4.

## STRUCTURE.

A. Introduction

The area is divided into five structural belts dominated by greywacke and each separated by a major zone of dislocation (Fig. 23). From north to south these are:

- A. Auchinleck - Glenlee belt
- B. Blackcraig - Ironmacannie belt
- C. Cairnsmore - Mossdale belt
- D. Barholm - Drumglass belt
- E. Knockeans - Castramont belt

Major high angle thrusts or reverse strike faults, marking the boundaries of the belts are associated with zones of intense minor faulting. These are referred to as thrust zones (Fig. 23) and consist of Schuppen produced by tectonic slicing of Birkhill and Hartfell shales during thrust movements (Weir, 1974a; Fyfe and Weir, in litt.). These zones decrease in complexity and width successively from north to south and this is attributed to one or both of two factors. Firstly the structural position of the thrust plane will influence the amount and width of the zone of tectonic slicing. It is envisaged, in accordance with Weir (1974a), that the thrust planes become less steep at depth and converge towards the northwest upon a flat lying basal décollement (Fig. 24), whilst in the other direction dips increase until they become reverse faults. It is apparent that larger numbers of Schuppen are associated with shallow thrust planes compared with higher

angle thrusts. As angles of dip on major fault planes increase from north to south (Fig. 24) so the thrust zones diminish in size and complexity. Secondly, the Talnothy and Blairbuias Thrusts may be of greater magnitude than those further south and consequently are associated with larger zones of Schuppenstruktur (Toghill, 1970; Fyfe and Weir, in litt).

The phases of deformation may be summarized thus:

PHASE 1. Caledonian.

F1. Folds with vertical or steeply dipping axial planes, equivalent to F1 of Rust (1965a) and Weir (1968), etc.

F2. Development of major monoclines and tilting of F1 axial planes in the northern part of the area.

F1 and F2 equivalent to F1 and F2 in the Glencuce area (Gordon, 1962).

F2a. Associated with F2, a phase of drag and parasitic folding. May also be associated with strike faulting. Strike faults, high angle thrusts, reverse faults and development of zones of Schuppenstruktur. Translation of thrusts dominantly to the southeast with planes trending between  $055^{\circ}$  and  $070^{\circ}$ .

Axes of F1, F2 and F2a structures are all parallel to the regional strike and constitute the major fold phases.

PHASE 2. Caledonian.

F3. Cross folds with axes plunging to the north and trending  $010^{\circ}$  with vertical axial planes; probably related to wrench faulting. Sinistral and dextral wrench (strike-slip) faults. Sinistral wrench planes trend between  $350^{\circ}$  and  $010^{\circ}$  and dextral wrench planes between

110° and 160°.

Intrusion of granite and reactivation of wrench faults and reorientation of Caledonian structures adjacent to the margin. Mineralization along thrust and wrench fault planes.

PHASE 3. ?Hercynian.

F4. Refolds of F1 structures with flat lying axial planes dipping 10°-15° NW. and trending parallel to the regional strike. Probably equivalent to F4 (Hercynian) of Rust (1965a) and Weir (1968). Movement of the Loch Ken Fault.

PHASE 4. ?Tertiary.

F5. Dextral kink bands trending between 350° and 070°, and maybe equivalent to F5 of Rust (1965a) and Weir (1968).

B. Auchinleck-Glenlee Belt.

A northwesterly facing (F2) monocline (cf. Craig and Walton, 1959; Walton, 1961, 1963, 1965) dominates the structure of this belt (Figs. 23-27, maps 1-4). The ground between Penkiln Burn (24405693) and Craignell (25105752) is occupied by the (F1) folded, steeply dipping, inverted limb and the rest of the belt to the east by northwesterly dipping strata belonging to the upper limb. The axis of the monocline apparently dips at a shallow angle to the northeast, as in the Rhinns of Galloway (Kelling and Welsh, 1970).

This major structure is superimposed upon smaller (F1) folds with reorientated flat lying axes, in the inverted belt between Penkiln Burn and Craignell. In the west a number of these are developed adjacent to the upper

boundary fault of the Talnothy thrust zone. Axes trend  $070^{\circ}$  and planes dip  $15^{\circ}$  SE. Folds of comparable form also occur in exposures along the Pulnee Burn (24555720). Further east on Craignell folds of this type have a larger wavelength with axes trending between  $055^{\circ}$  and  $075^{\circ}$ . Dilatation of the country rocks as a result of intrusion of the granite has produced more northerly trending structures in this area (Fig. 32).

In the region of Clatteringshaws (25525764, maps 3 and 4) a later phase (F3) of deformation modifies F1 and F2 structures. The Talnothy thrust zone and greywackes of this belt are warped by an apparent dextral movement (Figs. 23 and 27). In consequence a northerly plunging anticlinal and synclinal double fold has been formed with axes trending  $015^{\circ}$ . It is impossible to determine how much the orientation of these flexures depends upon the original monoclinical structure. Poor exposure coupled with the fact that the Talnothy thrust zone is cut by the granite at this locality make it difficult to determine whether this structure is simply the result of drag on a major dextral fault plane, such as the Loch Ken Fault, described below. Certainly folds of this style and orientation are unknown in the surrounding areas.

Dextral kink bands with a trend of  $070^{\circ}$  are common to the east between Glenlee (26105802) and New Galloway (grid square 263, 577). These are the result of a late minor (F5) phase of deformation.

Wrench or strike-slip faulting occurs extensively across the belt and is recognised where it displaces axes



of minor folds and thick shale horizons. Sinistral wrenches trend a few degrees either side of north whereas the infrequent dextral wrench has a more westerly trend. Dilatation of the country rocks during intrusion of the granite and post-consolidation stress in the country rocks has produced a predominance of sinistral wrenches in the area to the northwest of the pluton (Fig. 32). Joints, gash veins and foliation within the granite are indicative of intrusion under the influence of a NW.-SE. directed stress system (Parslow, 1964, 1970).

Exposures in the ravine of the River Cree (24065667) north of Newton Stewart contain red and purple oxidized greywackes. This may be the result of deep weathering during the Permo-Triassic, facilitated by local faulting (cf. Mykura, 1960). Similarly altered greywackes occur in the eastern part of the area along the line of a proposed major dislocation, the Loch Ken Fault, described below (Fig. 23).

### C. Talnotry Thrust Zone

Rocks of the Craignell Formation in the Auchinleck-Glenlee Belt have been thrust into their present position by a series of faults constituting the Talnotry thrust zone (Fig. 23, maps 1-4). This belt of Schuppen is exposed to the south of the Auchinleck-Glenlee belt, between Newton Stewart (24105660) in the southwest and the Water of Ken (grid square 263, 579) in the northeast. Its outcrop width varies between 600 and 1400 metres, and subdivision into distinct areas based on structural style is undertaken:

- (i) Newton Stewart to Loch of the Lowes

- (ii) Loch of the Lowes to Clatteringshaws Loch
- (iii) Knocknairling Burn to Water of Ken.

(i) Newton Stewart to Loch of the Lowes

The greatest development of the Talnostry thrust zone occurs to the east between Newton Stewart and Loch of the Lowes (24685705, maps 1 and 2). Penkiln Burn cuts diagonally across the zone from Hawk Hill (24305687) to Minnigaff Church (24105666) and provides a section of discontinuous exposure (table 5). However poorer exposure between Craigdistant Hill (24575688) and Penkiln Burn makes geological boundaries in this area somewhat conjectural (map 1).

North of Minnigaff (grid squares 241, 566 and 241, 567) Schuppen contain interbedded grey and black mudstones of Upper Birkhill lithology which lie conformably below turbidites of the Basic Facies of the Craignell Formation. Within the greywackes minor drag folds have developed adjacent and to the north of strike faults bounding the Schuppen, and indicate translation of thrusts to the south-east. Schuppen traversing the zone from the upper boundary thrust along Penkiln Burn to Craigdistant Hill and Loch of the Lowes display the largest development of black mudstones in juxtaposition with Craignell greywackes.

New road cuttings alongside the Newton Stewart - New Galloway road contain exposures of structures associated with the major basal thrust, the Talnostry Thrust itself. Quartz-filled tension gashes in greywacke below this fault are considered to have formed in response to rotational

strain during thrusting, and are exposed in a roadside quarry on Craigdistant Hill (locality 672, 24515682). High angle reverse faults in a succession of greywackes and shales below the Talnothy Thrust, northeast of Craigdistant (locality 840, plate 7A, 24625690), are parallel or at an angle to the bedding. Fault-bounded segments of greywacke and black shales associated with the basal thrust are exposed a few hundred metres to the northeast (locality 867, 24645693, plate 7B). This latter locality demonstrates the difficulties in working out the complete structure when exposure is limited.

Exposures disclosing the type of faulting within the thrust zone are restricted. A band of black mudstones of Birkhill lithology cutting across the summit of Craigdistant Hill, is thrust over Craignell greywacke (locality 841, 24595690, Fig. 30B). Translation of the mudstones is towards the southeast and it is envisaged that many of the strike faults in the thrust zones are of this type. Higher angle faults, such as that cutting mudstones at the locality above, also contribute to the formation of Schuppenstruktur.

(ii) Loch of the Lowes to Clatteringshaws Loch.

The complexity of the Talnothy thrust zone appears to decrease in a northeastward direction. Between Loch of the Lowes and Black Loch (24975728, maps 2 and 3) it is composed essentially of three Schuppen. The central Schuppe consists mainly of black mudstone, but faulted wedges of greywacke representing subsidiary Schuppen are exposed in the bed of Grey Mare's Tail Burn, Talnothy

(24925726). This stream cuts across the thrust zone normal to the strike and provides a traverse of exposures (table 6). At the upper waterfall (locality 874, 24915737) black mudstones of Lower Hartfell type are thrust over one of these small Schuppe of greywacke (plate 8B). Along the thrust plane, which dips approximately  $40^{\circ}$ NW, is a complex zone of faulting, crushing and contortion of mudstones. All surfaces are slickensided and give a direction of movement at right angles to the strike. Thrusts in Craignell greywacke below the Talnothy Thrust are exposed adjacent to the lower waterfall, on the Grey Mare's Tail Burn (24785707, plate 8A).

Road cuttings at the side of the Newton Stewart-New Galloway road again contain exposures associated with the major basal, or Talnothy Thrust. Black and grey shales of Lower Hartfell lithology are highly crushed and contain sheared black shale bands (locality 868, 24785707, plates 5B and 6B). Adjacent to the thrust plane grey shales are contorted and the footwall greywackes fractured and sliced into wedges (locality 872, 24845713, plates 5A and 6A). All these exposures are on the northern side of the road; to the south Craignell greywackes of the Blackcraig-Ironmacannie belt appear relatively unaffected. It can be concluded from lack of exposure of the thrust plane on the hillside to the south of locality 872, that the angle of dip of the thrust is greater than  $15^{\circ}$ NW.

Topography in this area is controlled by the

strike faulting. The Newton Stewart-New Galloway road follows a well defined valley, ledge or break in slope determined by the position of the Talnotry Thrust between Craigdistant Hill and Talnotry (24885717). The faults at the base of the northwesterly or upper Schuppe occur at the base of crags between Well Burn of Talnotry (24755723) and Black Loch, along which the Old Edinburgh Road was driven. Erosion has taken place easily along fault breccia zones and undercut hanging wall rocks to produce valleys parallel to the strike with southeastward facing scarps.

Between Black Loch and Clatteringshaws Loch the thrust zone outcrop narrows to 500m and consists completely of dark grey mudstones. Consequently it is impossible to determine whether numerous Schuppen exist, although it is probable that any faults in this area are of low magnitude. A median thrust is exposed in the upper reaches of Pulran Burn (25205747) and eastwards is offset by a sinistral wrench, but it continues towards Clatteringshaws Loch, marked by a low line of southeastward facing crags.

A characteristic of the thrusts in the whole area of study is that they generally carry a sparse base metal mineralization. Contorted grey-black shales of Birkhill lithology associated with the median thrust described above and exposed in a new quarry near Clatteringshaws Loch (locality 521, 25375757), are veined with quartz containing small amounts of galena, pyrrhotite and chalcopyrite. A number of levels, shafts and spoil tips associated with former trials for lead ore are located along the line of the thrust running along the base of the crags between Black Loch and Craighandle (24775714) further west.

Numerous wrench faults cut across the thrust zone in this area, the characteristics of which were described with reference to the greywacke belt to the north (see above).

As a result of (F3) folding (see above) or faulting the thrust zone is cut by the granite in the region of Clatteringshaws and is absent eastwards for 6 km.

(iii) Knocknairling Burn to Water of Ken

Further simplification of style is evident on the reappearance of the Talnoiry thrust zone between Peal Hill and Knocknairling Burn (26135767, map 4). A single Schuppe containing hornfelsed Craignell turbidites is bounded by narrower Schuppe containing grey and black mudstones. These are cut by a number of wrench faults but terminate in the vicinity of the Water of Ken as a result of dextral translation by the Loch Ken Fault (see below).

The reduction in complexity of the thrust zone may be the result of a number of factors. If the major boundary thrusts have a high angle of dip the zone will be reduced in apparent thickness and probably will contain fewer Schuppen. A change in angle of dip of the fault planes may be explained by a slight tilt to the northeast reflecting that of the monocline to the north. As the thrusts probably become reverse faults at higher structural levels (see above), this tilt will promote an increase in dip on the thrust planes to the northeast (Fig. 27A). It is also possible, although the author feels less likely, that the intensity of thrusting decreases in a north-

easterly direction.

D. Blackcraig-Ironmacannic Belt.

For descriptive purposes this belt of Craignell greywackes may be conveniently divided into two areas separated by the granite intrusion (Figs. 1, 23 and maps 1, 4, 5).

The area to the west of the pluton consists of a monotonous series of northwesterly dipping and younging turbidites. Dip varies between  $30^{\circ}$  and  $60^{\circ}$  and may be attributed to low amplitude (F2a) flexures with wavelengths of a few metres and fold axes trending parallel to the regional strike. Dilatation of the country rocks in response to forceful intrusion of the granite manifests itself in reorientation of rocks close to the contact (Fig. 32).

Owing to a lack of distinctive lithologies and major folds, faults are difficult to locate. The mineral vein at Dallash (24715693) is associated with a fault trending approximately  $130^{\circ}$  and dipping at a high angle to the southeast. It has a similar orientation to dextral wrenches in the locality but structures confirming translation are absent. The N-S mineral vein at Bargaly and the barren quartz vein 200 m to the east (24675682) are undoubtedly emplaced along sinistral wrench faults associated with a major sinistral wrench fault system dislocating both the Taluotry and Blairbuies thrust belts and running approximately N-S. along Bargaly Glen (Fig. 23), designated as the Bargaly Fault.

Dextral (F5) kink bands are the only other structures observed, and they occur especially in the vicinity of Craignine Hill (24535674) trending between  $010^{\circ}$  and  $015^{\circ}$ .

In areas to the east of the pluton greywackes of this belt maintain their northwesterly dip. Strata adjacent to the granite have strike directions parallel to the contact and are vertical, or dip at a high angle away from the pluton.

#### E. Loch Ken Fault.

The area of low ground in the east of the region occupied by the Water of Ken, the northern part of Loch Ken (26505740), Mossdale Loch (26565710) and Woodhall Loch (26705675) is probably the result of preferential erosion along a major fault zone (Figs. 1, 23; maps 4-6). This has been deduced from indirect evidence such as the presence of exposures of red and purple oxidized greywackes. Deeper than normal oxidation of rocks will have been facilitated by the fracture zone (cf. Mykura, 1960) during Permian-Triassic times when the Southern Uplands was part of a continental massif. The occurrence of sandstone basins of Permian-Triassic age in the Annan and Nith Valleys and in the low ground between Loch Ryan and Luce Bay endorse this concept.

Displacement by the fault can be determined by correlation of the shale horizons in the western block with those further east (Figs. 1, 23). Moffat shales in Schluppen of the Talnoy thrust zone are correlated with those at Barlay (26885779), the Blairbuice thrust zone



with shales at Barend (26955730) and the Culcronchie Thrust with the Hensol inlier (26785699). The apparent horizontal dextral throw varies from 3500-4000 metres around New Galloway to 1500 m in the south near Mossdale (26625705). Continued southerly decrease in displacement is indicated by a lack of dislocation of the Tibble thrust zone between Castramont Burn (26005623) and Laurieston (26825648, fig. 1).

A comparable fault bounding the Stranraer New Red Sandstone basin is described as having a westward downthrow of 1525-1708 m, following a pre-existing Caledonoid dextral wrench orientation (Kelling and Welsh, 1970). Unlike Ordovician rocks of the Loch Ryan area, Craignell greywackes to the east of this region are devoid of distinctive marker horizons and structures which could be used to ascertain whether displacement is vertical, horizontal or a combination of both.

The trend of the fault follows neither of the Caledonian wrench sets although the pluton has probably played an important role in its location and orientation. Geophysical evidence suggests that the contact of the Fleet pluton adjacent to Loch Ken is very steep and may be fault controlled (Parslow and Randall, 1973).

Greywacke beds within the fault zone generally have reorientated strike directions as a result of drag along the fault plane (map 5). They tend to be variable but mostly dip to the east, which might endorse a downthrow in this direction anticipated from the displacement of the

northwestward dipping thrust zones. However it is possible to obtain eastward dipping beds by drag resulting from a purely horizontal translation of a northwestward dipping sequence. With present information the relative displacement cannot be resolved.

#### F. Blairbuies Thrust Zone.

The granite intrusion splits the Blairbuies thrust zone into two areas and each will be described separately (Fig. 23; maps 1, 5, 9).

##### (i) Blackcraig to Blairbuies Hill

The structural style of the Blairbuies thrust zone between Blackcraig (24425674) and Blairbuies Hill (24805675) is quite different to that of the Talnostry thrust zone immediately northwest (map 1). Faults bounding Schuppen appear to be parallel rather than inclined to the major boundary thrusts and exposures of grey mudstone are vastly subordinate to black mudstones. Differences in orientation of minor faults may be due to a slightly differing direction of translation, or to exposure of a different structural level. Certainly the structure of the Blairbuies thrust zone has a greater affinity with the northeasterly parts of the Talnostry thrust zone around New Galloway. This endorses the concept of increasing structural level of thrust planes towards the south, proposed previously (chapter 4, A). The effect of reorientation of structures by the granite intrusion is spectacularly displayed to the northwest of Blairbuies Hill where a band of black mudstone above the upper boundary thrust trends nearly north-south

(map 1).

The structure of this area of the thrust zone may be somewhat idealized, being based on exposures alongside a new forestry road cut into the western flank of the Cairnsmore of Fleet (table 7), and otherwise from rather limited exposure on the rest of the hillside. Many of the black shale bands form southeastward facing scarps resulting from increased resistance to erosion due to thermal metamorphism and undercutting along fractured thrust planes. At one point on Blairbuies Burn (24785669) the stream runs along the upper boundary thrust plane for a distance of 100 m before breaking through the black shale ridge and flowing onto the conformably overlying Craignell greywackes to the north.

Intensive quartz veining and silicification are characteristic of rocks adjacent to thrusts. In some instances this may be due to silica-rich solutions percolating along fracture zones during intrusion of the granite. On Blairbuies Hill minor chalcopyrite mineralization occurs in colourless and yellow Fe-stained quartz veins along the base of a black mudstone unit displaying minor faulting and puckered lamination (locality 562, 24795678, Fig. 28A). There is ample evidence of crushing and silicification in the vicinity; the latter is local and extends only 2 m above the thrust plane. To the east a scree contains fragments of brecciated, black, silicified mudstone cemented by smokey and pink quartz producing an open vuggy structure. Slickensides on black mudstone of the

main outcrop dip  $30^{\circ}$ W. and trend  $095^{\circ}$  on surfaces that dip  $40^{\circ}$ W. and strike  $150^{\circ}$ , owing to reorientation by intrusion of the granite. These could have been produced either by thrusting or later reorientation of the beds, although data presented later (see below) support the latter process.

Tracing this band southwards, further structures of the types described above are exposed and also a thin microgranite vein trending parallel to the strike of the black mudstones (locality 565, 24805672). Planes of brecciation dip  $20^{\circ}$ W. and strike  $047^{\circ}$  and slickensides dip  $20^{\circ}$ W. and trend  $110^{\circ}$ . Further south towards the base of the mudstones slickensides trend at an angle of  $70^{\circ}$  to the strike of planes in non-reorientated mudstones (locality 602, 24875660). Consistency in the latter two angles suggests that they were formed as a result of thrusting with a true translation of about  $110^{\circ}$  to  $120^{\circ}$  i.e. south-eastwards. The different angle obtained at locality 562 (above) is probably due to interplanar movements during reorientation. Low amplitude flexures in the bedding of black mudstones at locality 602 (above) have axes normal to the strike and are also the result of lateral movements during emplacement of the pluton.

The complete thrust zone is cut by the Bargaly Fault (see above) which has a sinistral displacement in this region of about 750 m. Further exposures of Moffat Shales associated with the thrusts occur in the southeast between Palnure (24555635) and Blackcraig (map 9).

A description of the detailed section alongside the new forestry road on the western flank of the Cairns-

more of Fleet is provided in table 7. Much of this additional information has been omitted from map 1 for the sake of clarity and because of its two dimensional nature.

(ii) Stroan Loch to Bennan Hill

A reduction in size and complexity comparable with that of the Talnothy thrust zone is apparent on the reappearance of the Blairbuies thrust zone at the eastern margin of the granite (map 5). The number of exposed Schuppen has reduced from over twenty to less than ten, and there are only four bands of black mudstone. The trend of greywacke and shale bedding and strike fault planes have been reorientated to a more southerly direction, as a result of dilatation during granite intrusion.

Black mudstones exposed at the side of a forestry road on Bennan Hill (locality 1039, 26495729) are fused to the granite at the contact and contain pyrite and chalcopryrite. Veins of granite, previously described by Hall (1815), have invaded the country rocks in this vicinity, probably along lines of weakness produced by strike faulting.

Further east along the line of Loch Ken and Mossdale Loch the thrust Zone is cut by the Loch Ken Fault. Exposures of black mudstone do not occur between these lochs, however this may be an effect of poor exposure (map 5). Nevertheless, extensive exposures of Moffat Shale in inliers at Barend, to the west of Loch Ken, are correlated with those of this thrust zone.

G. Cairnsmore-Mosssdale Belt.

To the west of the pluton between Bargaly Glen and Crammery Hill (24895647) Craignell turbidites and occasional thin black shales dip and young to the northwest (Figs. 23-25, maps 5, 6, 9). Minor (F2a) flexures cause variations in the dip of bedding and planes of lamination between  $30^{\circ}$  and  $50^{\circ}$ . Strike reorientation is not as apparent as in the belts further north although slight southerly readjustments occur along the southern margin of the belt between Knocktim (24985638) and Craig Hill (25245636).

Mineralization at Cairnsmore (24675635) is undoubtedly associated with the northwestward continuation of the dextral wrench dislocating Moffat Shales north of Blairs Hill (24705628). Veins at Blackcraig probably occur along the same line of fracture (map 9). This fault appears to be unaffected by the Bargaly Fault (see above) or the sinistral wrench east of Blairs Hill, which indicates that the dextral wrench is younger. This is in agreement with Weir's (1968) interpretation of wrench faults between Creetown and Gatehouse of Fleet to the south.

Between Slogarie Hill (26385678) and Mosssdale Loch in the east, greywackes dip away from the pluton, except towards the Blairbuies Thrust where they dip north. Trends have been affected by dilatation during emplacement of the granite and drag on the Loch Ken fault plane.

At two localities in this area minor structures associated with incipient shear have been observed. On

Bennan Hill (locality 1110, 26455686, Fig. 28C) kinked lamination in hornfelsed greywacke is the result of an incipient sinistral wrench fault trending  $002^{\circ}$ . Further east adjacent to the Loch Ken Fault (locality 1098, 26565717, Fig. 28B) a (?F5) kink band in reddened oxidized greywacke trends  $060^{\circ}$  and has been produced by vertical dextral shear.

#### H. Culcronchie Thrust.

Major strike faults to the south of the Blairbuies Thrust have associated zones of Schuppenstruktur or imbrication which are much narrower than those to the north. The Culcronchie Thrust may be traced across country from Blairs Croft (24655618) in the west, to Culcronchie Hill (25145637) where it becomes masked by high grade contact metamorphism (maps 7 and 9). Towards the east at Slogarie (26485687, map 6) dark grey-black mudstones of Birkhill lithology are again exposed along the continuation of the fault.

Between Blairs Croft and Culcronchie Mine (25115639) the thrust zone consists of up to three Schuppen containing either greywacke or black mudstone. Near Cuil (24705627) quartz veins in the mudstone have a parallel trend to the strike faults. Further east faulting and puckering of lamination is comparable with that exposed on Blairbuies Hill and is again a result of thrusting (locality 683, 24945634, Fig. 29B). A spectacular mullion is exposed in a small quarry on Knocktim (locality 684, 24975635, Fig. 29A), and has developed in response to thrusting rolling the incompetent black mudstones over a competent, rigid

600 mm thick band of greywacke. The trend of the axis of this mullion is  $095^{\circ}$ , which will be normal to the direction of translation of the thrust, estimated at  $185^{\circ}$ . A more southerly direction is obtained compared to that deduced for the Blairbuies Thrust (above) due to reorientation by the granite.

At Culcronchie Mine the black mudstone horizons are attenuated and represented by brecciation zones of silicified mudstone, between Schuppen containing hornfelsed greywacke. Three of these zones are exposed in the bed of Culcronchie Burn (locality 085, 25115639, plate 9A).

Fragments in the breccia are cemented together by yellow-brown, Fe-stained quartz containing sphalerite, galena and chaloopyrite, and comparable to the breccia on Blairbuies Hill (see above). Each zone is separated by a five metre width of greywacke hornfels. Mineralization associated with the northern and southern zones has been worked open-cast, whereas a level has been driven a short distance along the central zone, and is now occupied by the stream.

Two bands of Moffat Shales at Slogarie dip to the southeast, in contrast to most of the others in the area. They pass upwards conformably on their southern margin into turbidites of the Craignell Formation (locality 1119, 26525689). Greywacke between the bands of mudstone is intensively quartz veined as a result of faulting. The Culcronchie Thrust is probably a high angle reverse fault in this region, with a downthrow to the northwest. Lack of exposure will hamper any further investigation into the true nature of the faulting.



In the west between Muirfad Flow (24655620) and Blairs Hill, Schuppen are dislocated by a N.-S. trending sinistral wrench fault. Further west at the limit of exposures, in a disused railway cutting near Blairs Croft, the strike of black mudstones and greywackes has been pulled round to a more southerly direction. This is probably the result of drag along a large sinistral wrench fault plane immediately to the west, which may be a continuation of the Bargaly fault (see above). Further evidence of faulting is restricted to dislocation of the thrust zone by the Loch Ken Fault in the east.

#### I. Barholm-Drumglass Belt.

The western part of this belt is divided into northern and southern areas separated by the Pool Ness Thrust (Fig. 23). Evidence of the fault has not been detected further east and it is therefore envisaged as being of a lower magnitude than the other thrusts of the area (maps 6, 7 and 9).

In the region to the north of the Pool Ness Thrust between Blairs Hill and Moneypool Burn (24905602) exposure is extremely limited owing to a thick peat cover. Information from the few exposures that do exist suggests that the greywackes dip constantly between  $20^{\circ}$  and  $40^{\circ}$  NW. Two kilometres further east between Craig Hill and Moneypool Burn a number of upright (F1) folds with axes trending E.-W. have developed. The granite intrusion is again responsible for these trends. This belt of folds dies out towards the east and is replaced by a sequence of south-

eastward-dipping and younging Craignell greywackes, beyond the Big Water of Fleet (25555635).

Minor structures are represented by asymmetrical (F2a) parasitic folds on northwestward dipping surfaces, and (F5) kink bands trending at approximately  $010^{\circ}$ . Axes of minor folds are parallel to the regional strike and wavelengths are of the order of 0.5 m.

In the west of areas to the south of the Pool Ness Thrust poor exposure is again encountered, but greywackes appear to dip between  $30^{\circ}$  and  $40^{\circ}$  NW. In a comparable fashion to the northern area (above), a belt of upright (F1) folds occurs further east. Between Meikle Bennan (25475613) and Little Water of Fleet (25805630) the greywackes dip steeply southeastwards and are generally inverted. East of this region a further belt of upright or slightly overturned (F1) folds occurs and is well exposed alongside a new forestry road on Shiel Rig (25935628). Axial planes of these folds are vertical or dip at a high angle to the southeast and axes plunge at a few degrees northeast.

Craignell greywackes are folded into a large (F1) syncline in the area between White Top of Culreoch (26015634) and Derrygown Burn (26235623, map 6). This has been refolded by (F4) movements producing small folds with axial planes dipping at a shallow angle to the northwest. One of these folds is traced as far as Lochenbreck Loch (26435656) and marks a major change in the attitude of the bedding, (fig 30A).

Small low amplitude (F2a) flexures in the bedding on Pibble Hill (locality 629, 25265612, plate 9B) have fold axes trending  $070^{\circ}$  and plunging  $5^{\circ}$  NE.

A series of faults have also been recognised on the northern flank of Pibble Hill (25355607), where they cut black mudstone bands associated with the Pool Ness and Pibble Thrusts. Dextral wrenches are predominant as a result of dilatation during intrusion of the granite (Fig. 32). They trend between  $120^{\circ}$  and  $155^{\circ}$  and occasionally carry mineral veins, e.g. Pibble and Pibble Gulch Veins.

#### J. Pool Ness Thrust

Exposures of Schuppen and other structures associated with the Pool Ness Thrust stretch eastwards from Culcronchie Burn (25065613) to Shiel Rig (25925636). The outcrop width of the zone of faulting never exceeds 400 m and is commonly about 150 m (Fig. 23, maps 6 and 7). On the northern flank of Pibble Hill three Schuppen of black mudstone and two of greywacke are exposed. Dips of lamination in the shales are variable in direction and often steep. High angle reverse faults probably separate the Schuppen and may have been affected by (F4) fold movements. Asymmetric parasitic (F2a) drag folds occur on some of the northwestward dipping black mudstone bedding planes. Axial planes in these dip towards the northwest and the folds were probably formed as a result of southeastward translation along fault planes.

At Pool Ness, on the Big Water of Fleet (locality 1169, 25665623, plates 10A-B, 11A-B), strike faults marking the eastward continuation of the thrust zone are

exposed in the river bed. Greywacke and shales dip at a high angle and young to the southeast. A vertical strike fault at the northern end of the ravine (plates 10A, 11B), separates Craignell greywackes from crushed and contorted grey-black laminated mudstones of Birkhill lithology. To the south these mudstones, which are cut by numerous quartz veins, pass conformably into Craignell turbidites (plates 10B, 11A). A second fault a few metres further south separates the greywackes from extensive outcrops of black shale downstream (plates 10A, 11A). The curved southeastward dipping fault plane is again cut by quartz veins and is parallel to pressure induced jointing in greywackes on the footwall. It is impossible to determine the direction of translation of the faulted blocks from these exposures.

Levels driven into the hillside between Pool Ness and Upper Rusko Cottage (25655623) are old lead workings (Wilson, 1921, p. 55), and have probably been opened up along veins associated with the faulted southern boundary of the thrust zone. These appear to be of the nature of a trial and are comparable with workings along the Talnoy thrust zone (above).

Further east on Knock Derry (grid squares 258, 563; 259, 563) two bands of grey-black mudstone are exposed alongside a new forestry road. The northern contact with greywacke is veined with quartz and is undoubtedly faulted and the southern contact is crushed and brecciated. Between the black mudstones is a band of greywacke, but the nature of its contacts cannot be determined.

At the western end of exposures of the thrust zone, in a disused railway cutting near Culcronchie Cottage (locality 839, 25145615), the faulted southerly contact of a Schuppe of black mudstone is exposed. Lamination in the mudstone dips  $40^{\circ}\text{S}$  and strikes  $047^{\circ}$  and the fault plane dips  $80^{\circ}\text{N}$  and strikes  $067^{\circ}$ . Along the fault plane mudstones are crushed against greywacke and the southward dip probably represents drag due to high angle reverse faulting. On the northern margin of the Schuppe black shales dip  $70^{\circ}\text{N}$  and are again in faulted contact with greywacke.

#### K. Pibble Thrust

Exposures of black mudstone along the outcrop of the Pibble Thrust extend from Creetown to the Nick of Trestran (25435610), between Pibble Hill and Meikle Bennan. Here the thrust is displaced by two dextral wrench faults and thrown south into an area not covered in this survey. A black mudstone inlier exposed in Castramont Cleugh, (grid square 259,561) also not studied in this work, is probably associated with the eastward continuation of the fault (Figs. 1, 23; maps 6-8).

At Creetown northwestward dipping Moffat Shales, converted to graphitic phyllites by low grade regional metamorphism, crop out in the north face of a ravine cut by the Balloch Burn (24675586). At the base of the exposure, the stream undercuts a cliff along the quartz veined shatter zone of a high angle thrust plane, dipping  $45^{\circ}\text{NW}$ . Greywackes of the Knockeans Formation below this are in a

highly crushed state. A few metres upstream exposures of Moffat Shales abruptly disappear, owing to northward displacement by a sinistral wrench. Further east they are encountered again in the bed of the Balloch Burn (24965595) where they dip  $60^{\circ}\text{N}$  compared with  $30^{\circ}\text{NW}$  near Creetown. A continuation of this trend of increasing dip is observed in exposures on the western flank of Pibble Hill (25225600) and probably reflects an increase in dip of the thrust plane.

Moffat Shales on Pibble Hill are separated from those above by sinistral and dextral wrench faults, the latter is the locus of the major Pibble mineral vein. Dark grey-black mudstones in the vicinity of the old mine workings dip to the south and are probably inverted. Near the southern contact of the mudstone outcrop (locality 637, 25295605, Fig. 30C), a series of thrusts separate crushed greywacke from contorted black mudstone and drag folded greywacke, the latter indicating a southeastward translation. Below the sole thrust a level has been driven a short distance along the fracture zone, following the sparse mineralization that is invariably associated with these structures. The eastward increase in dip of black mudstones and phyllites between Creetown and Pibble Hill probably reflects a curving strike fault plane with a shallow plunge to the northeast, in accordance with axial plunges of local minor structures. This concept also compares favourably with the structure of the Talnotry, Blairbuies and Pool Ness Thrusts (Fig. 27A).

The thrust continues further east towards

Laurieston and is traced by small inliers of Moffat Shales. At the head of Castramont Burn dark grey-black shales are faulted between crushed and quartz veined greywackes (locality 1129, 26105633). Other exposures have not been investigated.

#### L. Knockeans-Castramont Belt

The Pibble Thrust separates greywackes of the Craignell Formation from those of the Knockeans Formation to the south (Fig. 1).

To the west between Balloch Burn and Kirkbride Burn (24935565), Knockeans turbidites dip to the northwest at an average angle of  $45^{\circ}$ , small (F2a) flexures accounting for some fluctuations. Further east towards the Nick of Trestran upright (F1) folds occur (cf. Barholm-Drumglass Belt, above) their axes trend NE and plunge at a shallow angle in this direction (maps 7, 8). At the head of Castramont Burn greywackes of this belt are inverted and dip steeply southeast (26135624).

#### M. Conclusions

Crustal segmentation comparable with that proposed by Weir (1974a) is the dominant structure of the area. Six belts of greywacke and shale are separated by strike faults of considerable magnitude (Figs. 23-25, 31). The planes of these high angle thrusts or reverse faults are nearly vertical or dip at various angles to the northwest. It is envisaged that they become less steep with depth towards the northwest and probably converge with a basal décollement (Weir, 1974a). The incompetent Moffat Shales are

interpreted as the locus of movements on this décollement, being situated between relatively rigid basement rocks of unknown nature, possibly Lewisian (Powell, 1970, 1972), and overlying greywackes of Llandovery-Wenlock age.

Southeastward translation of the belts of greywacke as a result of NNW.-SSE. compression, must have taken place during the Wenlock or Ludlow, and probably at the Caledonian climax in late Silurian (Weir, in prep.). The thrusts are interpreted by Weir (*ibid*) as being the result of crustal shortening due to the southeastward movement of Eocaledonia (Precambrian and Dalradian successions to the northwest of the Highland Boundary fault) against a stabilized cratonic block, formed from the Lower Palaeozoic successions of England and Wales. However Mitchell and McKerrow (1975) suggest their formation is related to subduction of oceanic crust beneath the Southern Uplands throughout the Late Ordovician and Silurian, and scraping of flysch successions off the oceanic plate. Age differences among the thrusts around the Cairnmore of Fleet granite cannot be detected at present, although significant differences are unlikely to exist as they are contained within an area representing a small fraction of the total width of the Southern Uplands.

The pre-thrust structure of the area of study is dominated by the limb between two northwesterly facing and descending (F2) monoclinial folds (cf. Craig and Walton, 1959). To the south this is buckled by tighter (F1) folding of lesser magnitude (Fig. 31). Following the main (F1 & F2) fold phase the monoclines are segmented by thrusts



and reverse strike faults, and subsequently sinistral and dextral wrenches, associated with a (?F3) fold phase. Emplacement of the Fleet pluton at  $390 \pm 6$  my (Brown et al., 1968) gives all these structures a Caledonian age. Later phases of folding (F4 & F5) are of minor importance and may be associated with Hercynian or Tertiary movements. The Loch Ken fault cannot be dated accurately, but is also probably Hercynian.

CHAPTER 5  
METAMORPHISM.

A. Introduction

A systematic survey of the thermal metamorphic envelope surrounding the Cairnsmore of Fleet granite has not been attempted previously, although certain features have been alluded to in a number of works. James Hall (1815) described the nature of granitic sheets intruded along bedding planes or joints in "killas" (greywacke) between the granite contact and Loch Ken (see 4F (ii) above). Mineralogical and textural changes in rocks of the contact zone were ascribed to the action of heat. Later research was also concentrated upon this area. Allport and Bonney (1889) described the effects of thermal metamorphism in a series of 'silty clays and greywackes' and proposed that differences in mineralogy were due to original lithological differences. Research by Gardiner (1890) was centred upon exposures of black mudstone and greywacke on Peal Hill (26135764), west of New Galloway. As the contact of the pluton is approached these rocks are progressively transformed into 'chiastolite and garnet-sillimanite schists'. Teall (in Peach and Horne, 1899, p. 632) gives a general account of the rocks and minerals present in the metamorphic aureoles of all the major intrusions in the Southern Uplands, based upon collections made by the Geological Survey.

Later research was extended to cover the whole of the Cairnsmore of Fleet aureole. Gardiner and Reynolds (1937) described the dominant rock type as 'quartz-biotite

schist and hornfels' with subordinate 'andalusite schist and cordierite hornfels'. The outer boundary of the aureole was mapped by Parslow (1964, 1968) on the first appearance of biotite in hand specimen, and the presence of minerals such as amphibole, andalusite, cordierite and garnet in the hornfels was attributed to original differences in lithology, rather than metamorphic grade.

In the present work the limit of the aureole, as defined above, has been remapped and continued into areas in the southwest not covered by Parslow (*ibid*). Samples of country rock collected from localities at or near National Grid intersections (Fig. 2) have been investigated in thin section to determine major mineral parageneses and subsequently metamorphic facies. Owing to the increased sensitivity of this method the outer limit of thermal metamorphic effects is further from the pluton than that defined in the field (Fig. 33).

Thermal metamorphic mineral transformations have been superimposed upon rocks approaching or within the muscovite-chlorite subfacies of the greenschist facies of regional metamorphism (Weir, 1974b). New minerals are generally produced, especially at low grades, by reactions between argillaceous components of greywackes and shales. Consequently susceptibility to transformation depends largely on the lutite content of the various sedimentary rocks. Three broad zones containing different metamorphic mineral assemblages have been detected in the aureole (Fig. 33) and are correlated with facies of contact metamorphism (Winkler, 1967).

- |                            |   |                                |
|----------------------------|---|--------------------------------|
| 1. Biotite-chlorite zone   | / | Albite-epidote hornfels facies |
| 2. Biotite-zone            |   | Hornblende hornfels facies.    |
| 3. Hornblende-biotite zone |   |                                |

Higher grade rocks of K-feldspar-cordierite hornfels facies are found in close proximity to the contact in a few areas. Analysis of  $H_2O^+$  in greywackes gives a measure of the dehydration resulting from contact metamorphism and compares with the observed occurrence of the mineral zones above (Fig. 35).

#### B. Regional metamorphism

Reorganisation of illite into sericite or muscovite and the abundance of chlorite in pelites and pelitic greywacke imply that the 'unaltered' rocks are on the threshold of greenschist facies of regional metamorphism (Müller, 1967). Arenites and argillites a few kilometers to the south are considered to be of the quartz-albite-muscovite-chlorite subfacies (Weir, 1974b). This subfacies has a lower temperature limit in the vicinity of  $300^{\circ}C$  and reactions are catalysed by deformation (Turner and Verhoogen, 1960; Winkler, 1967). Evidence discussed later (chapter 9,C) indicates that the granite crystallized at pressures in excess of 2000 bars, which is equivalent to 7.5 km depth, discounting tectonic and intrusive stress. Taking into consideration a normal geothermal gradient temperatures at this depth are approximately  $225^{\circ}C$ , and a depth of 10 km is required to obtain temperatures approaching  $300^{\circ}C$ . It is more likely however, that the pluton was emplaced at

higher levels and that directionally-operative stress was more important. Weir (1974b) relates greenschist facies metamorphism to pre-thrust (F1) deformation, and it is therefore possible that this took place when the sedimentary succession was at greater depth than when intruded by the granite.

Calcite is a typical constituent of the 'unaltered' greywackes and is observed to disappear at low grades of thermal metamorphism (Fig. 34). For this reason a diagenetic origin is favoured rather than the carbonate metasomatism proposed by Weir (ibid) to be associated with the granite intrusion.

Epidote has been observed in exposures of greywacke adjacent to the Loch Ken fault and its formation may be related to shearing stress (Deer, Howie and Zussman, 1966) induced during displacement.

### C. Contact metamorphism

#### (i) The morphology of the aureole

The shape and extent of the aureole is determined by the shape of the pluton at the surface and the batholith at depth, and the thermal conductivity of the country rocks. The width of the aureole in the northwest and southeast reflects the subsurface expression of the batholith rather than the outcrop of the pluton (Parslow and Randall, 1973; Batraukh, 1975). Batraukh's interpretation based upon gravity surveys shows that rock of granitic composition probably lies at depths of less than 3.5 km around and between the Carsphairn, Doon and Fleet plutons (Fig. 37). This in itself will not account for the very wide aureole

to the southeast of the Fleet pluton (Fig. 33). It is therefore proposed that rock of granodioritic composition (cf. Gardiner and Reynolds, 1932; Blyth, 1955) lies between the upper surface of the granite and the roof of the batholith, and is at very shallow depths beneath the wider parts of the aureole. Its absence from gravity interpretations is a result of the negligible density difference between granodiorite and greywacke. The Fleet granite has probably been forcefully intruded through the roof of the batholith and its granodioritic fringe, which explains the absence of a granodioritic marginal facies (cf. the Loch Doon pluton, Gardiner and Reynolds, 1932) and its steep contacts (e.g. the Clints of Dromore, Blyth, 1954). This concept is discussed further in chapter 11 (below).

(ii) Albite-epidote hornfels facies (chlorite-biotite zone)

The outer limit of this zone is marked by the first appearance of biotite or recrystallized chlorite in thin section (Fig. 33; plate 12A). At higher grades the inner contact with the hornblende hornfels facies is characterized by the disappearance of chlorite. Biotite increases in amount across the zone at the expense of chlorite, white mica (sericite and muscovite), iron oxides, ilmenite and rutile.

In a typical greywacke (73/H 45-67, plate 12A) the original clastic texture remains unaltered. However the pelitic matrix contains recrystallized muscovite, sericite and chlorite, and biotite occurs as a product of reaction between these.

(iii) Hornblende hornfels facies

a. Biotite zone.

Biotite is the dominant metamorphic mineral of rocks in this zone, chlorite and amphibole, which are characteristic of the zones on either side, are absent. Marked variation in outcrop width is the result of factors discussed previously (above); extreme attenuation in the region of Clatteringshaws Loch is probably due to the steep nature of the contact coupled with the absence of the proposed batholith roof at shallow depths (Fig. 33). The biotite zone extends along pelitic bands associated with the Talnoy Thrust in the northwest, as a consequence of their higher thermal conductivity and susceptibility to metamorphism.

Biotite and muscovite or sericite have crystallized in flakes lying parallel to the original bedding lamination in pelites and occasionally shows signs of rucking when an incipient strain-slip cleavage is developed (e.g. 74/H 46-70, plate 12B). A typical greywacke at lower grades contains randomly orientated metamorphic biotite surrounding unaltered detrital quartz clasts. Few original feldspar fragments remain but occasional crystals of zoisite/clinozoisite are the product of hydrothermal alteration of plagioclase or reaction between diagenetic calcite and the aluminosilicate fraction. Consequently calcite is not present in the bulk of the rock but occurs sporadically in narrow (1 mm) veinlets which are probably post-metamorphism in age.

At higher grades (74/H 47-69 plate 13A) hornfelses

have a schistose texture due to alignment of biotite flakes, and the presence of cordierite imparts a purple hue. Original detrital material consists mainly of quartz, quartzite and graphic intergrowths of quartz and K-feldspar. Fragments of chert have been recrystallized into microcrystalline aggregates and cordierite occurs in xenoblastic polycrystalline aggregates packed with inclusions.

Cordierite forms according to the reaction

chlorite + muscovite + quartz  $\rightarrow$  cordierite + biotite + H<sub>2</sub>O  
for which a temperature of about 500°C must be attained at an H<sub>2</sub>O-pressure of 2000 bars (Winkler, 1967).

Pelitic hornfels within 200 m of the contact in the northeast (74/H 59-77, plate 13B) exhibits a texture representative of the highest grade in this zone. Coarsely crystalline biotite and muscovite flakes are aligned and give the rock a slightly schistose or lepidoblastic texture. Long axes of quartz grains also appear to lie parallel to this planar structure. Orientation of metamorphic minerals will be due to crystallization in a stress field produced by forceful intrusion of the pluton, thus giving directional features usually associated with regional metamorphism.

#### b. Hornblende-biotite zone.

Higher grades of metamorphism within the hornblende hornfels facies are characterised by the appearance of amphibole (hornblende or ferroactinolite) in impure arenitic hornfels and garnet (spessartine or almandine) in pelitic hornfels. The hornblende-biotite zone reaches its greatest extent in the southwest and



continues around the rest of the pluton in a narrow band. Its presence along the north and east contacts has not been confirmed but it is probably very local in extent amounting to a zone a few metres in width.

Green and purple/brown banding in hornfels reflects amphibole- and biotite-rich laminae where the mineralogy is controlled by original differences in lithology and geochemistry. Many of the more arenitic rocks possess a randomly orientated hornfelsic texture (plates 14A and B). Crystals of biotite and green amphibole with lengths between 1.0 and 1.5 mm are set in a finer grained, decussate textured groundmass of quartz and embayed feldspar crystals. Larger detrital clasts of quartz and altered feldspar may still occur, the extent to which recrystallization takes place appears to depend upon their size and composition. Xenoblastic sieve textured aggregates of muscovite occur in diffuse patches which impart a pale spotted appearance to many of the hornfelses close to the contact. Cordierite is common and detrital augite remains unaltered in basic group hornfelses (see chapter 2, C) throughout the zone.

Pelitic rocks are characteristically spotted and contain spessartine or almandine garnet (plate 15A). The presence of almandine in thermal aureoles has been attributed by many authors as being the result of specific chemistry, notably the presence of manganese or physical conditions i.e. hydrostatic pressures greater than those normally attending high-level intrusions (Harker, 1939, p. 55). Tilley (1926)

suggests that almandine is more commonly found in 'wet' aureoles and Chinner (1962, p. 317) states that it is a stable phase in the hornblende-hornfels facies. However, Matthes (1961), on experimental evidence, rejects rock compositional interpretations and proposes that almandine-bearing hornfels should be placed in an almandine-hornfels facies, representing the high pressure equivalent of the hornblende hornfels facies. Many of the conditions for the formation of almandine, discussed by the authors above, are satisfied in the Fleet aureole. Almandine, as a metamorphic mineral, is only found in pelitic hornfels which are richer in manganese than more arenitic types (tables 2-4). High confining pressures and hydrous conditions during intrusion of the granite are indicated by the structures and minerals present in both the granite and aureole (see chapters 4, 7 and 9). It is probably the combination of all these conditions that promotes the formation of almandine. Spessartine is fairly common in thermal aureoles (Winkler, 1967) and both garnets occur as euhedral or subhedral porphyroblasts (plate 15A) including large amounts of quartz.

Textures produced in pelitic rocks by crystallization of biotite are lepidoblastic or hornfelsic depending on their proximity to the contact (see above). Large (5 mm x 2 mm) pale xenoblastic ovoid spots contain aggregates of muscovite and quartz.

Two premetamorphic intrusions are affected by metamorphism of hornblende hornfels facies. A diorite sill at Talnotry (24695704, see chapters 10 and 13) occurs at

the boundary between the biotite and hornblende-biotite zones. Spectacular in thin section, it is composed of radiating aggregates of red-brown biotite, green hornblende and pale green to colourless actinolitic amphiboles. Large plagioclase laths are heavily altered and yellow/green epidote occurs probably as a result of hydrothermal alteration, owing to the proximity of a mineral vein (see chapters 13 and 15). Feldspar-quartz boundaries are embayed and intergrown, and much of the quartz appears to be of secondary origin. Needles of apatite up to 2 mm in length are common in plagioclase phenocrysts and aggregates of anhedral sphene crystals are always associated with ferromagnesian minerals.

An intrusion of ultrabasic composition is exposed on Clanery Hill (see chapter 10) within the hornblende-biotite zone (24775629). It is composed almost completely of radiating fibrous aggregates of tremolite (plate 15B). Talc and biotite are also present with subordinate secondary quartz, altered plagioclase and globular sphene.

(iv) K-feldspar-cordierite hornfels facies.

In some rocks immediately adjacent to the contact sillimanite has developed as fine needles in muscovite associated with cordierite, feldspar and quartz (Allport and Bonney, 1889; Gardiner, 1890; Gardiner and Reynolds, 1937). This indicates a sporadic development of the K-feldspar-cordierite hornfels facies which is rarely associated with granitic intrusions, because its lower temperature limit at 2000 bars pressure is  $640 \pm 20^{\circ}\text{C}$  (Winkler, 1967). It has been discussed earlier (above)

that crystallization of the granite probably took place at confining pressures greater than 2000 bars and that the ambient temperatures at an equivalent depth (7.5 km) will be about 225°C (Parslow, 1964, 1971; see section B above). A temperature of intrusion of about 700°C may be assumed and the temperature rise in the country rock in the immediate contact area will be 60% of this figure (Jaeger, 1957). When added to the background temperature a value of approximately 650°C is obtained, which, taking into account the size of the pluton and the possibility of an increased temperature gradient owing to the presence of a large batholith below, would have been maintained for a considerable length of time. All indications point therefore to the possibility of K-feldspar-cordierite-hornfels facies developing in the immediate vicinity of the contact especially in areas where the proposed batholith is not far below (e.g. Peal Hill 26135764; Gardiner, 1890; map 4, section A-B).

(v) Hydrothermal alteration.

The occurrence of numerous mineral veins (Part 3) around the western half of the pluton are the result of a syn- or post-magmatic hydrothermal event. Areas of hornfels containing clinozoisite/zoisite (Fig. 34, plate 16A) may have been altered by events such as these or by 'wet' thermal metamorphism and consequent breakdown (saussuritization) of calcic plagioclase (Deer, Howie and Zussman, 1966, p. 62). Clinozoisite is however developed almost exclusively in rocks of the biotite zone and is therefore probably related to reactions taking place during thermal

metamorphism of low grade hornblende hornfels facies.

Further evidence of mineralogical breakdown by hydrothermal solutions is afforded by hornfels containing uralite (a indeterminate brown amphibole) in a localised area to the south-west of the pluton (74/H 50-60, plate 16B, 25005598, Fig. 34). The formation of this fibrous amphibole is ascribed to alteration of ferromagnesian, notably pyroxenes (Deer, Howie and Zussman, 1966, p. 174).

This localised area is coincidental with a larger area of hornfels containing clinozoisite and calcite, in the southwestern part of the aureole (Fig. 34). Calcite, which usually disappears during the lower grades of contact metamorphism is probably post-metamorphic in origin. This area of alteration and deposition of secondary calcite straddles the main localities of hydrothermal vein mineralization, i.e. Blackcraig-Cairnsmore and Pibble (see Part 3), and may be related to their formation.

It is possible that two hydrothermal phases have taken place, one associated with the 'wet' thermal metamorphism and the other associated with the hydrothermal vein mineralization. As most of the clinozoisite coexists with biotite which is unaltered it is probable that it is mainly the result of the former process. The calcite occurring in veinlets in biotite hornfels owes its origin to the latter event.

PART 2

THE GRANITE AND MINOR INTRUSIVE ROCKS.

## CHAPTER 6

## INTRODUCTION.

A. History of previous research

The earliest petrographical description of the Cairnsmore of Fleet granite was made by Teall (in Peach and Horne, 1899) who recognised both alkali and oligoclase feldspars, biotite and muscovite. Pringle (1935) briefly referred to the mass, but the first detailed account was provided by Gardiner and Reynolds (1937). They distinguished a marginal biotite granite from a central biotite-muscovite granite, and postulated that each represented a separate phase of intrusion. Detailed research in the vicinity of the Clints of Dromore (25455641) on the southern contact suggested that there was little variation in mineralogy, and that faulting and shearing are common in both granite and hornfels near the margin (Blyth, 1954). The Galloway granites were described by Read (1961) as 'newer Caledonian granites', emplaced by forceful intrusion and consequent elongation parallel to the regional strike of the country rocks.

Parslow (1964, 1968, 1971) has provided the most detailed petrological, geochemical and structural data on the granite to date. He recognised and mapped three main types of granite in the field. A marginal facies of coarse grained biotite granite is described as giving way with gradational boundary to an inner coarse grained biotite-muscovite granite. This is intruded by a younger fine grained biotite-muscovite granite, with sharp contacts in

some areas, but diffuse in others (*ibid*).

Most geochronological studies have indicated an age of emplacement between the Upper Silurian and Lower Devonian. An age of  $386 \pm 8$  my is given by a whole rock K-Ar estimate compared with  $365 \pm 1$  my from a biotite analysed by the Rb-Sr method (Kulp *et al.*, 1960). The marginal facies was given an age of  $390 \pm 6$  my in a later study using the K-Ar method (Brown *et al.*, 1968) which compares very favourably with the previous K-Ar date. It is apparent from these and other ages of emplacement for granites in the Southern Uplands (e.g. Lambert and Mills, 1961) that the biotite estimate (above) is too young.

More recent research has been of a geophysical nature. Batraukh (1975) compiling new data along with those of Bott and Masson-Smith (1960) and Parslow and Randall (1973), has proposed the presence of a granite batholith at shallow depths beneath and around the Carsphairn, Doon and Fleet plutons (Fig. 37). Detailed observations to the southwest of the Fleet pluton have indicated the presence of a granitic cupola lying at shallow depths and extending towards Wigtown Bay (Parslow and Randall, 1973). This accounts, in part, for the very wide metamorphic aureole in this area (see chapter 5, Fig. 33, above). All other contacts around the granite appear initially to be steep, but must flatten off at depths between 2.0 and 2.5 km (Batraukh, 1975).

Mention was first made of the minor intrusive suite around the Fleet pluton by Gardiner and Reynolds (1937). Subsequently four types of dyke rock were recognised (Blyth, 1949); porphyrites, microdiorites, quartz-mica-diorites



and sheared lamprophyres. The dyke-like nature of these intrusions was difficult to establish as they are invariably intruded into vertically bedded greywacke. Also intense carbonatization, especially in porphyrites, made their recognition very difficult. Subsequent work has enabled the distinction of a further group of porphyrite-porphyrines and subdivision of the lamprophyres around the Criffell-Dalbeattie pluton into spessartites and kersantites (Phillips, 1956).

Alteration is observed as a characteristic feature of all the minor intrusives in this area. It progresses from an initial stage of albitization with production of epidote and albite, to final calcite replacement, and is the result of passage of residual solutions highly charged with volatiles and  $\text{Na}_2\text{O}$  (Phillips, 1956). Alteration of lamprophyres and porphyrites is essentially comparable.

#### B. Introduction

The Cairnsmore of Fleet granite is the most acidic of the three major late orogenic intrusions of the Southern Uplands, and differs from the others by the absence of a distinct marginal facies of more intermediate composition. Forceful intrusion is indicated by extreme dilatation of the surrounding country rocks (see chapter 4, above) and granulation or shearing in granite adjacent to the contacts (Blyth, 1954). The country rocks comprise Lower Palaeozoic greywackes and shales characterized by zones of intense strike faulting (above), and elongation of the pluton is parallel to the strike of these (Fig. 1).

All visible contacts are sharply defined and usually vertical (e.g. Clints of Dromore, 25455641) or steeply dipping (e.g. Rig of Drumruck, 25805650, plate 17A). However the northern contact of the pluton in the vicinity of Craigdews Hill has a shallower dip (24975722, plate 17B), which gradually steepens northwards. This may indicate that the granite in this area is not far below the original roof of the pluton. Parslow (1968) deduced from gravimetric traverses that the roof probably lay 1.5 km above the present erosion level. The contact also appears to be less steep to the north of Peal Hill (26145765, see chapter 5) west of New Galloway, under the area of high grade contact metamorphism described by Gardiner (1890). A small outcrop of granite is encountered in the bed of Knocknairling Burn (26165774, map 4) where the stream has cut a steep sided ravine onto the shallow contact of the pluton.

The northern contact on Brochloch Hill (25155740, map 3) and the eastern contact on the flank of Cairn Edward Hill (26505730, map 5) are characterised by granitic sheets intruded parallel to the bedding of the country rocks. At both these localities orientation of the veins gives an impression of anticlockwise injection (Parslow, 1964, 1968), but this is simply due to the relative disposition of the Lower Palaeozoic strata and the intrusive contact (see chapter 4, F). Planes of easy access created by strike faulting appear to be responsible for their location. One of the sheets on the eastern flank of Bennan

Hill (26525723, map 5) is completely isolated from the main granite outcrop by approximately 250 m.

The contact of the central fine grained granite has been described previously (Parslow, 1964, 1968). In the north it is sharp but lacks any effects of chilling in either of the coarse or fine grained variants. Further southwest it is apparently more diffuse and may be gradational (ibid), although exposure is very poor in this area. From the present study it appears that the outcrop of the central intrusion in the west and east is greater than previously described (Fig. 38).

Most of the other physical and structural features have been adequately described by Parslow (1964, 1968) and will not be reiterated here. Mention, however, must be made of an area of inhomogeneous granite containing mineral banding, which is probably a relict sedimentary structure. It is exposed adjacent to a forest road where it crosses Acre Burn (26315712) to the west of Stroan Loch. Ptygmatically deformed quartz- and biotite-rich bands are surrounded by normal coarse grained biotite-muscovite granite (Fig. 39). A sample (73/G 63-71) taken <sup>from</sup> more uniform granite in the vicinity has a chemistry closer to the more highly fractionated coarse grained granites (Fig. 40), and is considered to be anomalous as a result of these inhomogeneties. This exposure occurs 2 km away from the nearest contact with sedimentary rock, but may represent a xenolith derived by sinking from the roof zone. The quartz- and biotite-rich bands probably represent original arenitic and pelitic horizons respectively.

CHAPTER 7  
PETROGRAPHY OF THE GRANITE

A. Introduction.

The geochemistry of the Cairnsmore of Fleet granite has not been adequately described previously and this is one of the major aims of the present work. Samples taken for geochemical analysis (Figs. 2, 40) were also examined under the microscope. These investigations show that although the three-fold division of Parslow (1964, 1968) may be useful in the field, a truer resolution of rock types is obtained by the use of thin sections. The subdivisions described here are the result of a purely petrographical classification of 81 samples and are later supplemented by geochemical data (see chapter 8, below).

The scheme of classification is based on that of Parslow (1964, 1968). Initially samples are subdivided on grain size, and further division depends upon the type and relative amounts of primary mica.

Six facies are recognised (Fig. 38):

1. coarse grained biotite granite
2. coarse grained biotite-muscovite granite
3. coarse grained muscovite-biotite granite
4. fine grained biotite-muscovite granite
5. fine grained muscovite-biotite granite
6. fine grained muscovite granite.

Coarse and fine grained refer to rocks with an average grain size of over and under 10 mm respectively. The coarse grained granites are usually porphyritic and

their grain size tends to vary more than the relatively equigranular fine grained granites. In naming the facies, the dominant mica precedes the subordinate species.

Comparison of the new subdivisions with those of Parslow (1964, 1968; Fig. 38) indicates that the distribution of the various rock types is more complex than previously described. The inner contacts mapped by Parslow are shown on Figure 38 as dotted or continuous lines. Dotted lines indicate that contacts are gradational or indeterminate. Three of the fine grained granites collected in this survey were from areas outside the outcrop of fine grained granites defined by Parslow. This is probably the result of limited exposure and the indistinct nature of the contact. As much of the new evidence is based on spot sampling it is impossible to demarcate the contact accurately.

In the following petrological descriptions the definition of myrmekite as a vermicular quartz-plagioclase intergrowth (Sederholm, 1916, p. 1; Shelley, 1964; Phillips, 1974; etc.) is strictly adhered to (e.g. plate 21B). Other larger and more globular intergrowths are described as graphic or micrographic and usually (but not always) occur as quartz blebs with the same optical orientation, within a host of K-feldspar (e.g. plate 26A), when they may be described as granophyric.

#### B. Coarse grained biotite granite

This facies is represented by ten of the sample set and they all tend to occur at or near to the margin of the pluton (Fig. 38), within the outcrop of the coarse

grained biotite granite defined by Parslow (1964, 1968).

The rock is porphyritic with subhedral phenocrysts of microcline attaining lengths of 20 mm, averaging between 10 and 15 mm. The mean grain size of the rock is greater than 10 mm.

In the vicinity of the contact on the western flank of Cairnsmore of Fleet, this facies contains numerous biotite-rich xenoliths. Within these, oligoclase is altered to sericite or paragonite and along interfaces with K-feldspar myrmekite is developed. Red-brown biotite has a random orientation and includes small numbers of anhedral zircon crystals which, due to decay of radioactive impurities are surrounded by obvious pleochroic haloes. Potash feldspar in the xenoliths is orthoclase rather than microcline; the latter lowest temperature form of potash feldspar (Deer, Howie and Zussman, 1966) is characteristic of the rest of the granite. Anhedral and interstitial quartz has highly undulose extinction indicative of crystallization or recrystallization under strain.

Adjacent to the northern contact near to Clattering-shaws Dam (25485781, 73/G 55-75, plate 18) the granite has a distinctly gneissose texture in hand specimen. Porphyritic microcline crystals are aligned and surrounded by flakes of biotite in parallel orientation. In thin section (plate 18) the rock shows signs of granulation especially along the edges of phenocrysts. Polycrystalline quartz aggregates have strained extinction and sutured contacts reminiscent of metamorphic rocks. The implications

of this texture are that the granite in this area was intruded into its present position whilst in a semi-solid or completely crystalline state. It is noteworthy that the metamorphic aureole is at its narrowest (approximately 500 m, Fig. 33) in the vicinity of these outcrops.

Overall, the coarse grained biotite granite is notably biotite rich, and invariably is distinctly foliated, especially near to the locality described above. Biotite crystals average 2 mm in length but may reach 4 mm. Pleochroism is distinct ( $\alpha$ ) dark red-brown to ( $\beta$ ) light yellow-brown and ( $\gamma$ ) pale straw-yellow. Slight alteration to a green chlorite with anomalous blue interference colours has taken place along the basal cleavage. Though Parslow (1964) described this as penninite, chemical analyses (see chapter 8, C) indicate a higher MgO/FeO ratio and a composition closer to pycnochlorite or brunswigite (Hey, 1954). Epidote and clinozoisite are commonly developed within or adjacent to chlorite, indicating a probable hydrothermal breakdown both of biotite and of feldspars. Biotite crystals have suffered local corrosion, indicated by embayed edges and subsequent replacement by quartz.

Small crystals (less than 0.25 mm in length) of muscovite, sericite or paragonite aligned along crystallographic directions in oligoclase are the products of secondary alteration. These, however, are present in only a few of the samples investigated.

Myrmekite is usually well developed along margins

of oligoclase in contact with microcline phenocrysts, and frequently within zones of granulation. Small euhedral crystals of plagioclase poikilitically enclosed by porphyritic microcline have an average composition of An 12, but vary between An 8 and An 18. Discrete larger crystals may also be euhedral or subhedral and are invariably zoned (normal and occasionally reversed), with a range in composition from An 18 to An 8, averaging An 13. Multiple twinning on the albite law is often reversed at the margins due to post-crystallization reactions. Besides the micaceous alteration products described above, oligoclase often poikilitically encloses biotite and shows alteration to zoisite.

Large (greater than 15 mm) subhedral microcline phenocrysts enclose biotite and oligoclase crystals. Poikilitic oligoclase may be corroded and replaced by a rim of quartz or completely transformed to myrmekite. Occasionally biotite in this position is surrounded by oligoclase or albite exsolved from the microcline host. Flame, string or globular microperthite (Augustithis, 1973) may be poorly or fairly well developed. Intergranular myrmekite (Phillips, 1974) has been observed within and between adjacent microcline crystals when they have differing orientations, and especially where granulation has taken place. At some localities fractures cutting across K-feldspar are infilled with quartz and quartz micrographic (granophyric) intergrowths infrequently occur.

Quartz invariably displays undulose extinction arising from post- or syn-depositional strain. Inter-



crystalline contacts between quartz are usually slightly sutured, and narrow zones of small rounded quartz grains are the result of granulation. Fragments of granulated granite containing well developed myrmekite have been observed within later crystallized quartz. Quartz crystals are anhedral and interstitial, and poikilitically enclose small crystals of biotite and oligoclase.

Accessory minerals such as sphene, apatite, zircon, ilmenite and magnetite are invariably associated with, or included along the margins, or within crystals of biotite. They are distributed more widely in the feldspars and quartz. Two generations of zircon are apparent, a large euhedral type and a smaller anhedral type. Both produce distinct pleochroic haloes when included within biotite.

#### C. Coarse grained biotite-muscovite granite

This variety occupies the largest outcrop area (Fig. 38) and consequently is represented by the largest number of samples (55). It occurs in both of Parslow's (1964, 1968) coarse grained granite divisions. Porphyritic microcline crystals are again common but have an increased range in size from 6 to 28 mm, but average 15 mm in length. The major difference between this and the biotite granite is in the extensive development of primary muscovite, both as discrete crystals and interlayer polycrystalline aggregates with biotite (plate 19).

Amounts of biotite exceed those of muscovite and individual crystals vary in length between 1 and 6 mm. The average size is 2 mm parallel to the cleavage and 0.5 mm across. Pleochroism is from ( $\alpha$ ) red-brown to ( $\beta + \gamma$ )

straw yellow. Alteration to chlorite is generally more extensive than in the previous facies (above), and is again associated with the occurrence of epidote and clinozoisite. Fewer zircons are included in biotite and these are mainly of the small anhedral variety, although a few large (0.2 mm) euhedral crystals occur. The presence of U and Th in small rounded crystals of apatite is indicated by the presence of an occasional pleochroic halo in surrounding biotite. Sphene associated with biotite is less common than in the biotite granite. Replacement of biotite by quartz within and along the margins of crystals, and vermicular quartz-biotite (symplectic) intergrowths have been observed rarely (plates 20A, B; 23B).

Muscovite crystals fall into three major categories namely, interlayer aggregates with biotite, discrete crystals, and replacements along crystallographic directions of oligoclase. Primary muscovite intergrown with biotite usually contains crystals of apatite and opaque minerals. The length of these crystals varies between 0.25 and 3.0 mm, but is commonly about 1.0 mm. Large crystals of biotite occasionally completely enclose muscovite. Two generations of discrete muscovite crystals are distinguished, primary muscovite enclosed by quartz and feldspar, and secondary finer grained muscovite cutting across quartz and feldspar crystals.

Fine grained aggregates of secondary muscovite are frequently associated with myrmekite in zones of granulation (plates 21B; 22A, B), or along margins of microcline phenocrysts. Larger crystals often replace or cut across

feldspars in radial aggregates. Vermicular quartz-muscovite intergrowths, comparable with myrmekite, are developed along some microcline crystal boundaries. Fine grained muscovite has also infilled fractures and replaced microcline along Carlsbad twin planes. At one locality it has been observed to have grown into microcline from a ragged and embayed crystal edge of biotite. Muscovite completely enclosed by microcline at another locality is surrounded by a replacement rim of quartz, which is intergrown with the feldspar. Smaller crystals of secondary muscovite, sericite or paragonite replace oligoclase (plate 23A) and are characteristically less than 0.5 mm in length.

Euhedral oligoclase crystals are poikilitically enclosed by microcline and also occur as discrete subhedral crystals elsewhere. Sericitization is fairly extensive, and is indicated by a turbid appearance in thin section (above). Crystal cores are more altered than the more albite-rich margins, which again show signs of reverse twinning. Occasionally oligoclase enclosed by microcline is nearly completely replaced by white mica, and is associated with products of hydrothermal alteration, such as clinozoisite and zoisite. Large subhedral crystals contain included biotite and commonly have a composition between An 12 and An 16, although the overall range is An 10 to An 18. Plagioclase enclosed by microcline tends to be more albitic with compositions between An 0 and An 16, which may be a result of exsolution of albite from microcline.

Porphyritic microclines occur more frequently than in the biotite granite and invariably enclose crystals of biotite, muscovite, micaceous aggregates, oligoclase, myrmekite and globular quartz. Simple twinning and microperthite of string and globular types are generally apparent, although flame, crystalline, ganglia and irregular forms (Augustithis, 1973) may also occur. Microperthite is developed occasionally along Carlsbad twin planes (plate 21A) and only rarely cuts across them. Open fractures in microcline are infilled with white mica, quartz or albite, the latter mineral is usually in the same optical orientation as coexisting microperthite. Included oligoclase and biotite crystals are invariably corroded and replaced by quartz and/or muscovite. Large single crystals or fine grained radiating aggregates of secondary muscovite may also replace and cut across microcline crystals; the margins between them are generally intergrown. Quartz-potash feldspar - muscovite intergrowths have also been observed. Granulation along the margins of microcline phenocrysts, and micrographic (granophyric) quartz-microcline intergrowths are common. Small anhedral microcline crystals enclosed by more porphyritic crystals are apparent by their differing optical orientations.

Everywhere quartz displays some degree of undulose extinction and poikilitically encloses biotite, muscovite, oligoclase and apatite. Wherever it is fractured or granulated, it is associated with myrmekite and secondary white mica. Intercrystalline quartz contacts are

invariably slightly sutured, and orientated globular intergrowths of quartz within quartz have been observed.

Crystals of zircon, apatite and opaque iron oxides are widespread but less common than in the biotite granite, and sphene is rare. Hydrothermal breakdown products such as clinozoisite and epidote are again associated with chlorite and oligoclase, but are more extensively developed.

D. Coarse grained muscovite-biotite granite.

Outcrops adjacent to the northeast contact of the fine grained granite, and in the vicinity of the northwest contact of the coarse grained granite around Craignelder (25005700, Fig. 38), are representative of rocks in this facies. The amount of muscovite exceeds that of biotite, and microcline phenocrysts occur in lengths between 10 and 15 mm in all four samples (plate 24).

Crystals of biotite are usually highly chloritized but where unaltered have a ( $\alpha$ ) red brown to ( $\beta + \delta$ ) straw yellow pleochroism. Enclosed opaque minerals occur preferentially along cleavage planes or more commonly within chlorite. Euhedral and anhedral zircon and apatite are also enclosed by the crystals which attain lengths of 2.5 mm, but average 1.5 mm. Spherulitic bodies of secondary chlorite have developed away from biotite in interstices between quartz and feldspar crystals.

Discrete crystals of muscovite average 2 mm in length, but may reach 4 mm, and usually have enclosed, or crystallized adjacent to biotite and chlorite. White mica again occurs as an alteration product along crystallographic planes of oligoclase and microcline microperthite.

Plagioclase composition varies from An 0 to An 16. Crystals are occasionally fractured and infilled with quartz, and myrmekite is developed extensively along contacts with microcline phenocrysts. At one locality adjacent to the western contact, plagioclase is altered to calcite (72/G 436, 24805690).

Porphyritic microcline crystals commonly enclose quartz but less usually oligoclase, muscovite and myrmekite. Crystalline, string and globular varieties of microperthite occur, but tend to be poorly developed. Granulation along margins of phenocrysts is fairly common, and shearing across a crystal at one locality has been observed to displace enclosed oligoclase crystals.

In common with the other coarse grained granites quartz is strained, and is occasionally found in microcrystalline aggregates confined to narrow zones, as a result of granulation especially in rocks close to the western contact. Muscovite has been observed to contain inclusions of quartz which may be due to corrosion and later crystallization.

Crystals of zircon, apatite and opaques are concentrated in and around biotite, and clinozoisite occurs as a product of the alteration of plagioclase feldspar.

#### E. Fine grained biotite-muscovite granite

Three out of the five samples of this facies come from exposures outwith the fine grained granite contact of Parslow (1964, 1968), for reasons outlined above (Fig. 38). Major differences between these and the coarse grained biotite-muscovite granite are:

- i) the smaller average grain size (less than 10 mm) and
- ii) the development of fewer and smaller microcline phenocrysts (all less than 15 mm, plate 25).

Under the microscope biotite has a lower absorption but retains a ( $\alpha$ ) red-brown to ( $\beta + \gamma$ ) straw-yellow pleochroism. Normally it occurs with muscovite and encloses opaque minerals, small anhedral zircons and apatites. Chloritization is widespread and again epidote occurs within the chlorite. Replacement by quartz is observed in many crystals, especially along planes of cleavage. Crystals of biotite may reach 3.5 mm in length but are usually about 1.75 mm.

Muscovite is subordinate to biotite and occurs as interlayer or randomly orientated aggregates with this mineral, crystals averaging 2 mm in length. Secondary muscovite is developed within plagioclase and replacement of the feldspar takes place in the form of discrete crystals up to 1.5 mm in length. Vermicular quartz-muscovite intergrowths are fairly common (plate 26B).

Individual plagioclase crystals vary in composition between An 0 and An 16, averaging An 11. Those enclosed within microcline have a range of An 0 to An 14, but few of this type have been observed owing to the scarcity of porphyritic crystals. Myrmekite and micrographic quartz intergrowths are fairly common. Quartz in the latter has been observed in the same optical orientation as in adjacent quartz-potash feldspar (granophyric) intergrowths. Some oligoclase appears to have been replaced by potash feldspar and quartz.

As porphyritic microcline crystals are infrequent in their development, microperthite is less typical, although globular, flame and string varieties sporadically occur. The finer grain size of this granite indicates more rapid crystallization as a function of an increased rate of heat loss, and consequently less time at elevated temperatures for unmixing of alkali feldspars. This concept and the role of other factors in the unmixing of feldspars is discussed below. Effects of granulation are rare, in contrast to the coarse grained granite. Microcline crystals poikilitically enclose biotite, oligoclase and muscovite; the latter mineral is often replaced by rims of quartz and vermicular muscovite-quartz intergrowths. Micrographic (granophyric) quartz-potash feldspar intergrowths and non-orientated inclusions of quartz are a recurrent feature (plate 26A).

Quartz encloses small crystals of muscovite, biotite and oligoclase, and may be moderately strained or relatively unstrained. Suturing between quartz crystal interfaces does not occur.

Accessory minerals other than those associated with biotite (above) are rare, although secondary clinozoisite occurs in chlorite and oligoclase.

#### F. Fine grained muscovite-biotite granite

All six samples representing this facies fall within the fine-grained granite outcrop of Parslow (1964, 1968; Fig. 38). They are fairly equigranular with a few microcline phenocrysts attaining lengths of between 10 and 20 mm (plate 27).



Biotite has a ( $\alpha$ ) medium red-brown to ( $\beta + \gamma$ ) straw-yellow pleochroism, and contains a few euhedral and anhedral zircons, apatites and opaque minerals. Chloritization and replacement of biotite by quartz along cleavage planes is widespread, and epidote and clinozoisite are common alteration products. Secondary spherulitic, interstitial chlorite does not contain epidote. Biotite crystals vary in length between 1.5 and 3.5 mm and are usually associated with primary muscovite.

Muscovite is well developed and exceeds the amount of biotite. Discrete crystals of about 2 mm length are usual, and many, obviously secondary in origin, cut across all minerals and replace oligoclase. Radiating masses also occur and are well developed in a locality on the western flank of Fell of Fleet (sample 73/G 58-70, 25795701, plate 28). Finer grained (less than 0.5 mm in length) white mica is again associated with alteration of oligoclase. Much primary muscovite has crystallized adjacent to, and occasionally encloses biotite, in crystals between 2.0 and 2.5 mm in length. Along the edges of large crystals vermicular intergrowths with quartz are common.

Plagioclase is generally altered, and discrete crystals are albitic in composition (An 0 - An 10). The few crystals observed to be poikilitically enclosed by microcline, have a similar composition. Myrmekite is far less common than in the rest of the granite and in some of the samples absent altogether, however micrographic quartz-albite intergrowths occur sporadically.

Microcline crystals tend to be equidimensional and contain poorly developed irregular, globular, string or flame microperthite. Enclosed minerals are albite, biotite and muscovite surrounded by quartz rims and intergrowths. Micrographic (granophyric) quartz-potash feldspar intergrowths and randomly orientated inclusions of quartz are prevalent.

Quartz may be moderately strained or relatively unstrained and encloses small crystals of muscovite, biotite and albite. Fractures in these included minerals are infilled with quartz in optical continuity with the enclosing quartz. Where comparable fractures pass through feldspars secondary white mica has crystallized.

Sphene has been observed rarely as aggregates, and apatite is commonly enclosed by quartz and feldspars. Xenomorphic aggregates of clinozoisite are usually associated with chlorite and oligoclase.

#### G. Fine grained muscovite granite

The outcrop of this variety appears to be restricted in extent, and is only represented by one of the sample set from a locality near to the centre of the fine grained intrusion, between Fell of Fleet and Benmeal (73/G 57-69, 25705692, plate 29).

Biotite is absent, and any that originally was present may have been completely converted to the very small amounts of chlorite observed in thin section. In contrast large amounts of muscovite surround quartz crystals and cut across feldspars, in crystals up to 3 mm in length.

Plagioclase is highly altered and appears 'dusty' in plane polarised light. Discrete crystals are albitic in composition whereas the few enclosed by potash feldspar average An 12. Myrmekite is absent, but micrographic plagioclase-quartz intergrowths occur more frequently than in the types above.

Microcline showing Carlsbad twinning encloses oligoclase and contains crystalline and globular microperthite, and is usually sericitized.

Strained quartz crystals infrequently enclose pale buff to pink anhedral and fractured spessartine garnets (plate 29). Composition of the latter was confirmed by X-ray analysis of the separated mineral, which gave dominant peaks at  $2.58\text{\AA}$ ,  $1.60\text{\AA}$  and  $1.55\text{\AA}$  spacings. The only other accessory observed within quartz and feldspar is apatite.

#### H. Summary and conclusions

The coarse grained granite is dominantly porphyritic, and microcline phenocrysts attain their maximum size (approximately 30 mm in length) in the biotite-muscovite granite, in regions away from the contact. Porphyritic feldspars become increasingly scarce towards the centre of the fine grained granite and consequently this rock type tends to be more equigranular.

The mica distribution in the coarse grained granite is more complex than previously described (Parslow, 1964, 1968, 1971). Although the biotite granite is marginal in the southwest and south, towards the northeast a band of

this facies cuts across the pluton from the margin around Benniguinea (25655760) to Bennan Hill (26485725) and isolates an area of biotite-muscovite granite, in the marginal area southwest of Knocknairling (26235765), from the main outcrop (Fig. 38). Also the biotite granite does not form a continuous outcrop around the southern and northern contacts. Very generally the total amount of biotite decreases from the biotite granite facies towards the centre of the pluton (cf. Parslow, 1971, p. 44), and also although its colour remains the same its facility for absorbing light decreases in the same direction.

Large (0.2 mm) euhedral and smaller anhedral zircons with very obvious pleochroic haloes occur in biotite of the coarse grained biotite granite. Both types decrease in quantity with increasing acidity of host rock, but the former more rapidly. The large euhedral zircons are probably primary magmatic minerals, decreasing in quantity as a result of depletion of Zr, with increasing fractionation of the melt. Smaller anhedral zircons may be the residue of granitization of pre-existing sedimentary rocks.

Primary muscovite increases in amount away from the biotite granite and towards the centre of the pluton. Secondary muscovite of all types occurs in all of the granite facies but more extensively in the fine grained granite, and towards the northwest contact of the coarse grained granite.

The average composition of plagioclase appears to be fairly constant at An 13-14 over the bulk of the coarse grained granite outcrop, but within the coarse grained

muscovite-biotite facies and the fine grained granite it is more albitic. Zoning, reversed zoning and reversed twinning are more common in the biotite-rich coarse grained granites.

Microperthitic microclines are more abundant in the coarse grained granites than the fine grained varieties, and there seems to be a correlation with the size of the phenocrysts. This may simply be an effect of the length of time temperatures were elevated in order to assist the subsolidus exsolution of the albitic phase, as mentioned above. Yund and McCallister (1970) suggest that internal factors such as impurities, imperfection and supersaturation, or external factors such as dry or hydrothermal pressures, may modify the kinetics of any exsolution reaction. Of the latter, increased reaction rate is probably primarily due to the presence of water, either participating in the reaction or acting as a solvent (*ibid*). It is unlikely that a process such as this enhanced the production of microperthite in the coarse grained granite because the presence of copious quantities of muscovite and alteration in the fine grained granite appear to indicate that the latter was probably more hydrous. Also it is impossible to determine with the present information how much albite is contained within microcline of the central intrusion and consequently available for exsolution.

Myrmekite is extensively developed throughout the coarse grained granite, and although it is present in small quantities in the marginal regions of the fine grained granite, it is absent from the centre of this mass. There

appears to be a corresponding increase in micrographic or granophyric quartz-feldspar intergrowths. This decrease in amounts of myrmekite towards the centre of the pluton endorses Phillips (1974) statement that amounts of myrmekite are directly proportional to the Ca content of the host rock. Ca content decreases towards the centre of the pluton (see chapter 8, D, below).

Various theories have been propounded to explain the formation of myrmekite and are reviewed by Phillips (1974). Myrmekite of three types is common in the coarse grained granite; i) normal myrmekite formed within potash feldspar at the contact with plagioclase crystals, ii) intergranular myrmekite developed within adjacent microcline crystals with differing orientations, and iii) myrmekite bordering muscovite cutting across potash-feldspar crystals (plate 21). This latter variety is indicative that at least some of the myrmekite owes its origin to a late or post magmatic process, because muscovite in such a position is probably hydrothermal in origin.

Parslow (1971) preferred Shelley's (1964, etc.) theory of stress assisted exsolution of albite from potash feldspar, and subsequent growth on a plagioclase seed crystal, enclosing strained quartz that was originally situated between the alkali feldspar and the plagioclase (or two adjacent plagioclase crystals). His reasons were that myrmekite was more extensively developed in sheared rocks and is virtually absent from the relatively stress-free central granite. Whilst agreeing that myrmekite is common in zones of granulation, the author believes that this

could also be a result of the ease with which solutions might percolate through the rock. The association of secondary muscovite with myrmekite in fracture zones adds weight to this concept.

An alternative proposal involves interleptonic (between crystal boundaries) quartz infiltration and replacement (Augustithis, 1973), and is based upon the presence of vermicular (symplectic) intergrowths between quartz and other minerals, such as muscovite and biotite. Potash feldspar is apparently not involved in their formation, and comparable intergrowths occur adjacent to quartz crystals in the Fleet pluton (plates 20A and 26B), although throughout the granite, obvious secondary quartz replacement of many minerals has occurred without development of symplectic intergrowths (plate 20B). Any theory, such as that of Augustithis (1973) above must explain the relative absence of myrmekite from the fine grained granite when much secondary replacement by quartz and development of vermicular quartz-muscovite intergrowths has taken place.

The occurrence of myrmekite and micrographic (granophyric) intergrowths of microcline and quartz are inversely proportional, and although the latter is never as extensively developed this may indicate that their genesis is related in some way. Granophyric textures may be readily ascribed to the rapid simultaneous growth of quartz and feldspar, without the necessity of reactions taking place under cotectic or eutectic conditions, with implications of thermodynamic equilibrium (Smith, 1974). The presence of micrographic quartz intergrowths with other

minerals such as biotite (plate, 23B) and oligoclase, with quartz occurring in the same optical orientation between such intergrowths, render the above process improbable in the Fleet pluton, although it may be explained by infiltration and metasomatism (Augustithis, 1973; Smith, 1974).

Quartz crystals in the coarse grained granite are invariably strained and have sutured contacts especially in granite close to the margin of the pluton, where granulation is also common. Although all these effects are observed throughout the coarse grained granite, they are virtually absent from the fine grained intrusion, and this is evidence for a less forceful emplacement of the latter.

Hydrothermal alteration of feldspars to epidote minerals is minor, but widespread. The dominant secondary hydrothermal mineral is muscovite which occurs in large amounts towards the centre and northwest margin of the pluton.

The presence of garnet (spessartine) in the most highly fractionated fine grained granite may indicate its extremely peraluminous nature (Carmichael, Turner and Verhoogen, 1974). Rutherford (1973) suggests that garnet may replace biotite if rock compositions requisite for the formation of biotite occur above the biotite stability field. This results only if coexisting feldspar cannot accommodate the Al otherwise incorporated in the biotite lattice. The absence of biotite in the garnet-bearing granite may indicate that a process such as this has taken place. Although metasomatism, which has also occurred in



the central granite, has been submitted as a mode of origin for garnet in igneous rocks (Deer, Howie and Zussman, 1966).

The original distribution of primary magmatic minerals has been modified to a certain extent by late magmatic processes of two types. Firstly, forceful intrusion and subsequent adjustments due to consolidation and regional stress have granulated, sheared and recrystallized quartz in the coarse grained granite, especially close to the contact. Secondly, a post-magmatic event probably hydrothermal and associated with metasomatism (see below) in the central parts of the pluton, has altered biotite to chlorite and epidote, produced muscovite, clinozoisite and zoisite from feldspars, and corroded and replaced all minerals with quartz to a minor extent. Effects of the first process may have facilitated the second in the coarse grained granites, but the most obvious results of hydrothermal alteration appear to be related to the more highly fractionated rocks towards the centre and northwest of the pluton. Production of myrmekite and other symplectic or micrographic (granophyric) intergrowths may be connected with these late stage processes.

## CHAPTER 8

## GEOCHEMISTRY OF THE GRANITE

A. Introduction

Parslow (1964, 1971) made a preliminary study of the geochemistry of the Fleet pluton. However, few significant conclusions can be drawn from this work, because of the small number and erratic distribution of the sample collection. For this reason, following Stephens (1972), samples have been collected from grid intersections (appendix 1, Figs. 2 and 38) where possible, and bulk chemical variations analysed by statistical techniques (appendix 2). Minerals separated from a selection of rock types have been analysed to determine variations in their chemistry in order to interpret 'whole-rock' chemical trends.

The means of major oxides in the Fleet pluton are comparable with those of world-wide Ca poor granites (Turekian and Wedepohl, 1961; tables 9 and 10), except for significantly higher contents of MgO and TiO<sub>2</sub>. All except TiO<sub>2</sub>, fall within the chemical limits defined for acid magmatic rocks associated with rare metal mineralization (Tischendorf, 1974; table 10).

Many of the trace element means vary considerably from the averages quoted for Ca poor granites (Turekian and Wedepohl, 1961). Notably Li, Be, Rb, Ni, Sr and Pb are enriched, whereas La and Ba are depleted. Li falls within the range for mineralized granites (Tischendorf, 1974), but Rb and Be are slightly below. The mean chemical composition of the Fleet pluton indicates that it is a highly

fractionated granite of a type often associated with mineralization. This is endorsed by the high average value of Differentiation Index (Thornton and Tuttle, 1960) obtained from the sample set, which at 89.6 is much higher than the average granite, 80. Differentiation Index is defined for oversaturated granites as the sum of CIPW-normative quartz (Q), orthoclase (or) and albite (ab).

#### B. Geochemical classification

An objective classification of the sample set using cluster analysis was undertaken in order to test the significance of the petrological subdivisions or facies. Considering the relatively small ranges in bulk chemistry, a close similarity exists between both petrological and geochemical classifications (Figs. 38, 40 and 41, tables 11 and 12). The sample set is divided into four clusters, two of which contain most of the coarse grained granites, and the others containing more highly fractionated coarse grained granites and all the fine grained granites (Fig. 41).

Cluster 1 (10 samples) contains all but one of the coarse grained biotite granite samples and one of the coarse grained biotite-muscovite granites. This underlines the validity of the coarse grained biotite facies even though it apparently has gradational boundaries with the coarse grained biotite-muscovite facies. The mean Differentiation Index (85.30) is, as expected, the lowest of all four clusters, but is slightly higher than that of the average granite (80, Thornton and Tuttle, 1960, see above and tables 11 and 12). Relative to the mean of the total sample set average amounts of  $\text{SiO}_2$  and Rb are

significantly lower and  $TiO_2$ , FeO, MgO, CaO, Sr, Ba, La, Ce, Nd and Zr are higher. The cluster is enriched in the more basic constituents which is consistent with its lower Differentiation Index.

Cluster 2 represents 48 samples out of a total of 76, 46 being coarse grained biotite-muscovite granites (Figs. 38, 40 and 41). No significant differences occur between the chemical means of this cluster and those of the total sample set (tables 11 and 12), although a trend consistent with increased fractionation occurs between clusters 1 and 2 (Fig. 42), paralleled by an increase in the mean Differentiation Index (89.43). Clusters 1 and 2 are joined at a fusion coefficient of 12.85 to form a single new cluster containing 58 out of a total of 64 coarse grained granite samples (Fig. 41).

Samples in clusters 3 and 4 geochemically form a distinct group containing the most highly fractionated rocks. Changes in gradient of many of the trends in mean chemistry occur between clusters 2 and 3 (Fig. 42). The inclusion of some of the coarse grained granites in cluster 3 indicates that trends in chemical fractionation of the two intrusions overlap. Some of these coarse grained granites are from localities adjacent to the outcrop of the fine grained granite, but a number occur elsewhere. Two are from the northwest margin of the granite in the vicinity of the break in the biotite facies of Parslow (1964, 1968), one of which has been classified in the present work as a muscovite-biotite granite. The anomalous chemistry of another towards the eastern contact of the pluton has

already been attributed to inhomogeneity (73/G 63-71, see chapter 6, B). Highly fractionated samples occurring away from the central regions of the pluton infer that a simple model with increasing fractionation in situ towards a central point, characteristic of for instance the Criffell-Dalbeattie pluton (Stephens, 1972), is not applicable in the Cairnsmore of Fleet granite.

The mean Differentiation Index for the sixteen samples of cluster 3 is 91.53, close to that for alkali granites (93, Thornton and Tuttle, 1960), although the mean peralkalinity index ( $Al_2O_3/(Na_2O + K_2O)$ ) is greater than one (1.49), indicating that they are not peralkaline.  $SiO_2$  is significantly higher and  $TiO_2$ , FeO, MgO, CaO, Sr, Ba, La, Ce, Nd, Zr and Zn lower than the means of cluster 2 (Fig. 42) and the total sample set (tables 9, 10 and 12).

Cluster 4 contains two very highly fractionated samples, one of which (73/G 57-69) is the single representative of the muscovite granite facies. Both are extremely enriched or depleted in certain elements, and this is attributed to primary magmatic fractionation coupled with late stage alkali metasomatism and/or a hydrothermal event. Sample 73/G 58-70 contains well developed radiating aggregates of secondary muscovite (chapter 7, F; plate 28), and spessartine garnet occurs in 73/G 57-69 (chapter 7, G; plate 29) and may be the result of metasomatism or fractionation of a peraluminous melt (see chapter 7, H above). Their mean Differentiation Index is very high (95.83), and they are enriched in  $SiO_2$ ,  $Na_2O$ , Li, Rb, Be and Y and depleted in FeO, MgO, CaO,  $K_2O$ , Sr, Ba, La, Ce, Nd, Ni, Zn and Pb compared to the total sample set (tables 9 and 12,

Fig. 42).

### C. Geochemistry of separate mineral phases

Before interpreting overall chemical trends within the pluton it is necessary to understand variations in chemistry taking place in individual minerals during fractionation. For this reason twelve samples of granite (Fig. 40, 1-12) and one pegmatite were separated into their component minerals, by methods outlined in appendix 1 (below). Micas were completely analysed for major elements when in sufficient quantity, but only partial analyses were undertaken on quartz-feldspar mixtures (appendix 7). Locality numbers 1 to 12 (Fig. 40) refer to relative positions in the pluton and in each geochemical and petrological facies. Lower numbers have been given to localities both near to the margin and the biotite facies, whereas higher numbers refer to samples from the more highly fractionated and usually central parts of the intrusion. This type of approach was employed for easy comparison of a small number of mineral separates with trend surface and contour maps of the total sample set. These more subjective numbers are used in preference to units such as Differentiation Index, because the latter is complicated by late magmatic, metasomatic or hydrothermal processes.

#### (i) Biotite

Ten samples of biotite have been analysed, the raw data and numbers of ions per formula unit are tabulated in appendix 7 (below). Their position on the ternary diagram

$A = Al_{vi} + Li$ ,  $B = Fe^{3+} + Fe^{2+}$ ,  $C = Ti + Mn + Mg$  (Fig. 43) showing the octahedral occupancy, straddles the Fe biotite and Li-Fe biotite fields (Lange et al., 1972). Hercynian granites of the Erzgebirge (D.D.R.) contain biotite micas which trend in composition from Mg-biotite to zinnwaldite with increasing acidity and decreasing age of intrusion (*ibid*). There is a steady increase in  $Al_{vi}$  and Li in the octahedral site relative to Fe, Mn, Ti and Mg, accompanied by an increase in  $Fe^{2+} + Fe^{3+}$  relative to  $Mn + Ti + Mg$  (Fig. 7). Analyses of biotites from the Cairnsmore of Cairnsphairn igneous complex (Deer, 1936) are included on the ternary diagram for comparison. As might be expected from less acidic rocks, they plot more towards the Mg-biotite field.

The single complete analysis of biotite from the fine grained granite (10, 56-70B), for which a structural formula can be calculated, plots more towards the annitic apex (100%  $Fe^{2+} + Fe^{3+}$ ). Annitic micas are characteristic of alkaline granites which tend to be enriched in Fe relative to Mg (P. Bowden, pers. comm.). This coupled with  $Na_2O$  enrichment in the central parts of the fine grained granite may indicate an alkaline trend. If a total  $H_2O$  value is computed for sample 9 (54-68B) from the fine grained granite, it plots on a similar trend but closer to the biotites of the coarse grained granites. Further confirmation of this trend is presented later in investigations into the chemistry of chlorites (chapter 8, C (ii)).

$Al_2O_3$  and FeO are steadily enriched in biotites during fractionation, and  $SiO_2$  and MgO are correspondingly

depleted (Fig. 44). Similar variations have been recorded from Portuguese granites, but between rather than within individual plutons (de Albuquerque, 1973). Nockolds (1947) observed that the  $Al_2O_3$  content is always highest in biotites coexisting with muscovite, and that  $SiO_2$  shows the inverse relationship. This is consistent with chemical trends in biotites of the Fleet pluton.  $Li_2O$  is less simply distributed, increasing towards the more highly fractionated parts of the coarse grained granite, and apparently decreasing in the fine grained granite. This decrease may be a result of crystallization of larger amounts of muscovite and depletion of Li available for inclusion in the biotite lattice. Muscovite in the fine grained granite contains more  $Li_2O$  than in the coarse grained granite (chapter 8, C (iii), below).  $K_2O$  decreases in biotites further from the margin of the pluton probably reflecting more intense hydrothermal alteration. For this reason also, the  $Rb_2O$  distribution is variable between the eight samples analysed for this oxide. MnO, Zn and Be are all enriched and Cr and Ni depleted in biotites from more acidic host rocks. The  $TiO_2$  content is approximately constant.

According to Blaxland (1971) biotites from muscovite-bearing granites contain relatively low amounts of Zn and high quantities of Fe. Although this relationship is confirmed for FeO in Fleet biotites, the reverse obtains for Zn. Comparable enrichment of Zn in biotites from muscovite-rich granites has been reported previously (Kozlov, 1968, and others). The mean Zn concentration in Fleet biotites is 668 ppm, with a range of 305 to 1150 ppm.



Biotites from mineralized Cornish Hercynian granites have a mean of 350 ppm and a range of 200 to 650 ppm, whereas the mean of barren Caledonian granites in Britain is 330 ppm (Bradshaw, 1967). It is thus apparent that biotites from the Fleet pluton are significantly enriched in Zn.

The mean Cu content (38 ppm) of Fleet biotites is higher than both mineralized and non-mineralized British granites (Bradshaw, 1967). Ni usually occurs within the range 40 to 90 ppm, but one sample (10, 56-70B) from the central fine grained granite is extremely enriched (495 ppm Ni), and for this reason is not included on the variation diagram (Fig. 44). The previously described hydrothermal event may be responsible for this enrichment (see chapter 7, H). Values of Ni are higher than in Cornish granitic biotites (14 to 41 ppm, Bradshaw, 1967), but within the range of other Caledonian igneous rocks (granites, 44 to 150 ppm, Bradshaw, 1967; various intermediate and acid plutonic rocks, 30 to 150 ppm, Nockolds and Mitchell, 1946).

Concentrations of Rb in biotites from the mineralized Cornish granites fall within the range 900 to 2000 ppm and compare with Fleet biotites. The latter vary between 711 and 1217 ppm Rb, with a mean of 1005 ppm. These values are higher than biotites from other Caledonian granites (all less than 800 ppm Rb, Bradshaw, 1967), but lower than the mean (1300 ppm) of thirteen Caledonian igneous rocks ranging in composition from diorite to adamellite (Nockolds and Mitchell, 1946).

Sr concentrations in Fleet biotites (0-17 ppm) are also comparable with Cornish samples, but significantly lower than other Caledonian granites. The mean Cr value (129 ppm) is also lower than other biotites from Caledonian plutonic rocks (Nockolds and Mitchell, 1946). Differences in Zr content of biotites from Cornwall and Scotland are not significant (Bradshaw, 1967), but those from Cornwall tend to have lower concentrations overall, and are slightly lower than Fleet samples (mean 45 ppm Zr).

Some close similarities exist between the trace element contents of biotites from mineralized Hercynian granites in Cornwall and those from the Fleet pluton. Base metal mineralization occurs within and around the pluton, but the major controlling factor is undoubtedly its high degree of fractionation. Contents of base metals (e.g. Cu, Zn and Ni) that are higher than average, may be related to primary crystallization, or to secondary enrichment due to the detected late stage metasomatic and/or hydrothermal event.

(ii) Chlorite

Chlorite is considered to be a secondary alteration product after biotite, and it is suggested that variations in its chemistry reflect, at least in part, corresponding variations in chemistry of the original biotite.

All the analysed chlorites are unoxidized i.e. they contain less than 4%  $\text{Fe}_2\text{O}_3$  (appendix 7), and therefore may be termed orthochlorites. The classification of Hey (1954) has been adopted, and most plot between the pycnochlorite, brunsvigite and Fe-rich diabanite fields (Fig. 45). They

are relatively Fe-rich reflecting the composition of original biotites.

On the  $Al_{vi} + Li, Fe^{2+} + Fe^{3+}, Ti + Mn + Mg$  ternary diagram they form a trend comparable with the biotites (Figs. 43 and 45), but are slightly enriched in octahedral Al and Li. The annitic trend in biotites from the central fine grained granite described above is endorsed by the position of sample 11 (57-69C) closer to the  $Fe^{2+} + Fe^{3+}$  apex. This is assuming that the original biotite had a similar Fe/Ti + Mn + Mg ratio, which seems reasonable on comparison with other coexisting biotites and chlorites (e.g. samples 3, 8 and 10). This sample plots in the Fe-rich ripidolite field (Fig. 45), because of its high Fe/Mg ratio and its deficiency in  $SiO_2$ .

Trends in major and trace element chemistry (Fig. 46) are, as expected, similar to those of biotite (Fig. 44).  $SiO_2$  and MgO decrease, whereas  $Al_2O_3$  and FeO increase with fractionation. Chlorites from the central fine grained granite become depleted in  $Li_2O$  in response to uptake of this oxide by primary and secondary crystallization of muscovite, and confirms the trend observed in biotite (above). Variations in MnO, Zr, Cr and Ni are essentially equivalent to those in biotite, except for an extreme enrichment of Ni and depletion of Zn in sample 11 (57-69C). Chlorite in sample 10 (56-70C) contains 45 ppm Ni and 1459 ppm Zn, in contrast to coexisting biotite (56-70B) containing 495 ppm Ni and 1150 ppm Zn. Fluctuations in base metal concentrations are undoubtedly the result of hydrothermal

activity responsible for the conversion of biotite to chlorite and the recrystallization of large quantities of muscovite in the fine grained granite.

(iii) Muscovite

Muscovites plot in the Li muscovite field on a Li,  $R^{2+}$  ( $Fe^{2+} + Mn^{2+} + Mg^{2+}$ ), octahedral  $R^{3+}$  ( $Al^{3+} + Fe^{3+}$ ) +  $Ti^{4+}$  ternary diagram (Foster, 1960; Fig. 47). The ideal muscovite end member with a half cell formula  $[Al_{2.00}(Si_{3.00} Al_{1.00})O_{10}(OH)_2] K_{1.00}$  occurs at the octahedral  $R^{3+}$  (Al, Fe) +  $Ti^{4+}$  apex, and lithian muscovites, lepidolites and polyolithionites plot in a field adjacent to the octahedral  $R^{3+}$  - Li sideline (ibid). Biotite analyses from the Fleet pluton are also plotted on this diagram for comparison of octahedral occupancy (Fig. 47).

When plotted on an  $Al_{vi} + Li, Fe^{2+} + Fe^{3+}, Ti + Mn + Mg$  ternary diagram, the muscovites display a trend of increasing octahedral occupancy by  $Al_{vi}$  and Li, associated with a slight increase in the  $Fe/Ti + Mn + Mg$  ratio in these sites, with continuing fractionation. This broadly corresponds to the trend in biotite (Figs. 43 and 47). Increased fractionation promotes the inclusion of Al and Li into octahedral positions, which is related to depletion of Fe and Mg in the melt, as a result of their removal during crystallization of biotite. Foster (1960) has observed that an increase in Li is accompanied by a decrease in octahedral and tetrahedral Al, and an increase in Si and overall octahedral occupancy. None of these trends are apparent from these data, although compositional variations are small, and  $SiO_2$  does not have a significant trend.

However this may be the result of the lack of discrimination between primary and secondary muscovite.

Amounts of  $Al_2O_3$ ,  $Li_2O$ ,  $MnO$ ,  $Ni$  and  $Be$  all increase with fractionation (Fig. 48).  $Ni$  has the reverse trend of that in biotite, and whereas absolute quantities are lower the inverse relationship may indicate competition for  $Ni$  during primary crystallization of the micas, or increased alteration of biotite towards the centre of the pluton, releasing larger quantities of  $Ni$  for inclusion in the lattice of secondary muscovite.

Little previous research has been carried out into trace element variations in muscovite. Fleet muscovites are very rich in  $Li$  (mean 1840 ppm) compared to one other analysis of a Caledonian muscovite (10 ppm, Nockolds and Mitchell, 1946). The  $Be$  content fluctuates but appears to increase with fractionation. Amounts of  $Zr$  and  $Sr$  (0-25 ppm and 0-11 ppm respectively) are lower than the Cornish and Weardale granites (Bradshaw, 1967). Mineralized granites of Cornwall contain muscovites with a mean  $Zn$  concentration of 130 ppm as compared with Weardale, 240 ppm and Fleet, 159 ppm. The mean  $Rb$  content (1157 ppm) is comparable with those of Cornwall, but  $Ni$  (mean 39 ppm) is much higher than these and muscovites from the Weardale granite (Bradshaw, 1967).

Trends in major and minor element chemistry of muscovite are much as expected from previous research, even though large quantities of secondary muscovite occur in the fine grained granite intrusion.

(iv) Feldspar and quartz mixtures

The presence of many intergrowths between feldspars and quartz (chapter 7, above) would make any attempt at their separation difficult, if not impossible. These minerals were therefore left as a mixture after removal of the micas (appendix 1). Variations in the major oxides  $K_2O$ ,  $Na_2O$  and  $CaO$  are directly attributable to amounts of microcline and plagioclase, and to the composition of the latter. This proposition does not take into consideration albite in solid solution or exsolved as microperthite in K-feldspar.

The concentration of  $K_2O$  increases from the biotite facies into the less fractionated parts of the biotite muscovite facies of the coarse grained granite, and  $Na_2O$  and  $CaO$  correspondingly decrease (Fig. 49). This indicates a decrease in quantity of plagioclase and an increase in microcline. Further fractionation promotes a lowering of the  $K_2O$  content towards the centre of the fine grained mass. Within the coarse grained granite both  $Na_2O$  and  $CaO$  remain approximately constant, but in the most highly fractionated rocks  $CaO$  is depleted and  $Na_2O$  markedly enriched, which may be the result of alkali metasomatism. On a ternary diagram of these components (Fig. 50) an initial trend takes place towards the  $K_2O$ - $Na_2O$  sideline, with a slight increase in the  $K_2O/Na_2O$  ratio, followed by a later trend towards the  $Na_2O$  apex running parallel to the  $Na_2O$ - $K_2O$  sideline, in both coarse and fine grained granites. Comparable trends in whole rock analyses have been reported from granites of the Erzgebirge (Lange et al., 1972, see section E below).

Certain of the trace elements show significant variation with fractionation (Fig. 49). Sr decreases owing to the lowering of the anorthite component of plagioclase. Fractionation promotes the continuous enhancement of Rb values and the consequent decrease in the K/Rb ratio, equivalent to that observed previously (Bradshaw, 1967; Lange et al., 1974, p. 474). The mean K/Rb value of Fleet feldspars is 158 (range 72 to 253) compared with feldspars from Cornish granites, 70 and Caledonian granites, 350 (Bradshaw, 1967). Feldspars from the Fleet pluton are more closely comparable to the mineralized granites of Cornwall with respect to K/Rb ratio.

Ca/Sr ratios vary between 13 and 87 and have a mean of 53, but have a more complicated trend than K/Rb above. There is an initial rapid decrease indicating enrichment of Sr relative to Ca, but in the highly fractionated fine grained granites Sr is very depleted, and there is a consequent decrease in the ratio. Values are similar to both Cornish and Weardale granites (Bradshaw, 1967) and are the result of a high degree of fractionation.

Amounts of Li in feldspars of both the granites increase during fractionation, but a distinct break occurs between the coarse and fine grained granites, and is marked by an overall lowering of the Li content of these minerals (Fig. 49). The absolute decrease of Li in feldspars of the fine grained granite is probably associated with the crystallization of copious quantities of

Li-bearing primary and secondary muscovite (see section C, (iii) above). It is apparently unusual to have a Li concentration of greater than 5 ppm in feldspar (Ahrens and Liebenberg, 1945), therefore those from the Fleet pluton are very enriched.

Analyses plotted on a Rb, Li (x 10), Sr ternary diagram (Fig. 50) show two trends; the coarse grained granite feldspars increase in Li relative to Rb and Sr, and the Rb-rich feldspars from the fine grained granite become depleted in Sr relative to Li and Rb.

The mean Be content of the feldspar/quartz fraction is 6 ppm (range 3 to 13 ppm), most of which is contained within the lattice of plagioclase (Hörmann, 1969).

Amounts of Y increase with fractionation (Fig. 49, range 4-21 ppm, mean 12 ppm) and are enriched relative to Y analyses quoted from plagioclase and K-feldspar in a leucogranite from Southern California (8.5 ppm and 4.7 ppm respectively, Towell *et al.*, 1965), although some Y may be contained within included apatite.

Cu varies within very narrow limits (10-13 ppm) and has a mean value of 11 ppm. Assuming approximately one-third of the mixtures are quartz, which is reasonable from data presented by Parslow (1964, 1971), and that this mineral is barren of trace elements (Bradshaw, 1967), the feldspars average about 16 ppm Cu. This is lower than the mean value (25 ppm) obtained by Bradshaw (1967), who demonstrated that no statistical difference is detectable in the Cu content of feldspars from mineralized and non-mineralized granites of Britain.



Zn concentrations of feldspar/quartz mixtures occur within the range 0 to 10 ppm and average 6 ppm. Accounting for quartz (above), a mean value of 9 ppm is obtained and is comparable to the mean Zn content of non-mineralized Caledonian granites (Bradshaw, 1967).

The Pb content of feldspars decreases with increasing fractionation, and K/Pb ratios vary inconsistently between 697 (1, 55-75 F) and 1272 (12, 58-70 F). Concentrations of Pb in the feldspar mixtures are not proportional to the amounts of K-feldspar ( $K_2O$ ) present and fluctuations in the K/Pb ratio are apparently the result of differences in amount of K-feldspar. K/Pb ratios of Fleet feldspars plot in the overlapping fields for mineralized and non-mineralized granites (Bradshaw, 1967), but it is apparent that these fields are determined more by %K than a combination of the two variables.

The pegmatitic quartz/feldspar mixture (73/517 F) is more closely allied to those from the coarse grained granite with respect to  $K_2O$ ,  $Na_2O$  and  $CaO$ , but shows comparable variations in trace element chemistry (Rb, Li, Sr, Zr) with felsic mixtures from the fine grained granite (Fig. 50).

#### v. Conclusions

Trends in the major and trace element chemistry of biotites, chlorites, muscovites and feldspars have been presented and are generally consistent with those presented elsewhere (e.g. Nockolds and Mitchell, 1946; Foster, 1960; Lange et al., 1972). Minerals from the Fleet granite also show many similarities in trace element chemistry to

the mineralized granites of Cornwall (Bradshaw, 1967). One reservation to Bradshaw's approach is that comparisons or contrasts are made between mineralized Hercynian granites from Cornwall and non-mineralized Caledonian granites from Northern England and Scotland. A more useful exercise would have been to characterise mineralized granites by comparison with non-mineralized granites of the same age and from the same batholith. Many of the trends in chemistry observed within the Fleet pluton and by Bradshaw (1967) in the Cornish granites, are undoubtedly the results of a high degree of fractionation, which itself may be, but is not necessarily indicative of mineralization.

#### D. Areal variations in bulk chemistry and mesonormative minerals.

It has been mentioned previously that variations in bulk major oxide chemistry in the Fleet pluton are fairly small (see section B above, table 9). Likewise, many variations do not form simple trends from margin to centre as in the Criffell-Dalbeattie pluton (Stephens, 1972) because of, i) the non-concentric distribution of the coarse grained biotite facies, ii) the slight overlap in the fractionation trend between the coarse grained and later fine grained granites (Figs. 38 and 40) and iii) the occurrence of a late stage alkali metasomatism and/or hydrothermal event. Percentage fits of trend surfaces (table 13) therefore tend to be low, and many are significant only at higher orders, compared to those of Stephens (1972).

##### (i) SiO<sub>2</sub>

SiO<sub>2</sub> increases towards the centre of the pluton in

relation to the increase in amounts of quartz and alkali feldspars over An-plagioclase and biotite. The contour map shows that the distribution is more complex than that given by the 2nd order trend surface (Fig. 51). Values of  $\text{SiO}_2$  less than 72.30% correspond approximately to areas covered by the coarse grained biotite facies. The gap in the marginal coarse grained facies of Parslow (1964, 1968) is indicated by higher (greater than 73.71%  $\text{SiO}_2$ ) concentrations in the northwest. Decreases in the  $\text{SiO}_2$  content of biotite and chlorite with increasing fractionation, do not affect the overall trend because they are minor compared to increases in quartz and feldspar.

(ii)  $\text{TiO}_2$

Most of the  $\text{TiO}_2$  in the granite is contained within biotite, chlorite, muscovite and ilmenite. The  $\text{TiO}_2$  content of biotite does not appear to decrease with increased fractionation, as it does in muscovite (section C, above). Overall reduction of  $\text{TiO}_2$  relates to its depletion in muscovite and reduction in total amounts of biotite (Fig. 52). The 3rd order trend surface shows the break in the more basic marginal facies towards the northwest (cf. Figs. 38 and 40).

(iii)  $\text{Al}_2\text{O}_3$

The  $\text{Al}_2\text{O}_3$  distribution is complex and does not form a significant trend surface (Fig. 53). Cluster analysis (see section B, above, Fig. 42) demonstrates a slight decrease in the mean  $\text{Al}_2\text{O}_3$  content of clusters with increasing Differentiation Index.  $\text{Al}_2\text{O}_3$  is contained within all essential minerals except quartz, and changes in the relative quantities of these will result in

fluctuations in its concentration. Increase in fractionation promotes higher  $\text{Al}_2\text{O}_3$  contents in micas, but lower contents in feldspars, owing to a decrease in the anorthite molecule in plagioclase. Hydrothermal alteration may also redistribute some of the  $\text{Al}_2\text{O}_3$  in feldspars as secondary muscovite. The interrelationship of all these factors coupled with the small variation in total  $\text{Al}_2\text{O}_3$  (less than 3%), is responsible for the distribution obtained.

(iv) FeO

Variations in amounts of FeO are controlled by the distribution of biotite and chlorite, and to a lesser extent muscovite and Fe-Ti oxides. FeO increases with fractionation in biotite (and chlorite) but decreases in muscovite (section C, above). As a result of an overall lowering in the quantity of biotite during crystallization, FeO decreases in amount towards the centre of the pluton (Fig. 54). The distribution of areas with FeO greater than 1.56% approximates to the outcrop of the coarse grained biotite granite. The presence of more muscovite-rich granites in the north-west are responsible for depressed FeO values in this region.

(v) MnO

Very little variation in MnO concentration is apparent from the contour map (Fig. 53), or the means of the clusters (Fig. 42). Although MnO is enriched in biotite, chlorite and muscovite during fractionation, it also occurs in apatite and substituting for  $\text{Ca}^{2+}$  and  $\text{Na}^+$  in plagioclase (Nockolds and Mitchell, 1946). Lack of significant variation is the consequence of the inverse

relationship between muscovite and biotite, apatite or plagioclase.

(vi) MgO

As with FeO, MgO concentrations are related to the presence of ferromagnesian, the MgO contents of which decrease during fractionation (section C above, Fig. 55). Areas with MgO greater than 0.75% on the contour map correspond approximately to the coarse grained biotite granite outcrop.

(vii) CaO

CaO is contained within the lattice of the anorthite component of plagioclase and apatite, both of which decrease in amount during progressive crystallization (Fig. 56).

(viii) Na<sub>2</sub>O

No overall trend emerges from the complicated Na<sub>2</sub>O distribution (Fig. 57). It is primarily dependent on the amount and composition of plagioclase. Little variation occurs among clusters 1, 2 and 3 (Fig. 42), and the separated feldspars show an initial decrease followed by a slight increase in Na<sub>2</sub>O in the more highly fractionated coarse grained biotite-muscovite granites (section C, above). Superimposed upon this are the effects of a probable late stage alkali metasomatism in the centre of the pluton. It is enrichment of Na<sub>2</sub>O in feldspars at both ends of the fractionation trend which destroys any significant simple areal trend.

(ix) K<sub>2</sub>O

Variation in K<sub>2</sub>O content of the clusters is small (Fig. 42). As a result of alteration, amounts of K<sub>2</sub>O in

biotites decrease towards the centre of the pluton (Fig. 44), but no such variation has been observed with muscovite. The  $K_2O$  content of feldspars increases from the coarse grained biotite facies to the coarse grained biotite-muscovite facies, and subsequently decreases towards more highly fractionated rocks (Fig. 49). This relatively simple variation is complicated by the presence of large quantities of  $K_2O$ -rich biotite at the margins and muscovite in the centre of the pluton. The hydrothermal breakdown of microcline and biotite will have provided much of the  $K_2O$  in secondary muscovite, and this post-magmatic redistribution has given rise to a complex distribution (Fig. 57).

(x)  $P_2O_5$

Amounts of  $P_2O_5$  depend solely upon apatite and monazite (if present). The mean  $P_2O_5$  content of clusters 1 to 3 (Fig. 42) shows a normal trend of decreasing values with higher Differentiation Index. In cluster 4, which is represented by only two samples, a slight enrichment is apparent and in part complicates any simple trend (Fig. 57).

(xi) Lithium

Li is contained within many rock-forming minerals, and behaves differently within them during fractionation. Consequently its distribution is complex, and a trend surface is significant only at the sixth order (Fig. 58).

$Li^+$  probably substitutes for  $Mg^{2+}$  in octahedral sites in micas, due to their similar ionic radii ( $Li^+ = 0.68\text{\AA}$ ,  $Mg^{2+} = 0.66\text{\AA}$ ) and electronegativity (Goldschmidt, 1954; Krauskopf, 1967). It is likely that substitution

also takes place with octahedral  $\text{Fe}^{2+}$  ions although they have a larger ionic radius ( $0.74\text{\AA}$ ). As both  $\text{Fe}^{2+}$  and  $\text{Mg}^{2+}$  are divalent their charge densities are greater than univalent  $\text{Li}^+$ , and are consequently preferentially taken up in lattice positions during crystallization. Charge deficiencies due to the univalent state of the  $\text{Li}^+$  ion are made up by substitutions of  $\text{Fe}^{3+}$  and  $\text{Al}^{3+}$  for octahedral divalent ions (e.g.  $\text{Fe}^{2+}$ ,  $\text{Mg}^{2+}$  and  $\text{Mn}^{2+}$ , Figs. 43 and 47). In feldspars  $\text{Li}^+$  could substitute for  $\text{Na}^+$ ,  $\text{K}^+$  or  $\text{Ca}^{2+}$  only with great difficulty due to its smaller ionic size. Some of the Li in these minerals is undoubtedly in the lattice of enclosed secondary sericite or muscovite.

As expected from the discussion above, the Li content of muscovite increases with the acidity of the host rock (section C, above). Li is also enriched in late stage biotite and feldspars in the coarse grained granite, but depleted in the fine grained mass. This drop in Li content in the later granite is probably a result of increased crystallization of both primary and secondary muscovite.

The bulk of Li in the coarse grained granites is held within the lattice of biotite, but in the central granite it is mostly in muscovite. Therefore the overall content of Li in the three main geochemical clusters does not vary significantly (Fig. 42), but there is a slight enrichment in the granite affected by late magmatic, metamorphic and/or hydrothermal processes. None of the trends described above is dominant and they generally interfere with each other and result in the observed distribution (Fig. 58).

(xii) Rubidium

Rb, like Li, is contained within the lattices of feldspar (microcline), biotite and muscovite, wherein it substitutes for K. Although both micas contain more Rb than the feldspar, the bulk of Rb in the granite is held within microcline, as a result of its greater abundance. Trends in the Rb content of biotite tend to be erratic (appendix 7), but a steady enrichment occurs in late stage muscovite and feldspar (section C, above).

$\text{Rb}^+$  has a slightly larger ionic radius than  $\text{K}^+$ ,  $1.47\text{\AA}$  and  $1.33\text{\AA}$  respectively, although their electronegativities are the same (Krauskopf, 1967). As a result of its smaller size and higher charge density,  $\text{K}^+$  is expected to be taken into lattice sites in preference to  $\text{Rb}^+$ . Rb is therefore concentrated in the residual melt, as is demonstrated by a decrease in K/Rb ratios in all K-bearing minerals, with fractionation.

The second order trend surface (Fig. 59) gives an impression of the normal concentration of Rb due to the processes of fractionation. It is obvious, however from both the contour and residual maps that an area of very enhanced values is superimposed upon this. The area corresponds to that affected by alkali metasomatism, and contains granites with abundant primary and secondary muscovite, with  $\text{Rb}_2\text{O}$  contents between 0.16% and 0.18%. Feldspars are also enriched in Rb in this area (Fig. 49).

(xiii) Beryllium

Be shows little variation among clusters 1, 2 and 3, although a slight enrichment takes place with increasing



Differentiation Index, followed by more extreme enrichment in cluster 4 (Fig. 42). The mean value of Be in cluster 4 is 16 ppm, and is comparable with the average amount in albitised and muscovite-bearing granites (10 ppm, Beus, 1961), but is higher than biotite granites (5 ppm Be).

In accordance with previous research (Beus and Sobolev, 1963), Be appears to be slightly more enriched in both biotite and muscovite of the Fleet granite. Albite and muscovite have been reported to be the main carriers (ibid). Increased values of  $\text{Na}_2\text{O}$  in the felsic fraction of metasomatised fine grained granites are accompanied by an enhancement of Be to 13 ppm, compared with a mean of 6 ppm.  $\text{K}_2\text{O}$  rich felsic minerals from a pegmatite (73/517 F) are depleted in Be (2 ppm).

As a result of the very small size of the  $\text{Be}^{2+}$  ion ( $0.35\text{\AA}$ ) it is not easily incorporated into the lattices of rock forming minerals, and is therefore concentrated in residual liquids. This is apparent by the increase of Be in micas during fractionation (section C, above), and also by enrichment of Be in rocks affected by metasomatism.

#### (xiv) Strontium

Concentrations of Sr and Rb show an inverse relationship, the former decreases in amounts with higher fractionation, due to earlier crystallization of its host minerals, anorthitic plagioclase and apatite (Fig. 60).

$\text{Sr}^{2+}$  has a larger ionic radius ( $1.12\text{\AA}$ ) than  $\text{Ca}^{2+}$  ( $0.99\text{\AA}$ ), and as they have virtually the same electronegativity (Krauskopf, 1967)  $\text{Sr}^{2+}$  is expected to be

concentrated relative to  $\text{Ca}^{2+}$  in later stages of crystallization. Also because of its higher charge density it is incorporated into the lattice of plagioclase in preference to  $\text{Na}^+$ .

Ca/Sr ratios of feldspar therefore decrease towards the centre of the pluton (appendix 7), although in the altered rocks (samples 11 and 12, 57-69F and 58-70 F) Sr is depleted, and there is a consequent increase in the ratio.  $\text{Sr}^{2+}$  may also substitute for  $\text{K}^+$  in microcline (Nockolds and Mitchell, 1946), but this does not alter the trend significantly, as  $\text{Sr}^{2+}$  is taken up mainly in first formed crystals owing to its higher charge density.

(xv) Barium

$\text{Ba}^{2+}$  substitutes for  $\text{K}^+$  in potash feldspars as a result of their similar ionic size ( $1.34\text{\AA}$  and  $1.33\text{\AA}$  respectively) and electronegativity. Early crystallized feldspar will contain most of the  $\text{Ba}^{2+}$  due to its higher charge density. This accounts for the trend of decreasing Ba values towards the centre of the pluton (Fig. 61). Depletion comparable to that of Sr has taken place in the centre of the pluton.

(xvi) Yttrium

Although Y varies only slightly within most of the pluton, there is a marked enrichment in the rocks which have undergone extensive late stage alteration (Fig. 62).  $\text{Y}^{3+}$  (ionic radius  $0.92\text{\AA}$ ) may substitute for  $\text{Ca}^{2+}$  (ionic radius  $0.99\text{\AA}$ ) and is significantly enriched in apatite formed late in the crystallization sequence (Nockolds and Mitchell, 1946).

Y is concentrated in micas in the Fleet pluton (appendix 7), but  $P_2O_5$  and Zr contents are too low for it all to be contained within included apatite and zircon. It probably therefore occupies some lattice position, and enrichment at the centre of the pluton will be due to the presence <sup>of</sup> greater than normal quantities of muscovite. The slight but variable increase in Y in felsic minerals during fractionation is probably the result of enrichment of Y in enclosed apatite.

(xvii) Lanthanum

La occurs mainly in apatite and biotite in granites that do not contain monazite (Towell et al., 1965). Late stage apatites normally contain less La than those formed earlier in the sequence of crystallization (Nockolds and Mitchell, 1946). La decreases in amount during fractionation as a result of its early inclusion into biotite, apatite and  $Ca^{2+}$  lattice sites in plagioclase. Areas with low values of La (Fig. 63) correlate with the highest fractionated parts of the pluton, i.e. the centre and northwest margin.

(xviii) Cerium

The distribution of Ce in granitic minerals is affected by the same controlling factors as La above (Fig. 64). Areas of over 100 ppm Ce on the trend surface map closely correspond to the outcrop of the coarse grained biotite granite.

(xix) Neodymium

The distributions of the light rare earth elements, La, Ce and Nd tend to be comparable as a result of their similar ionic size (Fig. 65).

(xx) Zirconium

Zr concentrations are directly attributable to the amounts of zircon present in the granite. Zircon is an accessory mineral which forms early in the magmatic sequence and has been observed to decline in amounts during fractionation (see chapter 7, above). Consequently Zr is depleted in the highest fractionated rocks (Fig. 66).

(xxi) Nickel

Ni is concentrated in biotite, chlorite and muscovite but is not detected in the felsic fraction (section C, above).  $\text{Ni}^{2+}$  (ionic radius  $0.69\text{\AA}$ ) probably substitutes for  $\text{R}^{2+}$  (e.g.  $\text{Mg}^{2+}$ ,  $\text{Fe}^{2+}$ ) cations in micas due to their similarities in size. The Ni content of biotites decreases, and of muscovites increases with fractionation, but absolute abundances are higher in biotite (mean 68 ppm, excluding sample 10) than muscovites (mean 38 ppm). As a result of the breakdown of biotite secondary muscovite may contain more Ni than the primary mineral, and this redistribution is probably responsible for the complicated pattern obtained (Fig. 62).

(xxii) Copper

Whole rock Cu abundances do not vary significantly (Fig. 62). Cu is very slightly concentrated in biotite (mean 38 ppm), but it also occurs in muscovite and feldspar. Of these, muscovite is the only mineral to show a significant trend with respect to Cu concentration (Fig. 48), but this is masked by Cu in feldspar and biotite.

(xxiii) Zinc

The most important Zn-bearing minerals in the

granite are biotite and chlorite, which have means of 668 ppm and 970 ppm Zn respectively. Moderate amounts also occur in muscovite (mean 285 ppm) compared with the felsic minerals (mean 6 ppm).

$Zn^{2+}$  has the same ionic radius ( $0.74\text{\AA}$ ) as  $Fe^{2+}$  and is expected to fill octahedral lattice sites in micas after  $Mg^{2+}$  ( $0.66\text{\AA}$ ). This is reflected by an increase in both Fe and Zn in biotite during fractionation (Fig. 44), although a similar trend does not occur in muscovite. Consequently areal variations are controlled by amounts of biotite. Although the Zn-content of biotite increases with fractionation total amounts of biotite decrease and more than compensate for this, resulting in a Zn depletion in areas of highly fractionated granite, (Fig 67).

(xxiv) Lead

Pb is held within the lattice of potash-feldspar where  $Pb^{2+}$  (ionic radius  $1.20\text{\AA}$ ) substitutes for  $K^+$  ( $1.33\text{\AA}$ ). The Pb content of the feldspar fraction in the coarse grained granite is variable, but a decrease takes place in feldspars of the fine grained granite during fractionation. Chlorite, however, contains over 100 ppm Pb in the fine grained granite and will compensate for the low values of Pb in the felsic minerals.

Variations in the bulk Pb concentration tend to be low, and this coupled with redistribution by hydrothermal processes has destroyed any simple primary magmatic trend (Fig. 53).

(xxv) Mesonormative minerals.

Trend surface maps of mesonormative minerals

(appendix 5) show some of the variations in mineralogy expected from investigations into the petrology and geochemistry of the pluton.

The second order trend surface of mesonormative quartz (Q) (Fig. 68) increases towards the centre of the pluton, and compares with a trend surface of modal quartz reported earlier (Parslow, 1971, p. 44). The trend is slightly off centre owing to the highly fractionated granite close to the northwest margin (cf. Fig. 38).

The distribution of mesonormative orthoclase (Or) is complex (Fig. 69) because amounts of microcline initially increase and subsequently decrease during fractionation. Also Or values are too high in the muscovite-rich granites as  $K_2O$  in muscovite cannot be accounted for in the mesonormative calculation procedure.

The occurrence of albite is controlled by two processes. A primary magmatic trend results in a decrease in the albite molecule in plagioclase during crystallization. Superimposed upon this, in the Fleet pluton, is a late stage process of albitization or alkali metasomatism, reflected by high values of mesonormative albite (Ab) at the centre of the pluton (Fig. 69).

Although trend surface analysis of mesonormative anorthite (An) has produced a significant surface at a high order (6th), the magmatic trend of decreasing an-plagioclase is apparent. The high order surface is the result of a rapid initial depletion of anorthite (see section C, above), followed by a more gradual lowering in amounts with further fractionation, (fig 70).

The trend surface of mesonormative biotite (Bi) is

comparable with the distribution of the various facies (Figs. 38 and 71). Areas containing biotite (Bi) in excess of 5.61% correlate with the coarse grained biotite granite. Amounts of biotite (Bi) computed from analyses of muscovite-bearing granites tend to be high, because all MgO and FeO is placed in biotite (Bi), whereas some is contained within muscovite.

Mesonormative corundum (Co) gives an indication of the amount of muscovite that could be present as a result of excess  $Al_2O_3$ . Low values (less than 1.69%) occur in marginal areas (Fig. 69), but also in the area of altered granite in the centre of the pluton. This is due to high concentration of  $Na_2O$  in this area, resulting in additional  $Al_2O_3$  required to make albite (Ab) in the normative calculation. Secondary processes have modified any simple trend expected from investigations into the petrology.

Mesonormative sphene (Sp) is calculated from all the  $TiO_2$  in the analyses, though most of the  $TiO_2$  is probably contained within biotite and muscovite. Consequently the trend surface obtained (Fig. 72) is broadly comparable to that of  $TiO_2$  (Fig. 52, above).

The trend surface of mesonormative apatite (Ap) is consistent with the trend expected on petrological grounds (Fig. 73).

#### (xxvi) Differentiation Index

As mentioned previously the Differentiation Index (Thornton and Tuttle, 1960) gives an impression of the extent to which the processes of magmatic differentiation or fractionation have taken place. Both contour and trend surface maps compare favourably with the distribution of

various facies within the pluton (Figs. 38 and 74). Areas with an index lower than 87.6 closely correspond to the outcrop of the coarse grained biotite granite, and those above 92.1 cover most of the fine grained granites, but also some of the more fractionated coarse grained rocks.

All indices are above that for average granite (80) and approach or exceed the value for average alkali granite (93, Thornton and Tuttle, 1960). This is consistent with the highly fractionated nature of the Cairnsmore of Fleet granite and its chemical proximity to the granite residual system,  $\text{SiO}_2\text{-NaAlSi}_3\text{O}_8\text{-KAlSi}_3\text{O}_8$  (D.I. = 100).

E. Variation between geochemical variables and meso-normative minerals

Matrices of the significant product moment correlation coefficients of the chemical and normative data in clusters 1, 2 and 3 and the total of these, are provided on figures 75 to 78. The two samples representing cluster 4 have not been included for correlation purposes, as much of their chemistry is considered to be the result of late or post-magmatic processes, rather than normal fractionation.

More correlations are significant for the total set compared to clusters 1 to 3, owing to its greater overall variation. In many cases clusters appear as groups without having any significant internal correlation.

In general, variations between both elements and mesonormative minerals are consistent with those expected from the normal processes of fractionation, and therefore only a few of the more significant pairs will be alluded to.



FeO and CaO of the total data set both have positive correlations with MgO (Fig. 79). In each case samples in cluster 1 plot at the upper end, and clusters 3 and 4 at the lower end of the best fit line. This indicates the depletion of the melt in these oxides as a result of earlier crystallization of biotite and an-plagioclase. The importance of the variables Ce and MgO in the cluster analysis classification is displayed by the absence of overlaps between clusters in the scatter diagram (Fig. 79). Positive correlations exist between MgO and both Ce and Zr, and all three clusters have significant internal correlations between Zr and MgO.

The Zr- $P_2O_5$  diagram shows a different trend (Fig. 79). The total data set (i.e. clusters 1 to 3) has a positive correlation which is consistent with depletion both of zircon and apatite during fractionation. However the samples in cluster 3 have a reverse trend which explains the complex nature of the areal distribution of  $P_2O_5$  (see section D, above).

$SiO_2$  is the basic co-ordinate of Harker diagrams designed to show changes in chemistry with acidity. As expected there is a negative correlation between  $SiO_2$  and Sr (Fig. 79), due to the uptake of the latter in early formed minerals.

Bivariate plots of trace elements illustrate some of the extreme differences existing between cluster 4 and the rest of the sample set (Fig. 80). Invariably cluster 3, containing highly fractionated coarse grained granites and fine grained granites, falls on the overall chemical

trend. However the Sr-Rb diagram shows that there is no significant difference in Rb content between clusters 2 and 3, which may be explained with reference to the chemistry of the felsic fraction (see section C, above). The Rb content of feldspar does not increase continuously with fractionation, but reaches a maximum of about 200 ppm (Fig. 49). Only in the samples of cluster 4 (11 and 12, Fig. 49) does enrichment occur as expected from a continuation of the chemical trend initiated in clusters 1 and 2.

The positive correlation between mesonormative biotite (Bi) and Zr is consistent with trends taking place during fractionation (Fig. 81). As described earlier (section D, above) biotite contains most of the Zn and Ce in the granite, as indicated by their positive correlation (Fig. 81). Mesonormative orthoclase (Or) generally increases with falling biotite content. It might be expected from the trends in the chemistry of feldspars (section C, above) that biotite and orthoclase would have a positive correlation. This reversal of the forecast is due to the fact that the only K-bearing minerals of the mesonorm are orthoclase (Or) and biotite (Bi), and it is not strictly appropriate for muscovite-bearing granites. Correlations within each cluster on the mesonormative orthoclase (Or)-quartz (Q) diagram more closely correspond to the variations expected from data presented earlier (section C, above).

Mesonormative albite (Ab) and biotite (Bi) decrease in the samples of cluster 1 (Fig. 81), but an inverse trend

occurs in cluster 2. This is probably the result of albitization of some of the coarse grained biotite-muscovite granites. Little albite (Ab) variation is seen in cluster 3, but extreme enrichment occurs in cluster 4. This is consistent with the chemistry of the felsic mineral fraction (see section C, above). Within clusters 1 to 3 there are negative correlations between mesonormative albite (Ab) and quartz (Q), and the gradient of the best fit line i.e. the variation in albite (Ab), decreases from cluster 1 to 3 (Fig. 82). Albite-rich samples from clusters 2 and 4 have probably undergone alkali metasomatism, as mentioned above.

The Differentiation Index (D.I.) is a useful quantity to use in variation diagrams as it is based upon sound petrological principles (Thornton and Tuttle, 1960). Correlations between D.I. and  $\text{SiO}_2$ , FeO, MgO, CaO and mesonormative biotite (Bi) illustrate some of the trends occurring during fractionation (Fig. 82). Variation diagrams between D.I. and Ce, Sr, Zr and Ba show the extreme depletion of these elements in cluster 4 (Fig. 83). Again Rb shows enrichment in cluster 4 far above values expected from the normal chemical trend in clusters 1 to 3 (Fig. 83).

As modal data <sup>are</sup> ~~is~~ not available, CIPW-normative quartz (Q), orthoclase (or) and plagioclase (ab + an) have been plotted on the ternary diagram recommended by the IUGS Subcommittee on the Systematics of Igneous Rocks (Fig. 84). Most of the analyses plot close to the centre of the triangle, in granite subfield B, and therefore may be classified as monzogranite or adamellite.

Variation among  $\text{Na}_2\text{O}$ ,  $\text{K}_2\text{O}$  and  $\text{CaO}$  in feldspars has already been discussed (section C, above, Fig. 50). The distribution of whole rock analyses on the ternary  $\text{Na}_2\text{O}$ ,  $\text{K}_2\text{O}$ ,  $\text{CaO}$  diagram is comparable but displaced towards the  $\text{K}_2\text{O}$  apex, as a result of additional amounts of this oxide obtained from micas (Fig. 85). Fields of each petrological type overlap but nevertheless form a discernable trend comparable with the feldspars.

Rb, Ba and Sr show a simpler trend of enrichment in Rb over Ba and Sr during fractionation (Fig. 85). A comparable trend is illustrated on Figure 86, among Rb, Sr and Zr. Significant overlap between the coarse and fine grained rocks is restricted to the coarse grained muscovite-biotite facies.

## CHAPTER 9

CRYSTALLIZATION OF THE GRANITE IN RELATION TO EXPERIMENTAL  
MINERALOGICAL STUDIES.A. The system  $\text{NaAlSi}_3\text{O}_8\text{-KAlSi}_3\text{O}_8\text{-SiO}_2\text{-H}_2\text{O}$ 

Fleet analyses fall in a field on the feldspar-quartz eutectic in the system  $\text{NaAlSi}_3\text{O}_8\text{-KAlSi}_3\text{O}_8\text{-SiO}_2\text{-H}_2\text{O}$ , at the  $700^\circ\text{C}$  liquidus isotherm with an  $\text{H}_2\text{O}$  pressure of 2000 bars (Fig. 87A; Tuttle and Bowen, 1958). Under isothermal conditions ( $755^\circ\text{C}$ ) in the same system, they occur away from the ternary minimum and the highest density of points plots on quartz-alkali feldspar boundary curve again at 2000 bars (Fig. 88A). The field containing Fleet samples is displaced towards the or apex compared with the area of highest concentration of rocks with more than 80% normative ab + or + Q from Washington's Tables. Higher normative or content is due to the presence of micas in the granite. Coincidence of the bulk of granite analyses with the minimum is, according to Tuttle and Bowen (1958) evidence for the importance of crystal-liquid equilibria in the formation of acid igneous rocks.

B. The system  $\text{NaAlSi}_3\text{O}_8\text{-KAlSi}_3\text{O}_8\text{-CaAl}_2\text{Si}_2\text{O}_8\text{-SiO}_2$ 

In a section cut through the  $\text{CaAl}_2\text{Si}_2\text{O}_8\text{-NaAlSi}_3\text{O}_8\text{-KAlSi}_3\text{O}_8\text{-SiO}_2$  tetrahedron at An3, Fleet analyses plot in the field of potash feldspar adjacent to the two feldspar boundary curve at 1000 bars (Fig. 87B; James and Hamilton, 1969). A comparable position is obtained on the an-ab-or face of the tetrahedron containing the univariant curve projected from the Q saturated surface (Fig. 88 B). Most granite analyses plot to the left of the two-feldspar curve

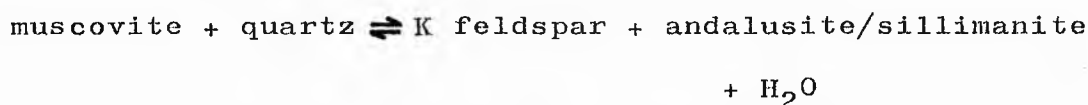
and the position of Fleet analyses is probably the result of enhanced or values due to factors mentioned above. However, this system has been investigated at pressures lower than those relevant during crystallization of the Fleet pluton. An increase in pressure trends to depress the quartz-feldspar boundary curve away from the Q apex, and to shift the two-feldspar curve towards the ab apex (Fig. 88A). This would result in the Fleet analyses occupying a position straddling the quartz-potash feldspar boundary curve, comparable to that in Figure 88A, but completely to the right of the two-feldspar curve and in the potash feldspar field in Figure 88B.

Truly residual acid plutonic rocks formed completely by fractionation processes are restricted to the field of plagioclase feldspar (Carmichael, 1963; Barth, 1965). Rocks which plot in the primary field of quartz or potash feldspar probably do not represent derivatives from a more basic magma, unless they have been modified by assimilation of acid material (Carmichael, 1963). Compositions of liquids produced by melting of sedimentary rocks such as greywacke and shale, obey crystal-liquid equilibria which can be predicted from the synthetic system Ab-Or-An-Q-H<sub>2</sub>O (James and Hamilton, 1969). Melts of similar composition may produce granitic liquids (Ab/Or equal or less than unity) at one kilobar, and granodioritic liquids (Ab/Or larger than unity) at five kilobars. Rocks of the Fleet pluton and the Southern Uplands batholith are therefore probably the products of melting of Lower Palaeozoic and ?earlier sedimentary rocks deep in the Caledonian orogen.

### C. Muscovite

Parslow (1971), following Yoder and Eugster (1955) and Velde (1964), has suggested that the presence of primary muscovite is due to crystallization from a granitic melt, with sufficient  $Al_2O_3$  and depleted FeO and MgO, at an external confining pressure and/or an internal intrusive pressure maintained above 2 kbar ( $\approx$  7.5 km depth). The relationship of the breakdown curve of muscovite to the minimum melting curve of granite shows that it is only possible for muscovite to form on the liquidus of the granite system above 1500 bars. Below this pressure muscovite can only form in the solid state (Yoder and Eugster, 1955, p. 267).

However, Evans (1965, p. 660) has demonstrated that muscovite in equilibrium with quartz requires a  $PH_2O$  of at least 3.5 to 4.0 kbar for crystallization. The intersection of the quartz stability curve:



intersects the granite melting curve above 4 kbar.

It appears therefore that a much higher  $PH_2O$  is required for crystallization of primary muscovite than earlier considered necessary. Yoder and Eugster (1955) point out that muscovite-bearing granites are usually those containing two feldspars (K-feldspar and plagioclase). If the water vapour pressure is as high as is evidently required for crystallization of muscovite, then feldspar solidus curves in the system  $NaAlSi_3O_8 - KAlSi_3O_8 - CaAl_2Si_2O_8$  will be depressed, allowing crystallization of two

feldspar phases to take place (Tuttle and Bowen, 1958).

The presence of secondary muscovite both as fine grained sericite and hydrothermal muscovite can be accounted for by leaching of  $K_2O \cdot 0.6SiO_2$  from K-feldspar. At low pressures i.e.  $PH_2O$  less than total pressure, this can take place in the solid state. The muscovite breakdown curve lies at lower temperatures, and the minimum melting curve of granite at higher temperatures, than those indicated for  $PH_2O =$  total pressure (Yoder, 1955; Yoder and Eugster, 1955).

#### D. Biotite

Experimental evidence suggests that the stability of biotite is dependant upon its composition. Fe-biotite is not stable in granitic liquids below 4 kbars if F and Ti contents are low (Rutherford, 1969), and the stability field of the assemblage Fe biotite-alkali feldspar is reduced by Na substituting for K. The Al content of biotite is a function of temperature,  $PH_2O$  and  $fO_2$ , and Al-rich biotite is stable on the minimum melting curve for syenite at fluid pressures as low as 1 kbar (Rutherford, 1973). An increase in  $PH_2O$  decreases the Al content of any biotite on the solidus.

All the above data have been deduced from experiments with synthetic biotite, and are of limited use in the determination of physical conditions in natural systems. Biotite from the Fleet granite contains Al and Ti, and probably F. However, the fact that alkali metasomatism i.e. a high Na feldspar activity, may cause biotite to completely break down (Rutherford, 1969) is consistent with petrographical observations made on the fine grained



granite (see chapter 7, E-H).

### E. Conclusions

The Fleet pluton is a typical subsolvus granite (Tuttle and Bowen, 1958) because:

1. most of the Na is present as discrete albite or albite-oligoclase crystals,
2. it does not contain a Na-Fe amphibole or Na pyroxene,
3. it is a large plutonic mass,
4. it contains both biotite and muscovite.

Tuttle and Bowen (ibid) suggest that subsolvus granites are metasomatic in origin, and formation of two feldspars may be due to unmixing in the solid state, aided by the presence of volatiles (e.g.  $H_2O$ ). The texture of the Cairnsmore of Fleet granite, however, indicates magmatic crystallization of both plagioclase and potash feldspar, with later unmixing of microcline to form microperthite in the solid state. Contents of CaO were evidently high enough to allow the crystallization of primary plagioclase (Parslow, 1964).

High concentrations of  $H_2O$ , i.e. enough to saturate the acid magma during slow cooling, will depress the two feldspar solvus in the system  $NaAlSi_3O_8$ - $KAlSi_3O_8$ - $CaAl_2Si_2O_8$ , and allow crystallization of two feldspars from a melt with a comparable composition to Fleet granites in this system (Fig. 88B). Continued slow cooling coupled with factors described previously (chapter 7, H, above) promote extensive exsolution of albite from K-feldspar on intersection of the alkali feldspar solvus. Therefore two generations of feldspar exist; a primary magmatic and a secondary exsolution product (Carmichael, Turner and

Verhoogan, 1974).

The mineralogy, texture and chemistry of the Cairnsmore of Fleet granite corroborate the existence of high H<sub>2</sub>O vapour pressures during crystallization. The hydrous nature of the melt is most obviously demonstrated by the presence of copious quantities both of primary and of secondary mica. Late stage processes, such as alkali metasomatic and hydrothermal breakdown of primary minerals, and the intrusion of pegmatites and aplites are consistent with this.

## CHAPTER 10

## THE MINOR INTRUSIVE SUITE.

A. Introduction

A selection of the minor intrusive rocks surrounding the Cairnsmore of Fleet granite have been investigated in this work. Most show signs of the alteration previously reported (Blyth, 1949; Phillips, 1956) to be so characteristic of the dyke rocks in Galloway. Albitization results in the alteration of plagioclase in porphyritic microdiorites and lamprophyres, to epidote, albite and quartz. Ghosts of original feldspar phenocrysts remain, but mafic minerals are more or less completely altered to chlorite (penninite), and secondary sericite or muscovite are characteristic. The passage of solutions rich in volatiles and  $\text{Na}_2\text{O}$  has been proposed as the mechanism of this breakdown (Phillips, 1956).

B. Lamprophyres(i) Spessartites

These melanocratic grey-blue dyke rocks are often difficult to distinguish from vertically bedded low grade greywacke hornfels. In hand specimen they invariably display patchy diffuse lighter areas, marking the positions of pseudomorphs of altered plagioclase.

Original hornblende in the Drumcleigh dyke (24585720, map 2) is altered to tremolite and epidote and surrounds plagioclase phenocrysts, which have been altered to sericite and/or paragonite. The groundmass shows fewer signs of alteration although fine grained clinozoisite or epidote occur. Some albitized plagioclase is very fresh, the rest is altered and indeterminate.

The spessartite in Waterside dyke (26085810, map 4) is much fresher and more even grained. Greenish-brown pleochroic hornblende is the dominant mafic constituent, and occurs in crystals up to 1 mm in length, in a groundmass of zoned plagioclase laths and hornblende. Primary porphyritic plagioclase crystals are rimmed by tangentially orientated hornblende crystals, and are replaced by calcite, quartz and antigorite. Interstitial antigorite also occurs in pale green to colourless fibrous aggregates. Calcite, opaque Fe and Ti oxides and sphene are common throughout the groundmass.

(ii) Kersantites

Biotite is the dominant ferromagnesian in the kersantite dykes, and has usually crystallized in aggregates which are slightly altered to chlorite.

The dyke adjacent to Drumlawhinnie Loch (24645698, map 1) contains biotite with a pale brown to pale straw-yellow pleochroism, and is associated with tremolite-actinolite amphibole. Plagioclase is altered to white mica, but where fresh has a composition of approximately An 30. Edges of crystal laths in contact with quartz are usually embayed and occasionally granophyrically intergrown. Quartz crystals invariably display undulose extinction as a result of strain during or after crystallization. Numerous crystals of sphene and apatite are present in a kersantite alongside the Grey Mare's Tail Burn (24875732, Map 2), the latter reaching lengths of 1 mm. Secondary minerals include antigorite and clinozoisite, and the latter when enclosed by biotite may be surrounded by a pleochroic halo, owing to the presence

of radioactive elements such as U and Th. Large amounts of calcite are present in the interstices between feldspars and biotite aggregates.

A pale pink weathering, highly altered dyke rock, intruded along a strike fault zone west of Cumloden (24165676), was probably originally a lamprophyre. The original texture has been completely destroyed and feldspars are altered to calcite, sericite/muscovite, antigorite and kaolinite. Plagioclase feldspar, which is present in large amounts, appears to have undergone albitization. Any original ferromagnesian minerals have been completely removed, and the only other minerals present are opaque Fe-Ti oxides, pyrite, sphene and strained interstitial quartz.

The dyke adjacent to the Grey Mare's Tail Burn (above) contains a pale grey-green leucocratic portion of more albitized kersantite. Biotite is completely converted to chlorite and associated with opaque minerals, sphene, epidote and clinozoisite. Altered plagioclase is generally albitic in composition, between An8 and An10. Approximately equal amounts of quartz, potash feldspar and plagioclase make up 95% of the rock. Intergrowths of a granophyric type are developed between quartz and both plagioclase and potash feldspars. Plagioclase commonly has embayed edges against quartz, and the intergrowths appear to be an intermediate stage in total quartz replacement. Both types of feldspar are altered to white mica and replaced by calcite, which also occurs in veins.

#### C. Porphyritic microdiorite

The only porphyritic microdiorite (porphyrite)

recognised in this survey outcrops as a dyke on Glenquicken Moor (25165586, map 8), 5 km south of the granite contact. Indeterminate feldspars occur as subhedral phenocrysts with embayed edges, and are intergrown with quartz. All original ferromagnesian minerals have been altered to chlorite or globular anhedral aggregates of epidote and sphene. Interstitial quartz is strained and feldspars in the groundmass are altered to sericite and muscovite.

#### D. Talnoy diorite sill.

A thermally metamorphosed sill of intermediate composition occurs in hornfelsed greywacke close to the contact of the granite, near Talnoy (24785703, map 3). It is obviously pre-granite in age, and is cut at its southern extremity by a fault, along which a mineralized vein containing pyrrhotite, chalcopyrite, pyrite and Co-Ni arsenides, has been emplaced (see chapter 13, below).

Away from the zone of alteration of this vein the rock contains biotite with a red-brown to colourless pleochroism, and (ferro-) actinolite which is pale green to colourless. Sphene is invariably associated with aggregates of these minerals. Plagioclase has an average composition of An 32, and has embayed and intergrown edges with quartz. Sericite and epidote occur sporadically as a result of hydrothermal alteration.

#### E. Clanery Hill ultrabasic intrusion

A dark greenish-grey intrusive rock of ultrabasic composition is exposed on Clanery Hill (24875630), but its relationship with the surrounding greywacke hornfels is unknown. It is pre-granite in age and has been transformed

by thermal metamorphism to a rock with a hornblende-hornfels facies mineralogy (see chapter 5, above). Radiating aggregates of tremolite and talc are the dominant minerals, with subordinate red-brown to nearly colourless biotite/phlogopite. Sphene occurs in subhedral aggregates, and small amounts of interstitial quartz and heavily altered plagioclase feldspar are also present.

#### F. Geochemistry

The chemistry of the Drumcleigh spessartite (73/I 854, appendix 6) is similar to the spessartite quoted in Phillips (1956, p. 115, analysis 4), from the Criffell-Dalbeattie area. Major differences are the higher  $\text{SiO}_2$  content and lower  $\text{Al}_2\text{O}_3$  and  $\text{CaO}$  contents of the former. A less albitized kersantite (72/I 220B) contains lower concentrations of  $\text{SiO}_2$  and higher concentrations of  $\text{MgO}$  and  $\text{FeO}$ . Amounts of  $\text{SiO}_2$  and  $\text{Na}_2\text{O}$  tend to increase during albitization, and  $\text{MgO}$  and  $\text{FeO}$  are removed owing to the breakdown of ferromagnesian minerals. The highly altered lamprophyre from Cumloden (72/I 140) has enhanced values of alkalis compared to the less altered members of this suite.

The porphyritic microdiorite exposed on Glenquicken Moor (73/I 762) has a lower  $\text{K}_2\text{O}$  content than an analysis of a similar rock cited by Phillips (ibid. analysis 1), but is comparable in all other respects. The chemical characteristics of the diorite at Talnotry have certain features in common with both basic and intermediate rocks, and are described more fully below.

Comparison of the CIPW-normative feldspar compositions of the granite and minor intrusive rocks, on a

ternary an-ab-or diagram, shows a trend of decreasing acidity from the ab-or sideline towards the an apex. The effects of albitization displace points towards the ab apex (e.g. 220B and 221, Fig. 89). Alteration of the Talnoy diorite (004A and B, Fig. 89) is accompanied by a comparable alkali enrichment, but at this locality it is associated with hydrothermal processes.

The intrusive rocks all lie on a trend with increasing fractionation from the Sr apex to the Rb apex of a Rb-Sr-Zr ternary diagram. Zr reaches its peak of relative enrichment in rocks of more intermediate composition.

The chemical composition of the Talnoy diorite is comparable with the hornblende hybrid of the colourless or brown amphibole stages of the Cairnsmore of Carsphairn igneous complex (Deer, 1935, analyses 12 and 13). Mixing of tonalite with an earlier basic intrusion has been proposed as a mechanism for the production of these hybrids. The tonalite of this intrusion is also considered to be a hybrid produced as a result of the mixing of gabbro and granite at greater depths, and prior to intrusion (ibid).

However, rocks of dioritic composition may be produced by marginal contamination of granodioritic magma, in the roof-zone of the batholith. A shallow southward dipping roof-zone is exposed at the southern end of the Loch Doon pluton (Doig, 1972). Contamination of granodiorite by hornfelsed greywacke in this vicinity, has produced hypersthene diorite. Rocks of this type probably exist between the granitic parts of the batholith and the roof, at shallow depths between the Fleet and Loch Doon



plutons. The presence of granite at depths between 2.5 and 3.5 km in this area is indicated by geophysical evidence (Batraukh, 1975). It is envisaged therefore that the Talnotry diorite might represent material intruded from the contaminated margin of the roof zone, prior to the emplacement of the Cairnsmore of Fleet granite. Crustal dilatation above the batholith would promote the formation of tension fractures which could have acted as channelways for the igneous material.

The lamprophyres and porphyrites are either the same age or slightly younger than the granite. Alteration and albitization is very probably linked with the late stage metasomatic and hydrothermal processes taking place within the pluton.

## CHAPTER 11

## CONCLUSIONS AND INTRUSIVE HISTORY

Continental collision relating to the closure of the Southern Uplands Trough towards the end of the Silurian and the beginning of the Devonian, caused crustal melting and production of magma beneath the newly formed Caledonian orogenic mountain ranges (cf. Dewey, 1971; Mitchell and McKerrow, 1975; Weir, in prep). In response to decreased density as a result of melting, magma of granite-granodioritic composition migrated upwards through the earth's crust, and formed a high level batholith in the area of the Fleet, Doon and Carsphairn intrusions (Batraukh, 1975).

In a belt adjacent to the roof zone of the batholith, contamination of granodioritic magma resulted in the crystallization of more basic hypersthene diorites (Doig, 1972). Some of this material was intruded along fractures above the roof to form minor dioritic sheets.

Away from the influence of the marginal area the normal processes of fractional crystallization took place, with rocks of greater acidity crystallizing further away from the marginal more intermediate rocks. Crystallization would be taking place in response to decreasing temperature owing to upward heat loss and/or decreasing pressure associated with the upward passage of the mass through the earth's crust.

In the more acidic stages, depletion of Mg and Fe in the magma due to crystallization of biotite, coupled with a high  $H_2O$  pressure, promoted the crystallization of

primary muscovite and both plagioclase and potash feldspars.

When the bulk of the upper zones of granite-granodioritic material had consolidated, the Fleet pluton broke through the roof-zone of the batholith in response to the relatively low density of the highly fractionated material. Forceful intrusion of this viscous mass is indicated by sheared and gneissose margins, and dilatation of the country rocks. Since crystallization, at least at the margins was nearly complete, no chilling effects occur at the very sharp contacts and very little, if any, local contamination has taken place. Xenoliths are therefore uncommon and the large granitized sedimentary raft described above (chapter 6), probably sank to its present position from the roof zone above.

As the bulk of fractionation had taken place prior to intrusion, the distribution of the coarse grained biotite facies had already been imprinted, and was a consequence of irregularities in the roof of the batholith. Owing to these irregularities more basic rocks, which would lie in a belt parallel to the roof, are neither concentrically disposed nor necessarily marginal with respect to the present intrusive contact. This situation is endorsed by the presence of some of the most highly fractionated coarse grained granites adjacent to the northwest contact.

Subsequent slow cooling, perhaps associated with hydrothermal activity, allowed the subsolidus exsolution of albite from microcline to take place, especially in regions away from the contact. Decrease in pressure as a result of upward movement may have produced disequilibrium conditions, which in turn may have promoted the replacement

of earlier formed minerals by quartz and also the development of myrmekite. Granulation and fracture zones developed during intrusion or as a result of later stress, would aid the passage of fluids responsible for alteration.

Fractionation was still taking place at depth when a second intrusion took place centrally within the coarse grained granite. Some overlap in the fractionation trends is apparent from geochemical studies. Chilled contacts do not occur in this mass, because the coarse grained granite was still hot. Lack of granulation and shear suggest that crystallization of the later granite was not as advanced as that of the coarse grained granite during emplacement. This concept is backed up by the fact that some of the contacts appear to be diffuse and the marginal fine grained granite may contain xenoliths of coarse grained granite (Parslow, 1964, 1968).

Heat loss was more rapid due to the higher level of emplacement and/or dissipation by  $H_2O$ , which was undoubtedly highly concentrated in the residual melt. The grain size of the later granite is consequently smaller and microperthite is poorly developed. Fractionation took place in situ and resulted in a concentric arrangement of facies, increasing in acidity towards the centre of the mass. The  $H_2O$  pressure was still high enough to allow crystallization of primary muscovite, and the absence of myrmekite except in contact areas may be the result of reduced shearing stress.

Continued crystallization owing to temperature and/or pressure decreases, promoted  $H_2O$  enrichment, which

was probably accompanied by a decrease in the  $H_2O$  pressure. Throughout the central parts of the pluton, hydrothermal solutions caused the breakdown of biotite and feldspars to form chlorite, epidote, clinozoisite, zoisite and muscovite. This stage was associated with alkali metasomatism, which may have caused a breakdown of biotite or a reduction in its stability field, resulting in the production of spessartine garnet, in a restricted area in the centre of the intrusion. Also associated with this hydrous late stage phase are veins following tension gashes, containing cryptocrystalline silica, jasper, quartz, chalcopyrite and pyrite (see chapter 13).

Lamprophyre and porphyrite dykes intruded in the environs of the granite during or soon after emplacement, show signs of alteration and albitization which are the result of comparable late stage processes.

PART 3  
THE FLEET OREFIELD

CHAPTER 12  
I N T R O D U C T I O N

A. Introduction and previous research

Traces of mining activity are encountered over the whole of the Southern Uplands, but are nowhere more prolific than in the Newton Stewart and Leadhills-Wanlockhead districts (Fig. 90). Dewey (1920) and Wilson (1921) collated all previous information (Heddle, 1901, and others), and classified the mineral deposits according to their mineralogy and location. Later work has been concentrated upon individual occurrences or districts. Gregory (1927) described in detail the interesting Ni-Co deposit at Talnoy, in the Newton Stewart district. The comprehensive work of Temple (1955) on the economically important Leadhills-Wanlockhead Pb-Zn vein deposits was followed by MacKay (1959). More recently U deposits have been described from the environs of the Criffell pluton (Miller and Taylor, 1966; Gallagher et al., 1971).

The Fleet orefield, which includes the Newton Stewart district mentioned above, covers approximately 300 sq. km of the Fleet pluton and the country rocks around its western margin (Figs. 90 and 91). Over twenty five mineral veins occur containing the most diverse suite of minerals in the Southern Uplands (Fig. 92). Nearly all of these are fissure infillings and occupy faults with a Caledonoid trend in Lower Palaeozoic greywackes and shales. Two major groups of veins occur (Fig. 93); those trending between  $280^{\circ}$  and  $320^{\circ}$  along dextral wrench fault planes, and others

trending between  $350^{\circ}$  and  $020^{\circ}$  along sinistral wrench fault planes (see chapter 4, below). Veins of a third minor group are encountered along the planes of large strike faults trending WSW.-ENE. The mineral deposits fall into groups of similar types forming zones around the western margin of the pluton (see below, Figs. 91 and 94), and therefore are obviously related at least spatially, to the granite.

B. Spatial relationships between the mineralization and the granite batholith.

As mentioned previously (see chapters 5, C and 6, A, below) recent geophysical investigations in the southwestern part of the Southern Uplands indicate a large area of negative gravity anomalies around and between the Fleet, Doon and Carsphairn plutonic masses (Bott and Masson Smith, 1960; Parslow and Randall, 1973; Batraukh, 1975). Batraukh accounts for these by proposing the existence of a granite batholith at fairly shallow depths (Fig. 37). The model gives only an estimate of the minimum size of the batholith because granodiorite, one of the major components of most of the plutons, has a similar density to the greywacke country rock, and consequently cannot be resolved in this type of gravity investigation.

The distribution of rocks of granitic composition beneath the southwestern parts of the Southern Uplands is compared with the localities of mineralization on Figure 37. The following features are of importance. The Fleet, Doon and Carsphairn plutons are all postulated to be connected by granitic rocks at depths of less than 3 km,



whereas if the Criffell pluton is connected with the others by rocks of this composition, it is at depths exceeding 10 km. A wide shallow shelf of granite is suggested to extend to the west and southwest of the Fleet pluton (Parslow and Randall, 1973; Batraukh, 1975), and to coincide with much of the Fleet orefield. As a result of these interpretations it now appears that most of the mineralized localities in the southwest of the Southern Uplands occur within 3.5 km of granitic rock.

Investigations, detailed herein, into the distribution of mineralization in the Fleet orefield disclose a zonal arrangement clearly related to the exposed areas of the pluton (Figs. 91 and 94). The pattern is similar to that occurring in the Cornish deposits (Dewey, 1925) except for the absence of Sn, W and Sb ores. An inner zone dominated by copper ores with siliceous gangue includes the granite and adjacent parts of the aureole, narrowest around the western margin of the pluton and having wider extensions to the north and south. High temperature hydrothermal minerals such as molybdenite, arsenopyrite and pentlandite are confined to this zone. The inner zone is replaced outwards gradationally by a zone typified by the occurrence of zinc (sphalerite) and carbonate (ankerite, calcite, etc.) minerals with the quartzose gangue. The outermost zone contains ores of lead, with a carbonate gangue, containing minor barytes at some localities. A small area of zinc mineralization alongside the River Cree does not follow this simple zoning pattern (Figs. 91 and 94). It should be emphasized that ores of Cu, Pb and Zn occur throughout the orefield,

and zones have been named according to the dominant ore metal and subdivided on the nature of the gangue. Also all changes in mineralogy and the nature of the veins are gradational and consequently the zones overlap.

CHAPTER 13  
THE MINERAL DEPOSITS

A. Deposits of the copper zone

Major copper mineralization occurs both within and around the granite, although for clarity only its distribution within the country rock is shown (Figs. 91 and 94). Twelve veins (1-12, Fig. 91) are included in this zone, only one occurring entirely within the pluton. Two subdivisions are erected on gangue mineralogy, an inner of quartz-rich gangue and an outer, confined to the southeast, of quartz and carbonate.

(i) Quartz subzone

(a) Orchars vein (25785730)

This vein (1, Fig. 91) follows a line of fracture in the coarse grained biotite-muscovite granite facies, having a similar orientation to gash veins described by Parslow (1964, 1968). It was detected in the present survey through the occurrence in the Nick Burn 200 m downstream of the outcrop, of anomalously high values of Pb (890 ppm) and As (150 ppm), in a regional survey of stream sediments. Likewise the White Burn, having a parallel course but 150 m to the west, yielded anomalous values of 1700 ppm Pb and 400 ppm As. (Average and threshold values of Cu, Ni, Zn and Pb in stream sediments from the Fleet pluton are given on table 14).

The vein trends  $010^{\circ}$  and the exposure forms a small cascade in the Nick Burn. Granite in the vicinity is cut by small and vuggy quartz veins trending between  $330^{\circ}$  and  $010^{\circ}$ , and is stained with hematite along joints.

The main vein, which is five metres thick, consists of a multiple intrusion of white and smokey-grey quartz, surrounding a breccia of altered granite and earlier vein quartz. Certain phases of the mineralization are characterized by colloform jasper and silica, specular hematite, chalcopyrite and pyrite (plate 30A and B). The colloform nature of the jasper is particularly impressive when viewed under cross polarized reflected light, even though the silica has divitrified.

A paragenetical sequence deduced from studies of slabs of vein material and polished sections is as follows:

1. brecciation and alteration of granite wallrock.
2. quartz-veining.
3. brecciation followed by deposition of quartz, chalcopyrite and specular hematite.
4. deposition of colloform silica and jasper with specular hematite occurring in bands and infilling vugs.
5. deposition of quartz, chalcopyrite and pyrite.
6. brecciation followed by deposition of colourless quartz and pyrite.
7. deposition of cryptocrystalline pale pink or grey amorphous silica.

Summary:

quartz	_____	_____
colloform silica/jasper		_____
hematite	_____	
chalcopyrite	_____	_____
pyrite		_____

The granite wallrocks are reddened in the vicinity of the vein, and a detailed description of this alteration is given in chapter 15, below.

(b) Clugie Linn vein (24875712)

Veins containing quartz with sparse molybdenite mineralization occur along the exposed contact of the granite in the bed of the Palmure Burn at Clugie Linn, south of Talnotry (2, Fig. 91). The contact hornfels in the vicinity contains numerous quartz veins and the granite in the proximity of the contact is xenolithic. At this locality the stream flows over granite and undercuts the hornfels along the contact, on the northwest bank.

Molybdenite mineralization tends to belong to the pegmatitic-pneumatolytic or high temperature hydrothermal stages (Ramdohr, 1969), which is confirmed by its occurrence adjacent to the granite contact. The presence of anomalously high concentrations of molybdenum in stream sediments (up to 60 ppm), especially over the Fleet pluton, indicates that other veins or disseminations of molybdenite may exist, although as yet remain undiscovered (Fig. 105). Streams draining the granite in the vicinity of Clugie Linn contain sediments with concentrations of Mo varying between 2 and 25 ppm compared to a background value of about 2 ppm.

(c) Talnotry vein (24785703, map 2)

Although the Ni, Co and As deposits near Talnotry have previously been treated as separate occurrences (Dewey, 1920; Gregory, 1927), they are now considered either as parts of one vein, or branches of a connecting vein (3, Fig. 91; Fig. 95).

Though the workings at the eastern arsenopyrite

deposit, where the granite contact is cut by the Palnure Burn (24805702), are now overgrown, spoil tips yield good specimens of ore. Other than the tips, evidences of previous working are restricted to open-cast cuttings and the metal beam of a pumping engine. The vein coincides with the granite contact, trends northeast and hades to the northwest (Dewey, 1920). Pale steel-grey arsenopyrite occurs in a white quartz gangue surrounding brecciated and altered muscovite granite. All vein rocks show signs of granulation with a strong development of undulose extinction in quartz crystals especially around crushed, brittle arsenopyrite crystals (plate 31A). All these features are evidence for post-depositional stress. The granite wall-rocks have a similar mineralogy to coarse grained muscovite-biotite granite elsewhere in the Fleet pluton, except that much of the K-feldspar is altered to secondary muscovite and in zones of granulation some plagioclase is replaced by calcite, as a result of hydrothermal alteration.

A simple paragenesis has been obtained from the samples investigated:

1. brecciation and alteration of wallrocks.
2. deposition of arsenopyrite and colourless quartz.
3. rebrecciation, followed by deposition of colourless quartz, or solution and reprecipitation of pre-existing quartz.

In all probability this vein bifurcates north of the Palnure Burn and a more northerly extension trends  $130^{\circ}$  along a fault plane (Fig. 95). Where fault and vein cut the southern end of a diorite sill, described earlier (see chapter 10, D), a different mineralization occurs.

At this locality (24785703) the fault fades steeply to the north, diorite forming the hanging wall and silicified greywacke hornfels the footwall (Gregory, 1927). The lens-shaped lode which has a maximum width of 3 m, occurs on the hanging wall in brecciated, impregnated and replaced diorite. The ore consists of smaltite (i.e. cobaltian skutterudite), niccolite, chalcopyrite, pyrrhotite, pentlandite and pyrite (plates 31B-33B), with a very minor quartz gangue. Sulphides and arsenides are scarce in the footwall rocks, which are more resistant to fracture, less chemically reactive and therefore are relatively unaltered.

Investigation of polished sections reveals that initial deposition was of smaltite, which has developed in euhedral crystals with a hexagonal or trapezoid cross section (plates 31B and 32A). Deposition of anhedral niccolite closely followed, although Leitch (in Gregory, 1927) observed an occasional reversal of this sequence, demonstrating that overlap in the sequence of crystallization has taken place.

Paragenesis:

1. alteration and brecciation of diorite.
2. deposition of euhedral smaltite.
3. deposition of anhedral clusters of niccolite.
4. replacement of diorite by chalcopyrite, pyrite, niccolite, pyrrhotite and pentlandite (plate 33A and B).
5. deposition of chalcopyrite, pyrrhotite and pentlandite with minor quartz gangue (plate 32B).
6. deposition of pyrrhotite and pentlandite with minor quantities of quartz gangue.
7. deposition of quartz, infilling available open spaces.

## Summary:

smaltite	—————
niccolite	—————
pyrite	—————
chalcopyrite	—————
pyrrhotite	—————
pentlandite	-----
quartz	-----

As mentioned previously (chapters 5 and 10) the diorite has been subjected to thermal metamorphism and is therefore older than the granite. Wallrock alteration in the vicinity of the vein has promoted the removal of biotite and hornblende, and production of tremolite/actinolite amphibole. Plagioclase is also highly altered and becomes more albitic as a result of this (see chapter 10, Fig. 89). Replacement by ore is commonly observed along the cleavages of amphiboles and micas (plates 33A and B).

An extension of the vein, previously unrecorded, occurs further to the northwest (Fig. 95), and is marked by a small open-cast operation on the western side of Glen of the Bar (24775703). Wallrocks at this locality are completely of hornfelsed greywacke, and the vein consists of quartz, arsenopyrite and pyrite with minor occurrences of realgar and orpiment (plate 34 A).

## Paragenesis:

1. deposition of translucent, colourless quartz.
2. deposition of pyrite and quartz.
3. deposition of arsenopyrite and quartz.
4. brecciation followed by deposition of white quartz, realgar and orpiment.
5. deposition of white quartz and orpiment.

not confirmed by  
ore microscopy  
and microprobe  
at Royal Scottish  
Museum Feb. 1980



## Summary:

quartz	_____
pyrite	_____
arsenopyrite	_____
* realgar	_____
orpiment	_____

Overall it appears that vein mineralogy at Talnotry is influenced by the nature of the enclosing wallrocks. Arsenopyrite and quartz occur where wallrocks are relatively siliceous (e.g. granite and hornfelsed greywacke) and unreactive. With lower overall  $\text{SiO}_2$  and higher FeO contents in wallrocks, the vein material is mainly of arsenopyrite, pyrite and quartz (e.g. Glen of the Bar). Where wallrocks are more basic (i.e. diorite and greywacke) very little quartz gangue occurs with Ni-Co arsenides and Ni, Fe and Cu sulphides.

The veins at Talnotry have some features in common with 'Cobalt type' ore deposits. The major ore minerals in this association are pyrite, arsenopyrite, chalcopyrite, galena, native silver and bismuth, niccolite, smaltite and cloanthite (Stanton, 1972), many of which occur at Talnotry. Pyrrhotite has been observed in a few deposits of the 'Cobalt type' (Bastin, 1939), but the occurrence of pentlandite is unusual. The form of the Talnotry vein as an infilling along a fault plane, cutting an intermediate sill associated with a felsic intrusion, is essentially comparable to 'Cobalt type' deposits. There is little doubt that ores of this type have originated from solutions derived from igneous intrusions, and in many cases have been observed to merge into base metal

veins of a normal granite-granodiorite affinity (Stanton, 1972).

The sequence of deposition of ores at Talnotry is comparable to that of Cobalt, Ontario (cf. Petruk, 1968). The absence of fine dendritic ore textures and the presence of pentlandite in the Talnotry vein are the major petrographical differences between the deposits. The texture of the ore minerals at Talnotry has greater affinity with normal hydrothermal base metal vein deposits.

Minerals such as pentlandite and arsenopyrite are restricted to high temperature vein deposits (Ramdohr, 1969) and as might be expected only occur in the vicinity of the granite contact.

(d) Blairbuies vein (24795678, map 1)

Minor chalcopyrite mineralization is associated with Fe-stained quartz, in veins emplaced along the upper boundary thrust of the Blairbuies thrust zone, exposed on the western flank of the Cairnsmore of Fleet (see chapter 4, F; 4, Fig. 91). The veins occur within 200 m of the granite contact.

Brecciated and silicified black hornfelsed mudstones occur in a zone trending nearly due north along the outcrop of the thrust plane. The style of mineralization is comparable with the upper veins at Culcronchie (see below).

(e) Culcronchie veins (grid square, 250, 563, map 7)

Workings associated with three subparallel veins occur intermittently for 1 km along the upper reaches of

the Culcronchie Burn (5, Fig. 91). The middle vein appears to have been the most productive.

An open-cast trial (25045633) marks the site of the lower workings. Sparse chalcopyrite mineralization associated with a gangue of quartz and minor amounts of calcite or ankerite occurs in fragments of hornfels obtained from a small spoil tip alongside the stream. The vein is not exposed, but is shown to trend a few degrees south of east on the one inch Geological Survey map (sheet 4).

The middle workings have been fairly extensive and consist of a shaft and level sunk onto the vein at about 740 feet, and a cross-cut adit further downstream at 725 feet (25075637, map 7). Adjacent to the shaft are the remains of a water wheel. Around the levels and shaft and alongside the burn, areas of spoil yield fragments of quartz-rich vein material carrying chalcopyrite and pyrite mineralization.

The vein trends a few degrees south of east and contains a breccia of highly silicified greywacke hornfels welded together by the gangue and ore. Under the microscope pyrite tends to be markedly anisotropic, which is an indication of distortion of the lattice due to the presence of impurities (Uytenbogaardt and Burke, 1971). This is confirmed by high values of Ni and Co in an analysis of the ore (0.74/1167, appendix 8).

**Paragenesis:**

1. brecciation and silicification of the hornfels wallrocks.
2. deposition of colourless quartz.

3. deposition of pyrite, often in euhedral crystals and smokey grey quartz.
4. deposition of chalcopyrite and smokey grey quartz.
5. deposition of quartz and cryptocrystalline silica (chalcedony).
6. deposition of Fe-stained quartz and minor chalcopyrite.

Summary:

quartz \_\_\_\_\_  
 pyrite \_\_\_\_\_  
 chalcopyrite \_\_\_\_\_

Further upstream open-cast workings and a level indicate the site of the upper veins (25115638, map 7). The level, struck into the hillside along one of the veins, has been breached at its upper end and is now occupied by the stream, enabling open-cast operations to have been undertaken in the original stream bed (plate 9A). Three veins, 5 metres apart, are associated with zones of brecciation trending  $100^{\circ}$  and which are the result of reverse strike faulting or thrusting (see chapter 4, H). The ore is mainly sphalerite, associated with subordinate amounts of colourless or Fe-stained quartz gangue. Black pelitic hornfels wallrocks have undergone silicification (see chapter 15, above).

1. brecciation and silicification of pelitic hornfels, and crystallization of minor quantities of pyrite and chalcopyrite with grey or colourless quartz.
2. deposition of sphalerite and minor quantities of chalcopyrite and galena.

3. introduction of colourless quartz and cryptocrystalline silica (chalcedony).
4. deposition of chalcopyrite.
5. precipitation of cryptocrystalline silica.
6. deposition of colourless and Fe-stained quartz.

Summary:

quartz/silica -----  
 pyrite -----  
 chalcopyrite -----  
 sphalerite -----  
 galena -----

(f) Clatteringshaws vein (25385758)

Sparse mineralization associated with strike faulting in the Talnothy thrust zone has recently been exposed in a quarry on the western side of Clatteringshaws Loch (6, Fig. 91). Pyrite, pyrrhotite, chalcopyrite, sphalerite and galena occur in lens-shaped masses of white quartz within crushed, chloritized and slickensided dark grey shales.

Paragenesis:

1. brecciation and alteration of pelitic wallrocks.
2. crystallization of white quartz, pyrite, chalcopyrite and pyrrhotite.
3. deposition of minor quantities of pink calcite, sphalerite and galena infilling fractures.

This very mixed ore type may be the result of telescoping in response to crystallization down a steep

thermal gradient. Coincidentally, the thermal aureole is very narrow in this vicinity, (Fig. 33).

Sediments from a stream draining the thrust zone 500 m to the west of the quarry contain anomalously high amounts of Cu (34 ppm), Ni (135 ppm), Zn (550 ppm) and Pb 410 ppm). This may indicate that mineralization along this line of faulting is more than localized in extent.

(g) Drumruck vein (25875637, map 7).

This vein and its extensive workings are situated on the eastern flank of the valley of the Big Water of Fleet near Drumruck (7, Fig. 91). The vein is associated with a felsite dyke (Wilson, 1921) and has a trend of  $115^{\circ}$  and a southward hade of  $14^{\circ}$ . Four levels have been driven into the hillside on the outcrop of the vein at 460, 425, 360 and 280 feet. The lower level may have been a trial only, but the 360 foot level had a length of about 800 feet (Wilson, 1921). All levels, except the upper in which supporting timbers still remain, are now blocked. The workings were drained by an adit, the entrance of which is at 240 feet and close to the foundations of various mine buildings.

Chalcopyrite is the major ore and often shows secondary alteration to cuprite, chalcocite and azurite. Galena occurs in minor quantities in the gangue consisting mainly of Fe-stained quartz, which surrounds bleached and silicified greywacke hornfels. The spoil tips yield fragments of cuprite-rich gossan from the

oxidized upper zones of the vein. Barren orange ankerite veins containing carbonatized wallrock fragments are also exposed in the vicinity. Wallrocks at the entrance to the upper level are highly silicified and cut by anastomosing barren milky quartz veins.

Paragenesis:

1. brecciation and silicification of wallrocks.
2. introduction of white and orange (Fe-stained) quartz and chalcopyrite.
3. deposition of galena.
4. rebrecciation and local carbonatization of wallrocks followed by crystallization of ankerite, calcite and malachite in minor veins.
5. secondary alteration of chalcopyrite to chalcocite, covellite and cuprite.

(h) Craignell vein

The exact location of this vein is not known and it is probably submerged beneath Clatteringshaws Loch, which has been created as a reservoir this century (8, Fig. 91). The vein has been described as about 0.5 m wide, trending  $020^{\circ}$ , and containing quartz, calcite, chalcopyrite and sphalerite (Wilson, 1921).

(i) Craigencallie vein (25045780)

Again the exact location of the vein is unknown (9, Fig. 91). Wilson (1921) describes it as being about 2 m in width, trending  $105^{\circ}$  and hading to the southwest, with an infilling of quartz, pyrite and chalcopyrite. It

is probably comparable to the middle vein at Culcronchie (above).

(j) Kings Laggan vein (25635578)

Exposed in the stream bed immediately behind Kings Laggan farmhouse, this vein was worked mainly open-cast (10, Fig. 91). It trends NNW., hadees WSW., and is approximately 2 metres wide (Wilson, 1921). A few metres to the west of the surface workings a shaft has been sunk to strike the vein at depth. Greywackes in the vicinity dip at a high angle to the northwest, and are cut by numerous barren quartz veins.

The infilling is reminiscent of the Drumruck vein (above), consisting of brecciated pale green greywacke embedded in quartz and chalcopyrite, with secondary malachite and chrysocolla.

Paragenesis:

1. brecciation and silicification of greywacke wallrock.
2. intrusion of white quartz.
3. deposition of chalcopyrite.
4. crystallization of green (Cu-stained) quartz.
5. deposition of calcite and alteration of chalcopyrite to malachite.
6. alteration of the ore to cuprite and deposition of chrysocolla.

(ii) Quartz-carbonate subzone

In the extreme southwest of the area, over 5 km



from the granite outcrop, but closer to some small dyke-like masses probably comparable to the Kirkmabreck granodiorite in composition, the quartz-rich deposits of the inner copper zone give way to those containing a mixed quartz and carbonate gangue.

(a) Lauchentyre vein (25575574)

The only remaining evidences of mineralization at this locality are a blocked shaft and associated spoil tip (11, Fig. 91). Country rocks are dark grey phyllites and the vein contents comprise chalcopyrite, tenorite, malachite, sphalerite, quartz, calcite and dolomite (Wilson, 1921). Workings have been on a small scale and consist of a short adit level driven along the vein and the shaft mentioned above (ibid).

(b) Enrick vein (26205550)

Considerable mining activity was concentrated upon this vein in the earlier part of last century (12, Fig. 91). It trends  $110^{\circ}$  and contains brecciated country rock cemented by a gangue of calcite, dolomite and quartz, carrying chalcopyrite and malachite ore (Wilson, 1921). The vein is approximately 1.5 metres wide and has been worked by a number of shafts and levels.

The copper zone deposits have been described in order of increasing distance from the pluton and confirm the trends in mineralogy outlined earlier (above). These zones must relate to the granite as the nucleus of mineralization, and/or the presence of a gradient to lower temperatures in the country rocks during mineralization.

## B. Deposits of the zinc zone

The major zone of zinc mineralization forms a narrow band around the western margin of the Fleet pluton (Figs. 91 and 94), varying in distance from the contact between less than 1 km in the north to over 5 km in the south. The zone itself increases in width from north to south, being divided at its widest into quartz and quartz-carbonate subzones. Increased outcrop width of both the copper and zinc zones to the south of the pluton may be the result of a lower thermal gradient during mineralization, or decreased dip of the zones themselves. Both these criteria could be related to the presence of a mineralizing igneous body shelving at a shallower angle than in the west and north. Increased aureole width and the occurrence of a number of small dyke-like intrusions probably of granodiorite, to the south of the Fleet pluton, lend support to this proposal.

A small 'inlier' of zinc mineralization occurs farther west in the Wood of Cree area, north of Newton Stewart. This area does not fit into the otherwise concentric zoning pattern.

### (i) Quartz subzone, Dromore area

Three deposits (14-16, Fig. 91) to the south of the pluton represent this subzone.

#### (a) Dromore vein (25385622, map 7)

Open-cast workings along the outcrop of this vein occur immediately to the south of the Creetown-Gatehouse of Fleet road, near to the now disused Gatehouse of Fleet station (14, Fig. 91). Trending  $120^{\circ}$ , the vein follows the crush zone of a dextral wrench fault, the movement of

which can be determined by slickensides and contortion of lamination in the greywacke hornfels. It is about 1 m wide and has a  $10^{\circ}$  E. The infilling has been described (Wilson, 1921) as consisting principally of brecciated country rock with quartz and chalcopyrite-sphalerite ore. However, chalcopyrite is absent from all the samples collected in this survey, which were mainly of massive sphalerite and galena ore, from the footwall. Wallrock alteration appears to be restricted essentially to silicification, although it is not as intense as in the rocks associated with veins of the copper-quartz subzone (above).

Paragenesis:

1. silicification and minor argillic alteration of wallrocks associated with crystallization of minor amounts of pyrite.
2. introduction of colourless quartz and deposition of cryptocrystalline silica, pyrite, sphalerite and galena.
3. deposition of massive sphalerite and galena ore.
4. deposition of galena.
5. deposition of sphalerite.
6. brecciation followed by crystallization of quartz.
7. deposition of a fine grained sphalerite and quartz aggregate with minor galena.

Summary:

quartz	---	-----	-----
pyrite	---	-----	
sphalerite		-----	-----
galena		-----	-----

(b) Meikle Bennan vein (25535615, map 7)

The vein is situated on the northwestern flank of Meikle Bennan, 700 metres southwest of Upper Rusko Cottage (15, Fig. 91). The site of workings is marked by two blocked shafts at 785 and 850 feet, two cross-cut levels at 725 and 765 feet of which the lower is the adit, together with spoil tips and remains of mine buildings. According to Wilson (1921) the vein, which is less than 0.5 metres wide, trends  $075^{\circ}$  and hases  $30^{\circ}\text{S}$ . Brecciated and silicified low grade greywacke hornfels welded by quartz with pyrite, chalcopyrite, sphalerite and galena constitute the vein infilling.

Paragenesis:

1. brecciation and silicification of wallrock hornfels.
2. deposition of white crystalline quartz, pyrite, chalcopyrite and galena.
3. crystallization of orange (Fe-stained) quartz.
4. deposition of sphalerite and galena with minor amounts of chalcopyrite.
5. deposition of white quartz.
6. late stage infillings of dolomite or ankerite.
7. quartz veining.

## Summary:

quartz	_____	_____	_____
chalcopyrite	_____	-----	
galena	_____	_____	
sphalerite		_____	
dolomite/ankerite.			_____

(c) Pibble Gulch vein (25255615, map 7)

In common with many of the veins to the south of the pluton, the Pibble Gulch vein follows the line of a dextral wrench fault trending  $130^{\circ}$  (16, Fig. 91; Fig. 97). Signs of mining activity are restricted to a small open-cast trial along a stream and a spoil tip. Wilson (1921) described the infilling as brecciated country rock with quartz and sphalerite.

(ii) Quartz subzone, Wood of Cree area.

This area contains two veins of Zn-rich ores isolated from the main concentric zone of zinc mineralization, around the western margin of the pluton. Their mineralogy differs from the zinc-quartz subzone deposits above, in that they contain little gangue and the mutual relationships of the ore minerals are more complex.

(a) Wood of Cree vein. (23875695)

Workings on the vein started about 1870 and in the early part of this century the mine was extended and new machinery brought in (Wilson, 1921; 18, Fig. 91). It was the last operational mine in the Newton Stewart area. At present two levels open on to the lode from the open-cast site (Fig. 96). Vein material has been collected in situ from the entrance to the more northerly level. The vein

trends a few degrees west of north and fades to the west. Two shafts to the west of the outcrop have been sunk to strike it at depth. The ore-bearing ground is approximately 5 metres wide and is a shatter belt associated with a line of fracture running parallel to the River Cree (Wilson, 1921).

The major sulphide phases are intermingled sphalerite, galena and pyrite, and chalcopyrite occurs in minor amounts (plates 34B-36A). A chemical process was evidently required to separate the ore (Wilson, 1921). Wallrocks are bleached and markedly silicified, but there is a noticeable absence of well developed gangue minerals in the material collected. It is not known how representative these samples are, but the vein is placed in the quartz subzone because of the high degree of silicification of wallrocks and the presence of microcrystalline aggregates of quartz and sphalerite.

Compared with the veins previously described the paragenetical sequence is complex:

1. wallrock alteration including bleaching and silicification associated with crystallization of minor amounts of quartz and pyrite (see chapter 15).
2. deposition of euhedral, isotropic, yellow pyrite I (plates 34B and 35A, B).
3. deposition of polycrystalline aggregates of weakly anisotropic, paler coloured pyrite II (plate 34B). As mentioned previously (above) anisotropy may indicate lattice distortion due to the presence of impurities such as Ni and Co (Uytenbogaardt and Burke, 1971).
4. brecciation of ore.

5. deposition of quartz.
6. deposition of quartz and pyrite replacing pyrite II (plates 35B and 36A). Pyrite I is not replaced and may be a result of its purer state and high degree of crystallinity. Infilling of fractures by minor amounts of galena (plate 35B).
7. deposition of galena, replacing pyrite II (plate 35B and 36A), but again leaving pyrite I unaffected, and infilling fractures.
8. crystallization of microcrystalline aggregates of sphalerite and quartz, with minor amounts of galena.
9. brecciation followed by deposition of coarsely crystalline sphalerite, with quartz and minor galena.
10. sphalerite and quartz deposited with minor amounts of galena, and crystallization of carbonate (calcite, ankerite) in microfractures.
11. deposition of quartz-rich microcrystalline aggregates of sphalerite.
12. infilling of few remaining open spaces with sphalerite, galena and minor carbonate.
13. fracturing.

Chalcopyrite has not been observed in the material collected although it has been recorded previously (Wilson, 1921).

Summary:

quartz	-----
pyrite	--
sphalerite	-----
galena	-----
carbonate.	-----

(b) Coldstream Burn vein (23885698)

The vein trends a few degrees east of north, is vertical and where it crosses Coldstream Burn is between 0.75 and 1.0 metres wide (19, Fig. 91; Fig. 96). Two levels, one from the bed of the Coldstream Burn, the other at the side of a tributary to the north, have been opened up on the vein. A blocked shaft surrounded by extensive areas of spoil marks the site of the main working, although two others described by Wilson (1926), have undoubtedly been covered with debris. Further downstream along the Coldstream Burn, a trial level and open-cast excavation mark the site of attempts to locate a northerly extension to the Wood of Cree vein (Fig. 96).

Sphalerite, galena, pyrite and chalcopyrite associated with a quartz and minor carbonate gangue surrounding fragments of wallrocks, are the major vein components. The ore is essentially comparable to that at Wood of Cree, though bleaching of the wallrocks is less intense. It is not known whether these veins converge at depth. In some respects their parageneses may be correlated although a number of the early phases are missing from the Coldstream Burn vein.

Paragenesis (numbers in brackets refer to proposed equivalent phases in the Wood of Cree vein):

1. wallrock alteration, silicification and crystallization of quartz, euhedral pyrite and chalcopyrite.
2. deposition of pale sphalerite and quartz cementing wallrock breccia, with minor quantities of chalcopyrite, pyrite and galena (8).



3. deposition of dark (Fe-rich, see chapter 14) highly crystalline sphalerite and galena (9).
4. precipitation of cryptocrystalline silica followed by brecciation.
5. deposition of pale sphalerite, cryptocrystalline silica and microcrystalline galena in fractures (10 and 11).
6. deposition of calcite/ankerite and sphalerite (12).

Summary:

quartz/silica -----  
 pyrite -----  
 chalcopyrite -----  
 sphalerite -----  
 galena -----  
 carbonate -----

(iii) Quartz-carbonate subzone

Towards the outside of the copper-quartz subzone in the north and the zinc-quartz subzone in the south, carbonate gangue increases in amount to form a narrow band typified by Zn ores with mixed quartz and carbonate gangue (Figs. 91 and 94). Only two veins are representative of this subzone, but trends in the mineralogy of other veins in the vicinity have enabled its position to be mapped.

(a) Tonderghie vein (24985733, map 2)

Narrow anastomosing veins of quartz and calcite carrying a mineralization of sphalerite, galena and chalcopyrite, cut across the bed of Tonderghie Burn at the southern entrance to Tonderghie Glen (13, Fig. 91). Most trend  $020^{\circ}$ , parallel to the major strike faults of

the Talnothy thrust zone (see chapter 4, C). Their formation is probably the result of infilling of parallel tension fractures developed below the sole of the upper boundary thrust. Wallrocks are pale green, highly fractured and silicified or carbonatized according to the mineralogy of adjacent veins.

Paragenesis:

1. brecciation, silicification and/or carbonatization and argillic alteration of wallrocks, and crystallization of minor amounts of pyrite.
2. deposition of white calcite with minor amounts of quartz and either galena or sphalerite and chalcopryrite.
3. deposition of white calcite with minor amounts of quartz, and galena replacing sulphides of phase 2 (above).
4. crystallization of ankerite.
5. introduction of white quartz and sphalerite with minor galena.
6. deposition of barren white quartz.

Summary:

quartz	-----	-----
carbonate	-----	-----
pyrite	-----	
chalcopryrite	-----	
sphalerite	-----	-----
galena	-----	-----

(b) Chain Burn vein (25015608, map 7)

All that remains of workings associated with this vein are a blocked shaft and an overgrown spoil tip alongside the Creetown-Dromore road, although another shaft was originally present on the south bank of Moneypool Burn

(Wilson, 1921; 17, Fig. 91). The vein occurs along a line of fracture trending  $110^{\circ}$ , hading to the north and again probably a dextral wrench fault. Sphalerite and galena are the dominant ores, associated with a gangue comprising quartz, ankerite and ferroan calcite, surrounding fragments of hornfelsed greywacke and shale.

Paragenesis:

1. brecciation of wallrocks and argillic alteration; silicification is absent.
2. crystallization of white quartz with chalcopyrite, sphalerite and galena.
3. deposition of ankerite with increasing Fe content (deduced from stained sections, see appendix 1).
4. deposition of white crystalline quartz.
5. crystallization of ankerite again with increasing Fe content.

The mineralogy of these two veins is consistent with the decreasing importance of silica-rich gangue and associated silicification. Types of gangue in the various phases of intrusion alternate, probably reflecting the transitional position of the vein between carbonate and quartz dominated zones.

### C. Deposits of the lead zone.

Veins with a mineralogy typical of this zone occur in regions furthest away from the pluton towards the west and southwest, with the exception of the Wood of Cree area described above (Figs. 91 and 94). It is subdivided, in common, with the other zones, on the composition of the gangue.

(i) Carbonate-quartz subzone

The narrow discontinuous subzone of Pb ores in association with carbonate and quartz gangue, occurs between the zinc-quartz-carbonate subzone and the lead-carbonate subzone (Fig. 94). Two main areas are represented by two deposits. The mineralogy of the Pibble and Bargaly veins are considered to be transitional between both lead and zinc carbonate/quartz subzones, and chemically they have more affinity with the latter (see chapter 14).

(a) Pibble vein (25255605, map 7).

Much remains of the workings at Pibble mine (frontispiece and Fig. 97), and it was one of the most important in the area (20, Fig. 91). At the lower workings a water wheel pit large enough to accommodate an undershot wheel 16 metres in diameter, and probably used to drive the ore crushers, is still to be seen. This is adjacent to the lowest shaft (550 feet), and is fed from an artificial reservoir at the base of Pibble Hill. A water leat tapping the resources of many streams flowing northwards down the hill fed the reservoir. Foundations of mine buildings and the remains of a large engine house (frontispiece) comparable with those of Cornwall, which would accommodate an atmospheric or beam-type steam engine again used to drive crushers, are situated in the upper washing and dressing area. Around these are extensive areas of spoil, from which a pony track leads up the hill to the main workings.

Signs of mining activity of various degrees are scattered all over the northwestern flank of Pibble Hill. The upper shaft and level are adjacent at 875 feet,

apparently on a vein, but to the northeast of that marked on Figure 97 and the one inch Geological Survey map (sheet 4). Further east a small trial level at 975 feet has been driven a short distance along the fracture zone below a northwestward dipping thrust (see chapter 4, K). A lower shaft occurs at 850 feet, and most of the work appears to have been concentrated along levels over this part of the hill. The entrances to three levels occur between 800 and 850 feet and two others between 650 and 700 feet. It appears that levels were struck into the hillside at 10 fathom (60 feet) intervals. The entrance to the adit at 525 feet, is immediately below the waterwheel pit. From this a masonry-lined channel emerges which would originally have carried water drained from the mine, and is 10 fathoms (60 feet) below the lowest level exposed at present on the hillside. The workings are 250 feet (approximately 40 fathoms) in depth from the top level to the adit, but they probably extend below this.

The vein or veins trend  $125^{\circ}$  along the plane of a dextral wrench fault which offsets outcrops of black shales exposed across the top of Pibble Hill (Fig. 97). It contains an infilling of brecciated country rock embedded in quartz and carbonate gangue (barytes also occurs, Wilson, 1921) carrying an ore of galena, sphalerite and chalcopyrite with numerous secondary minerals. The vein material obtained in this work tends to be either quartz-rich (comparable with the Meikle Bennan vein, above) or carbonate-rich. The former is invariably barren or associated with chalcopyrite; the latter usually contains

chalcopyrite, sphalerite and galena.

Paragenesis:

1. brecciation and silicification and argillic alteration of greywacke and pelitic hornfels wallrocks.
2. crystallization of white quartz cementing breccia.
3. deposition of chalcopyrite.
4. deposition of orange (Fe-stained) quartz with minor sphalerite and white quartz.
5. deposition of dolomite and chalcopyrite.
6. deposition of sphalerite.
7. introduction of Fe-poor ankerite with dolomite and chalcopyrite.
8. deposition of Fe-rich ankerite.
9. deposition of Fe-stained ferroan calcite.
10. precipitation of cryptocrystalline silica.
11. introduction of colourless quartz.
12. deposition of Fe-stained orange quartz.
13. deposition of sphalerite and ferroan calcite.
14. deposition of galena with white quartz.
15. alteration of ore minerals; a. alteration of chalcopyrite to cuprite via the intermediates covellite and chalcocite (plate 36B), and production of anglesite and cerussite from galena. b. secondary (supergene) enrichment forming a gossan and replacement of primary minerals e.g. galena by native copper, covellite, chalcocite, cuprite and limonite (plates 37A and B).

Other secondary minerals identified include malachite, azurite, chrysocolla, pyrolusite, linarite and leadhillite. Reaction of solutions derived from the

alteration of primary ores of Pb and Cu has produced secondary minerals which have crystallized in vugs. For example in one sample, chalcopyrite is altered to cuprite and malachite ( $\text{CuCO}_3 \cdot \text{Cu}(\text{OH})_2$ ) adjacent to galena altered to anglesite ( $\text{PbSO}_4$ ). Between them linarite ( $(\text{Pb,Cu})\text{SO}_4 \cdot (\text{Pb,Cu}) (\text{OH})_2$ ) in beautiful azure-blue aggregates has formed as a result of reaction of the secondary solutions. In a similar manner leadhillite ( $\text{PbSO}_4 \cdot 2\text{PbCO}_3 \cdot \text{Pb} (\text{OH})_2$ ) forms by interaction of basic carbonate and sulphate solutions.

Summary:

quartz	_____	-----	-----	_____
chalcopyrite	_____	-----	-----	_____
sphalerite		_____	-----	_____
ankerite/dolomite		_____	-----	_____
calcite			_____	_____
galena				_____

(b) Bargaly veins (24665682, map 1)

Two intersecting veins occur, one trends a few degrees east of north and the other at  $160^\circ$  (21, Fig. 91). Two shafts have been sunk but are now blocked, one at the junction of the veins and the other on the north-south vein south of the junction. The northern and southern limits of the N.-S. vein have been worked open-cast. Ore from the NW. vein was won from a level struck along its length from the south bank of the Palnure Burn, and spoil tips around the entrance provide good specimens. Recently, forestry planting has destroyed most of the evidence of original mine workings south of the stream.

The veins carry galena and sphalerite with

carbonate and quartz gangue, surrounding sericitized wallrock breccia (see chapter 15).

Paragenesis:

1. brecciation and argillic alteration of wallrock and crystallization of pyrite.
2. impregnation of wallrocks by sphalerite and cryptocrystalline silica.
3. deposition of sphalerite and crystalline quartz.
4. crystallization of barren white quartz.
5. deposition of sphalerite with subsequent exsolution of blebs of chalcopyrite and crystallization of white quartz.
6. deposition of galena with minor sphalerite and chalcopyrite, galena replacing some of the sphalerite of phase 5 (above). Also crystallization of ankerite, ferroan calcite and calcite.
7. introduction of barren white quartz.

Summary:

quartz/silica	-----
pyrite	_____
sphalerite	-----
chalcopyrite	-----
galena	_____
carbonate	_____

(ii) Carbonate subzone

- (a) Blackcraig veins (grid square 244, 564; maps 1 and 9).

The mines at East and West Blackcraig produced the greatest quantity of ore of any mine in the Southern Uplands,



outwith the Leadhills-Wanlockhead area (22, Fig. 91). The main vein trends  $110^{\circ}$ , fades to the southwest and occurs in a shatter belt 15 to 20 metres wide. Ore has been encountered on the concave sides of a sinuous basic dyke (Wilson, 1921), which is similar to Permo-Carboniferous intrusions in Central Scotland (Gallagher et al., 1971). At West Blackcraig the vein bifurcates and the more northerly branch runs parallel to the main vein for a few hundred metres before dying out. A more detailed description with diagrams is given by Wilson (1921), and will not be duplicated here.

At the present day little is left of the surface features of the mine. Much of the spoil has been removed for use as ballast on forestry roads and good specimens of ore are rarely found. The engine shaft at East Blackcraig is still open and the cross-cut adit entrance may be located to the southeast of Craighton (24365647). A trial shaft on the northwesterly continuation of the vein east of Calgow (24355653) appears to have proved barren quartz only.

The brecciation zone along which the vein is emplaced is probably associated with a dextral wrench fault, which dislocates outcrops of black mudstones along the Culcronchie Thrust and also contains a southeasterly extension of the vein at Cairnsmore (Fig. 91, map 9 and see below). Minerals identified are galena, sphalerite, chalcopyrite, calcite, dolomite and barytes, with subordinate quartz, surrounding altered and brecciated wallrocks.

The breccia in some samples is very loosely cemented and full of open spaces, almost as if mineralizing solutions were of very low concentration, or conditions were adverse for precipitation. A paragenetical sequence could not be deduced from the samples obtained in this study.

(b) Cairnsmore veins (grid square 246,563; map 9).

Six depressions in a field southwest of Strathmadie (24655636) mark the sites of shafts sunk onto the Cairnsmore vein (23, Fig. 91). The vein is not exposed and all spoil has been removed, therefore samples of the ore cannot be obtained.

Two parallel veins, a few metres apart, trend  $105^{\circ}$  and hade to the south (Wilson, 1921). As mentioned above, they probably represent a southeastward extension of the Blackcraig veins, along the shatter zone of a dextral wrench fault (map 9). A trial open-cast extension on the eastern end of the southern vein has been cut into the bank of a tributary of Cairnsmore Burn (24695634).

Workings on the veins were evidently considerable and an account of these is given by Wilson (1921), who describes the ore of the main vein as consisting of galena and pyrite with calcite, dolomite and barytes surrounding brecciated country rock. From this description the ore appears to be comparable with that of Blackcraig (above).

(c) Palnure vein (24555637, map 9).

A level immediately below the road on the western bank of Palnure Burn, 500 metres north of Palnure, marks the site of the vein (24, Fig. 4). Wilson (1921) suggests that it may be a branch of the Blackcraig vein with a

comparable trend and hade.

(d) Silver Rig vein (23785729)

The sites of four shafts, a blocked level and an open-cast cutting occur along the length of the vein which trends  $100^{\circ}$  (25, Fig. 91). Foundations of old mine buildings and a water wheel pit are also present. Galena, described as being rich in Ag, was won from the vein, which is nearly 2 metres wide (Wilson, 1921). However an analysis of galena from this locality (G 74/889, appendix 8) does not confirm a high Ag content, but is not necessarily representative. The infilling is of brecciated altered fragments of wallrock greywacke embedded in ankerite and calcite carrying galena and sphalerite. Alteration of wallrocks appears to be mainly argillic or a result of carbonatization; silicification is minimal and quartz gangue absent. Loosely consolidated breccia ore occurs and is reminiscent of comparable material at Blackcraig.

Paragenesis:

1. brecciation and argillic alteration and/or carbonatization associated with crystallization of minor amounts of pyrite.
2. deposition of ankerite and sphalerite and minor amounts of chalcopyrite and pyrite.
3. deposition of ferroan calcite.
4. deposition of dolomite, sphalerite and galena with minor amounts of chalcopyrite.
5. deposition of ankerite and minor chalcopyrite.
6. deposition of calcite and minor chalcopyrite.

## Summary:

silica	-----
pyrite	-----
chalcopyrite	-----
sphalerite	-----
ankerite/dolomite	-----
calcite	-----
galena	-----

(e) Dallash vein (24715693, map 1)

Open cast excavations along the stream bed behind Dallash farmhouse mark the superficial workings on this vein, which trends  $125^{\circ}$ , fades to the east and appears to follow a fault (26, Fig. 91). Underground operations have been limited to a shaft, the site of which is adjacent to the forestry road, and a connecting level along the length of the vein (Wilson, 1921). Specimens of vein material have been obtained from the stream bed and the wallrocks on either bank, and consist mainly of calcite and galena with small amounts of sphalerite, chalcopyrite and pyrite. Fragments of brecciated greywacke hornfels within the vein are heavily carbonatized.

## Paragenesis:

1. brecciation and alteration of wallrocks.
2. introduction of quartz, chalcopyrite and sphalerite into fractures along the vein margins.
3. deposition of ferroan calcite, calcite, ankerite, sphalerite and chalcopyrite associated with carbonatization of wallrocks.
4. rebrecciation followed by deposition of ferroan calcite, pyrite, chalcopyrite and galena.

## Summary:

quartz	_____
chalcopyrite	_____
sphalerite	_____
carbonate	_____
pyrite	_____
galena	_____

(f) Balloch (Englishman's) Burn vein (24845588, map 8)

A level struck along the vein trending  $155^{\circ}$  and parallel to fractures in the stream bed, is the only sign of mining activity at this site (28, Fig. 91). According to Wilson (1921) the major ore is galena, but material is not available for investigation.

(g) Poolness vein (25665623)

Workings for Pb ore along the Poolness Thrust are indicated by the presence of a level and spoil tip to the west of Poolness on the Big Water of Fleet (27, Fig. 91). No samples of ore were retrieved from the dump although it is likely to be of the same general type as that at Clatteringshaws (above).

Numerous other small workings of this nature occur over the whole area, but are especially concentrated in the zones of major strike faulting. Many are found in the region of the upper waterfall on the Grey Mare's Tail Burn, Talnotry (24915726). Base metal anomalies in stream sediments from the surrounding area may be accounted for by mineralization along these faults.

D. Conclusions.

The distribution of various ores around the western margin of the Fleet pluton appears to be related to the

present outcrop and subsurface topography of the granitic intrusion. This is reflected in the tripartite mineral zoning, the sequence of which is mirrored generally in the paragenesis of the deposits. The zoning, which is comparable in many respects to that in Cornwall (Dewey, 1925) and sequences drawn up by Emmons (1936) and Lindgren (1937) can be summarized:

#### A. COPPER ZONE

1. Deposits in the granite intrusion containing chalcopryrite, pyrite, specular hematite, quartz, colloform jasper and silica. Other deposits, some of which probably contain molybdenite and other base metal sulphides are suggested by secondary dispersion anomalies but, as yet, remain undiscovered (see chapter 14, G below and Figs. 105 and 106).
2. Deposits of veins with a high temperature mineralogy at the granite contact e.g. quartz-molybdenite and quartz-arsenopyrite.
3. High temperature deposits in the thermal aureole including veins containing arsenopyrite, pyrite, pyrrhotite, pentlandite, chalcopryrite, niccolite, smaltite, realgar, orpiment and quartz.
4. Veins containing chalcopryrite and pyrite, minor amounts of sphalerite and galena, with occasional pyrrhotite and a quartz gangue.
5. Chalcopryrite-sphalerite ore with a mixed gangue of quartz, calcite and dolomite.

#### B. ZINC ZONE

1. Sphalerite with minor amounts of pyrite, chalcopryrite and galena with quartz gangue.

2. Sphalerite with minor amounts of pyrite, chalcopyrite and galena and a gangue of quartz, ferroan calcite and ankerite.

#### C. LEAD ZONE

1. Veins containing galena with pyrite, chalcopyrite and sphalerite, and a gangue of quartz, ankerite, dolomite, ferroan calcite and barytes.
2. As above except quartz gangue is absent. Veins further away from the granite may contain argentiferous galena e.g. Silver Rig (Wilson, 1921).

Veins which have been economically significant in the past occur in the outer zones only. The Wood of Cree and Coldstream Burn veins occur in an isolated area of zinc-zone ores 8 km away from the granite, and the Blackcraig, Cairnsmore and Pibble veins are all in the lead zone. In most of these deposits large amounts of all three major ores are usually present, but one is always predominant. The location of the major ore deposits does not appear to be controlled by the nature of the wallrocks, because all are greywacke and have been transformed by various grades of thermal metamorphism. It is relevant to note that the greatest overall production has been from veins with a WNW.-NW. trend (Fig. 93). Amongst these Pb ores are most important, whereas more northerly trending veins tend to be minor and contain dominantly Cu and Zn ores.

## CHAPTER 14

## GEOCHEMISTRY OF THE ORE MINERALS

A. Introduction

One of the aims of the geochemical investigation is to determine any significant differences in trace and major element contents of the ore minerals in different mineralogical zones. This may lead to conclusions related to temperature of formation and partitioning of elements between minerals at different stages of intrusion.

Samples of individual ore minerals were separated and analysed by the methods outlined in appendix 1. Lists of the veins from which chalcopyrite, sphalerite and galena were obtained and their locations are provided on Figures 98 and 99. Results of these analyses and others, of arsenopyrite, pyrrhotite and crude ore are tabulated in appendix 8.

B. Sphalerite

Sphalerite is one of the best minerals to use in this type of study, having a widespread occurrence, a varied trace and major element chemistry and a relative resistance to the processes of secondary alteration. Twelve samples were separated and analysed from various localities (Figs. 98 and 99, appendix 8).

Amongst the trace and minor elements Cd, Mn, Ni, Co and As are probably held in lattice sites (Fleischer, 1955). Cu and Ag may occur in separate mineral phases e.g. tetrahedrite and/or in the lattice. High Ag concentration in some of the sphalerites cannot, in many cases, be explained as being due to galena impurities,



because Ag contents are low in many coexisting galenas. Native silver, argentite or other Ag-bearing minerals have not been observed in polished sections, although they may occur as separate submicroscopic admixed phases. All Pb in sphalerites is assumed to be contained in galena contamination, high concentrations of this element reflect some of the difficulties encountered during separation of the ores.

Bearing these points in mind, a cluster analysis (appendix 1) was performed upon the results of the Zn, Fe, Cd, Mn, Ni, Co and Ag analyses. Two significant clusters emerge (Fig. 100) which are considered to have both a chemical and geographical connotation.

The first cluster includes sphalerites from East and West Blackcraig (1 and 2), Culcronchie (12), Chain Burn (7), Pibble (9), Dromore (11) and Meikle Bennan (8, Fig. 99). These tend to have a low content of all analysed minor and trace elements (table 15A, appendix 8). Geographically they all occur in the Blackcraig-Pibble area (Fig. 91). Within the clusters, sphalerites from the Pibble-Dromore (P, Fig. 99) and Blackcraig-Culcronchie areas seem to form internally comparable groups, but their significance other than geographical, may be low.

Sphalerites from Silver Rig (3), Dromore (10), Coldstream Burn (4 and 5) and Wood of Cree (6, Fig. 99) are contained within the second cluster. One of the most important differences between the clusters is that the samples in the second contain more Fe (table 15A). Within the cluster the Wood of Cree-Coldstream Burn sphalerites

form a group, probably again of low significance. Broadly, except sample 10 from Dromore, the cluster analysis has grouped together sphalerites on a geographical basis.

Correlations between elements in sphalerite (table 15B) show the predictable highly significant negative correlation between Fe and Zn. Fe and Mn have a significant positive correlation which is consistent with previously published data (Warren and Thompson, 1945; Fleischer, 1955; etc.). Positive correlations occur between Ag and Fe, and Ag and Mn. High temperature and/or low S vapour pressure may, depending upon the availability of Fe, produce a sphalerite rich in Fe (Kullerud, 1953; Barton and Toulmin, 1963, 1966). The correlations above indicate that similar conditions may promote the uptake of Ag into either lattice sites or as a separate phase in solid solution. A positive correlation of greater than 95% significance also occurs between Fe and Co.

(i) Iron

As mentioned above, cluster analysis separates the sphalerites into two groups, and these contain low and high Fe sphalerites with means of 2.20% and 7.35%. On a geographical basis those from the Pibble-Blackcraig area vary between 0.5% and 6% and the Silver Rig-Wood of Cree area between 6% and 10% Fe. Within these areas sphalerites from the lead zone have relatively lower Fe contents than those from the zinc zone (East and West Blackcraig,  $\bar{x}$  = 1.95% Fe; Silver Rig, 6.48% Fe). The most Fe-poor sphalerite is from the copper zone at Culcronchie, adjacent

to the granite, (fig 101).

Though further sampling is desirable, it appears that sphalerites from the zinc zones contain more Fe than those from the copper and lead zones. On Fe content alone it may be considered that either two separate phases of mineralization occurred, or the same phase was influenced by differing S vapour pressure in the two areas described above.

(ii) Cadmium

Compared with previous analyses (Fleischer, 1955) most of the sphalerites appear to contain average amounts of Cd, although one of the Dromore samples (10) and the Silver Rig sample (3) are enriched (appendix 8, Fig. 101).

Sphalerite from veins in the lead zone varies in Cd content from 0.41% to 0.80%. The Silver Rig sample (0.80% Cd) contains considerably more than the mean of the Blackcraig samples (0.43%). The Cd content of the copper zone sphalerite at Culcronchie (0.43%) equals the mean of the Blackcraig analyses (cf. Fe above). Sphalerites from the zinc zone in the Wood of Cree area are relatively low in Cd ( $\bar{x} = 0.17\%$ ) whereas those from the Pibble region contain more ( $\bar{x} = 0.38\%$ , Fig. 101). A ternary diagram of the relative Zn, Fe and Cd contents (Fig. 102) shows the chemical separation of the two areas of zinc zone mineralization.

High concentrations of Cd are more likely in moderate to low temperature veins, than those of high temperature (Stoiber, 1940; Warren and Thompson, 1945). In this context it is perhaps relevant that amounts of Cd

and Fe in sphalerites of the two zinc zone areas are inversely proportional.

As with Fe (above), Cd contents of sphalerites from the zinc zone of the Wood of Cree and Pibble areas suggest differing conditions during their deposition or different phases of mineralization (Fig. 101).

(iii) Manganese

Sphalerites of the Fleet orefield are comparatively poor in Mn (6-318 ppm; cf. Fleischer, 1955). As expected from the positive correlation with Fe (table 15B) the distribution of these elements is comparable (Fig. 101), although an overlap occurs in the Mn contents of the sphalerites from the zinc zone in the Pibble and Wood of Cree areas.

(iv) Nickel

Nickel concentrations are mostly on the limit of detection for this analytical technique ( $< 10$  ppm), except for two of the Fe-rich samples from the Wood of Cree and Coldstream Burn veins (34 and 31 ppm respectively). These low values are consistent with data published previously (Fleischer, 1955).

(v) Cobalt

The range of concentration of Co in sphalerite is between 8 and 119 ppm (Fig. 101), indicating a slight depletion compared with the norm (Fleischer, 1955). As with Fe and Cd two distinct groups exist. Zinc zone sphalerites from the Pibble region contain between 8 and 36 ppm Co, whilst those from the Wood of Cree region contain between 102 and 119 ppm. The lead zone sphalerites

have a range in Co concentration between 95 and 102 ppm and compare with those of the Wood of Cree zinc zone (Fig. 101). The Co content of the sphalerite from the copper zone (12) is intermediate between these groups (64 ppm). The distribution of Co in sphalerite is undoubtedly related to Fe content, as indicated by their positive correlation (table 15B).

(vi) Silver

Most of the sphalerites have an average Ag content (10-200 ppm; cf. Fleischer, 1955), but three are considerably enriched (4, 5 and 10, Fig. 101; 500-1400 ppm). The extent to which impurities of argentiferous sulphides contribute is unknown, because none has been identified by microscopy. If Ag is present in tetrahedrite, a positive correlation with Cu would be expected, but none exists, although it may have been overprinted by the presence of chalcopyrite inclusions. Nevertheless a sphalerite from Dromore (10) contains both the highest Ag (1357 ppm) and Cu (0.20%) concentrations, though the Cu:Ag ratio is low even for tetrahedrite.

Ag contents from sphalerites in the lead and copper zones range between 10 and 21 ppm, and in the zinc zone between 57 and 1357 ppm (Fig. 101). If sphalerites of the zinc zone are divided on a geographical basis as before, samples from the Wood of Cree area have a mean of 474 ppm and those from the Pibble area, 346 ppm, although a large overlap exists due to the Dromore sample (10).

Correlations between Fe, Mn and Ag have been discussed previously (above).

(vii) Lead and copper

Pb contents exhibit a wide range (0.01-8.45%) and are probably mainly the result of physically admixed galena. Separate sulphide phases, such as chalcopyrite and tetrahedrite contribute to the Cu concentrations (0.03-0.20%).

(viii) Arsenic

Concentrations of As are below the detection limit of the analytical technique ( $\approx 0.1\%$ ) in most of the sphalerites. However Fe-rich samples from Coldstream Burn (4) and Dromore (10, Fig. 99) contain 0.18% and 0.10% respectively.

(ix) Conclusions

It is appreciated that the interrelationships between the Zn, Fe, Cd, Mn, Ni, Co and Ag contents of sphalerite are complex. Data are broken down onto three ternary diagrams, Zn-Fe-Cd, Cd-Ag-Co and Cd-Co-Mn (Figs. 102 and 103). Fields of sphalerites from different mineralogical zones and geographical locations may be distinguished. More samples of sphalerite from chalcopyrite-bearing veins would be desirable to confirm data relating to ores of the copper zone. Certain of these trends are confirmed by Zn/Cd and Zn/Fe ratios in galena, chalcopyrite and crude ores (below).

C. Galena.

Eight samples of galena have been analysed (appendix 8, Figs. 98 and 99) for Pb, Zn, Cu, Ag, Mn, Cd, Cr, Fe, Ni, Co and As. Of these Ni, Co and As were under the detection limit, and significant quantities of Zn, Cd,

Mn, Cu, Fe and Cr originate from contamination by sphalerite, chalcopyrite, gangue and wallrock. Pb and Ag are the only analysed elements which can be ascribed definitely to the lattice of galena.

(i) Silver

The samples of galena may be divided into three groups on their Ag content, and these correspond to the mineral zones (Fig. 101). Galenas from the lead zone have a range between 17 and 19 ppm, the zinc zone 266 to 327 ppm; and the single sample from the copper zone 48 ppm. Additional samples from the Wood of Cree area are desirable to determine the relationship between galenas of the two zinc zones. Galena in this locality is highly intermixed with pyrite (plate 35A and B) and was considered unsuitable for separation.

Sphalerites and galenas in the zinc zone are notably enriched in Ag in comparison with their copper and lead zone counterparts. However the Ag content of galena in many other areas has been observed to increase away from the zone of major zinc ores, towards a zone of argentite-rich ore (Emmons, 1936). As noted above galena from Silver Rig described previously as argentiferous (Wilson, 1921), yielded only 17 ppm Ag in this survey.

High amounts of Ag detected in galenas and sphalerites from the zinc zone may be related to the association of argentiferous tetrahedrite which is often found in deposits of the outer copper zone (Emmons, 1936). But again this appears to be unlikely because the Ag content of most of the galenas exceeds the Cu content by

factors of between 2 and 20.

As all other analysed elements may be ascribed to the presence of impurities their concentration depends solely on amounts of admixed minerals.

(ii) Zinc/cadmium ratios

Zn and Cd occurring in large amounts in galena is the result of sphalerite contamination; actual amounts of Zn and Cd taken up as a solid solution in galena are low (Bethke and Barton, 1971). This concept has been tested by analysing coexisting galena and sphalerite from the Dromore vein (galena, 7; sphalerite, 10). The Zn/Cd ratio of the sphalerite is 78, and that of coexisting galena containing 0.30% Zn, is 83. However a low ratio (24) is obtained from a galena from the Pibble vein (sample 6) containing 193 ppm Zn, due to Cd contained within the crystal lattice.

The two galenas from the Bargaly vein (samples 4 and 5) contain sufficient Zn (1.13% and 0.19%) to apply the ratio. The results obtained (470 and 475) are of a similar order of magnitude as the Wood of Cree and Cold-stream Burn zinc zone sphalerites, which range between 275 and 380. They are indicative of low Cd contents in coexisting sphalerite, from which correlation between sphalerites from the zinc zone at Wood of Cree and Bargaly may be inferred.

(iii) Zinc/iron ratios

Zn/Fe ratios have been determined from galenas containing greater than 0.1% Zn and reflect the Fe content of coexisting sphalerite. Dromore galena (sample 7) yields



a Zn/Fe ratio of 11.5 which compares with that of co-existing sphalerite (sample 10), 10. Bargaly galenas (samples 4 and 5) have ratios of 12 and 20 which are similar to sphalerites from the zinc zone in the Pibble-Dromore area with a range between 10 and 46, and indicate sphalerites with Fe contents between approximately 3 and 6% (cf. Fig. 101).

(iv) Conclusions

It is apparent that sphalerite from the zinc zone at Bargaly has a comparable Cd content with sphalerite at Wood of Cree, and a comparable Fe content with sphalerite from the Pibble-Dromore area. It is perhaps relevant that the Bargaly vein is situated between these areas (Fig. 101). Relative amounts of Zn, Fe and Cd in galenas from the localities described above have been plotted on Figure 102, for comparison with sphalerites. As expected the galena (7) and sphalerite (10) from Dromore plot very close together. Bargaly galenas (4 and 5) occur between the Pibble and Wood of Cree zinc zone fields.

Galena samples are divided into groups, based on their Ag content, which correspond to the mineral zones. Bargaly galena compares on this basis with Pibble-Dromore galena from the zinc zone.

D. Chalcopyrite

Chalcopyrite, being very susceptible to post-depositional alteration, is considered less desirable for use in a geochemical study of this type. In the seven samples analysed it is proposed that Zn, Pb, Cd and Cr are the result of contamination by other sulphide phases and

wallrocks. High Ni and Co concentrations in chalcopyrite from Talnostry are probably due to enclosed niccolite and smaltite ( see chapter 13, A).

(i) Nickel and Cobalt

Discounting the obviously contaminated Talnostry ore, chalcopyrite increases in both Ni and Co content from the copper zone, through the zinc zone to the lead zone (Fig. 101). Means of Ni for the copper, zinc and lead zones are 37 ppm (range 21-52 ppm), 217 ppm (92-342 ppm) and 817 ppm (334-1300 ppm) respectively, and those for cobalt are 8 ppm (6-9 ppm), 63 ppm (0-126 ppm) and 152 ppm (63-241 ppm) respectively. High Ni and Co concentrations in chalcopyrite from West Blackcraig may be due to impurities of erythrite ( $\text{Co}_3\text{AsO}_8 \cdot 8\text{H}_2\text{O}$ ), which has previously been described from this locality (Heddle, 1901). However As contents are relatively low in this sample (appendix 8).

(ii) Silver

The Ag distribution follows a less clear pattern as the chalcopyrites from each zone have wider variations in the concentration of this element (Fig. 101). There is an increase in the mean Ag concentration away from the copper zone. Copper, zinc and lead zones have means of 188 ppm (range 109-370 ppm), 167 ppm (179-183 ppm) and 127 ppm (58-203 ppm) respectively, an inverse relationship to those of Ni and Co.

(iii) Arsenic

Arsenic concentrations in chalcopyrite do not fall into a regular pattern. The high As content of the Talnostry ore (0.43%) is probably related to Ni-Co arsenides, but that at Pibble (0.44%) is unaccountable as

a visible mineral contaminant. Lower values at Drumruck, Pibble and West Blackcraig may relate to As within the lattice.

(iv) Manganese

Chalcopyrites contain average Mn contents (cf. Fleischer, 1955) and these are considered to be related essentially to Mn in the lattice, although a minor contribution may be made from admixed sphalerite. Variations in concentration are large but excluding the Talnotry sample, ores from the lead and zinc zones appear to contain more Mn (3-27 ppm), than those of the copper zone (0-10 ppm). More data are desirable to confirm this trend.

(v) Zinc/cadmium ratios

It is assumed, as with the galenas (above), that high concentrations of Zn and Cd are related to an enclosed sphalerite phase. The mean Zn/Cd ratios for chalcopyrites from the copper, zinc and lead zones are 97 (54-139), 135 (55-215) and 68 (53-83) respectively. Zn zone sphalerites are consistently relatively Cd-poor (see above).

(vi) Conclusions

The Ag-Ni-Co ternary diagram displays the major differences in the chemistry of the chalcopyrites (Fig. 104). Away from the copper zone Ag decreases in amounts relative to Ni and Co, and there is a corresponding slight enrichment of Co relative to Ni. Pending analyses of further material the results can, however only be considered as preliminary.

## E. Pyrrhotite and Arsenopyrite

### (i) Pyrrhotite

One analysis was undertaken on hand picked pyrrhotite ore from the Talnotry vein (P 74/004, appendix 8), but it is probably contaminated with chalcopyrite, pentlandite, niccolite and smaltite. These account for the high concentrations of Ni (3.82%), Co (974 ppm) and Cu (832 ppm). The significance of Co/Ni ratios in relation to this deposit are discussed below.

### (ii) Arsenopyrite

Arsenopyrites from the Glen of the Bar (A 73/515) and Palnure Burn (A 72/005) deposits at Talnotry have been analysed (appendix 8). Arsenopyrite from the former locality is contaminated with small amounts of pyrite which accounts for its high S/As ratio (1.36, S has been calculated by difference, which is valid as all other major elements and quantities of insoluble material have been accounted for). The pure arsenopyrite from the granite contact is only slightly enriched in S (S/As = 1.03) which is consistent with other analyses (Clark, 1960a, 1960b). Ni, Co and Mn concentrations are within the average ranges for arsenopyrite (cf. Fleischer, 1955). Variations in trace element assemblages cannot be assessed without further analyses from these deposits.

## F. Crude ores

### (i) Orchars vein

Two samples of contrasting vein infillings from the vein at Orchars (chapter 13, A; 1, Fig. 91) have been analysed to compare Cu, Pb, Zn, Ni and As concentrations

with stream sediments collected downstream. Comparative data of primary and secondary dispersion of Cu, Pb, Zn and Ni are provided in table 14. As a result of incomplete sampling statistical analysis was not undertaken on As data, but the background appears to be below 40 ppm. Pb (890 ppm) and As (150 ppm) occur in anomalously high concentrations in stream sediments downstream from the outcrop of the vein. It is considered impossible for the quantity of Pb in the two ore samples (25 ppm and < 5 ppm, appendix 8) to be responsible for the highly significant secondary dispersion anomaly. The surrounding granite has a higher Pb content ( $\bar{x} = 31$  ppm), than the vein. Accordingly, it is proposed that other veins or a disseminated mineralization of a different mineralogy, are responsible for this and other Pb anomalies in stream sediments derived from the granite (see G below and Figs. 105 and 106).

The jasper-rich ore (0.73/507a), containing minor amounts of specular hematite and chalcopyrite, (plates 30A and B) contains lower quantities of all base metals compared with the quartz-pyrite ore (0.73/507b). Pyrite is the only opaque mineral identified in the latter type and thus accounts for the whole of the base metal assemblage. If the insoluble residue is accounted for, and the pyrite analysis recalculated to 100%, it appears to be significantly enriched in Co (ca. 6000 ppm), Ni (ca. 900 ppm) and As (ca. 1500 ppm; cf. Fleischer, 1955). Pyrite from high temperature deposits contains high amounts of Co, has a high Co/Ni ratio and is comparable with that from the Orchards vein (6.7). Large variations

have been observed in concentrations of Ni in pyrite from hydrothermal ore deposits, although again higher concentrations have been related to deposits with a high temperature of formation (ibid).

From paragenetical studies the Orchars vein is considered to be a multiple phase intrusion, comprising initial stages of low to intermediate temperatures of formation associated with deposition of chalcopyrite, specular hematite, colloform jasper and silica, followed by a high temperature quartz-pyrite stage.

(ii) Talnotry vein

Two samples of ore have been collected in situ from the Talnotry pyrrhotite deposit. Sample 0.73/513 is from the hanging wall at the margin of the lode and consists of sulphides impregnating and replacing altered and brecciated diorite wallrock. Sample 0.72/004c is from the centre of the lode approximately one metre from the footwall. Both ores contain pyrrhotite, chalcopyrite, niccolite and probably smaltite, which return high Cu, Ni and Co concentrations. However, low As contents in both ores indicate that most of the Ni is in the pyrrhotite.

Co/Ni ratios of the crude ores are 0.035 and 0.042 and the pyrrhotite (above) has a ratio of 0.025. All are comparable with values for ores of magmatic origin (Bastin, 1939). Typically Ni-Co-Ag veins contain ores with higher ratios, between 2.0 and 0.15. Although the vein at Talnotry has a similar mineralogy and setting to those of the Ni-Co-Ag type, the chemical characteristics and the presence of pentlandite are more closely related to ores of the differentiated magmatic sulphide deposits

(e.g. Sudbury, Bastin, 1939; Stanton, 1972). The reason for this is not clear.

(iii) Culcronchie vein

A mixed chalcopyrite-pyrite ore with a quartz gangue from the middle vein at Culcronchie, has been analysed (0.74/1167, appendix 8). Analysis of stream sediments immediately below the vein and spoil tips give the following results, and are compared with the ore:

	ORE	SEDIMENT	
		<100 m downstream	≈500 m downstream
ppm			
Cu	76500	86	34
Ni	900	295	50
Pb	424	830	180
Zn	714	6000	910
As	3600	300	40
Mo	-	4.0	<2.0

Analysis of the ore (above) and polished section indicate that approximately equal amounts of chalcopyrite and pyrite occur. This is not typical of ore of the middle vein at Culcronchie, in which chalcopyrite is usually in excess. The secondary dispersion figures (above) reveal the high solubility of Cu minerals (e.g. chalcopyrite) and the relative resistance of galena, sphalerite and pyrite. Ore from the upper vein which contains sphalerite and minor amounts of galena and chalcopyrite, may have contributed some of the Pb and Zn in these sediments.

Chalcopyrite from this vein contains very low amounts of Ni and Co (see above, 20 and 9 ppm respectively). It is assumed, therefore that the bulk of the Ni and Co in the crude ore is contributed by pyrite (endorsed by anisotropism observed under the microscope, above), which thus appears to be slightly enriched in these constituents (cf. Fleischer, 1955). This enrichment coupled with a Co/Ni ratio of 0.5 may indicate a high temperature of formation (ibid).

Partitioning of Ni and Co between pyrite and chalcopyrite appears to favour the former mineral and may as a result of decrease in amounts of pyrite and/or changes in physical conditions during crystallization, be the reason for the increase in concentration of these elements in chalcopyrites further away from the copper zone (see above). At lower temperatures of formation partitioning may favour chalcopyrite (e.g. Blackcraig).

The presence of sphalerite is indicated by a high Zn content (714 ppm), and the Zn/Cd ratio (179) is close to that determined from the upper vein at this locality (152, see above).

(iv) Tonderghie vein

The ore analysed is typical of vein infilling at Tonderghie, and consists of sphalerite, various carbonates and quartz (0.72/031, appendix 8). High concentrations of Mn and Fe relative to Zn are due to contamination by gangue carbonates (e.g. calcite, ankerite, etc.) and is unavoidable in any analysis involving acid extraction.

The Zn/Cd ratio is 135, close to the mean of the



lead zone sphalerites (128), but within the range of the zinc zone sphalerites from the Pibble area (78-280,  $\bar{x}$  = 201). If the Ag value is recalculated to 100% sphalerite (i.e. 67% Zn) a figure of approximately 50 ppm is obtained which is comparable to Pibble area zinc zone sphalerites. (57-1357 ppm,  $\bar{x}$  = 346 ppm). Zinc zone sphalerites separated from mixed quartz and carbonate gangue have a mean of 73 ppm Ag, and those from the lead zone with a pure carbonate gangue, 17 ppm. It thus appears chemically that sphalerite from the Tonderghie deposit has characteristics in common with both lead and zinc zones, and this is borne out mineralogically by the high proportion of carbonate in the gangue. Although the boundary between the lead and zinc zones has not been detected northwest of the pluton (Figs. 91 and 94), on this basis the zinc zone is probably very narrow.

(v) Pibble vein

Analysis has been undertaken on ore containing cuprite, covellite, chalcocite, native copper and iron oxides from the zone of secondary (supergene) enrichment at Pibble (0.74/639b, appendix 8, plate 37A and B). Galena has been replaced by chalcocite during enrichment by percolation of solutions containing Cu from the oxidation zone or gossan above, in accordance with Schürmann's series (Schürmann, 1888). The presence of both chalcocite and cuprite indicate that this ore was situated close to the fluctuating surface of the water table, which provided changing conditions of Eh.

### G. Secondary dispersion

Anomalous base metal concentrations in stream sediments over the granite outcrop pinpoint certain areas which may contain minor vein or disseminated base metal mineralization. The revised contact of the fine grained granite (see part 2, above) passes through a number of these areas, especially in the southwest (Fig. 105).

The Glengainoch Burn provides a continuous system of drainage across the inferred contact over which levels of Cu, Ni, As, Zn, Pb and Mo increase markedly and decrease downstream (Figs. 105 and 106). Levels of some elements increase again further downstream as a result of concentration of heavy minerals in less turbulent water, owing to a decrease in the gradient of the stream bed. Exposure in this area is so poor that the nature of the mineralization has not been ascertained.

Streams draining south from the fine grained granite in the vicinity of Craigwhinnie (25585690) and Benmeal (25685686) also contain sediments with very high or above threshold concentrations (table 14) of certain base metals, notably Pb and Mo (Fig. 105). Mo values are especially high near to or immediately downstream from the contact. These anomalies suggest that mineralization may be associated with the fine grained granite contact in this area. Other secondary dispersion anomalies over the granite may be the result of mineralization comparable with that at Orchars (above), but further investigation is required to confirm this.

### H. Summary and conclusions

It is admitted that because of the small number of samples studied only tentative conclusions may be reached. Nevertheless, certain trends appear to be significant and might reasonably form the basis of a more detailed study. The geochemical characteristics of the major sulphides in each mineral zone are tabulated below, although relative amounts of minor and trace elements refer only to ranges observed in the Fleet ore-field (table 16).

	COPPER ZONE	ZINC ZONE	LEAD ZONE
SPHALERITE	low Ag, Fe, Mn. mod. Cd, Co.	mod. to high Ag, Fe, Mn. variable Cd, Co.	low Ag, high Co mod. to low Fe, Mn. mod. to high Cd.
		WOOD OF CREE low Cd high Fe, Mn.	PIBBLE mod. to high Cd mod. Fe, Mn.
GALENA	mod. to low Ag	high Ag	low Ag
CHALCOPYRITE	high Ag low Ni, Co	mod. Ag mod. Ni, Co	low Ag high Ni, Co.

Low concentrations of Fe in sphalerites from the copper zone may be due to high S fugacity (Barton and Toulmin, 1963) and/or reduced availability resulting from partitioning of Fe towards pyrite and chalcopryrite, which may be more stable under these conditions. In the zinc zone conditions allow more Fe to be taken up by sphalerite, up to the amounts allowable in the Zn-Fe-S system at the prevailing temperatures and S fugacities. This may be associated with the crystallization of

relatively smaller amounts of Fe containing sulphides such as pyrite and chalcopyrite. Less Fe is accommodated in the lattice of sphalerite of the lead zone probably as a result of lower temperatures of formation (Kullerud, 1953). The excess Fe is probably contained within the ferroan calcite and ankerite gangue of these deposits, and perhaps indicates lower S fugacities.

Pyrite from high temperature veins often contains high concentrations of Ni and Co (Fleischer, 1955; e.g. Orchars and Culcronchie, above). This may explain the depletion of these elements in sphalerite and chalcopyrite of the copper zone. Towards the lead zone the amount of pyrite in the veins decreases as does its capability of holding large amounts of Ni and Co, due to reduced temperatures of formation. These elements are accordingly found in larger concentrations in sphalerite and chalcopyrite of the lead zone.

The Ag content of chalcopyrite is highest in the copper zone whereas it tends to be low in sphalerite and galena. The content of Ag in the latter minerals is highest in the zinc zone where amounts in chalcopyrite are only moderate. All three minerals are depleted in Ag in the lead zone. The initial inverse relationship is probably a result of partitioning at high temperatures, and the decrease in concentrations between the lead and zinc zones may be due to decreasing temperature of formation or overall depletion in Ag. It has been previously reported (Tischendorf, 1955) that the Ag content of galena decreases with decreasing temperature of formation. Emmons (1936) observes that separate Ag

phases, such as argentite, develop to the outside of a zone of lead ores, but such mineralization has not been recognised in the Fleet orefield

## CHAPTER 15

## WALLROCK ALTERATION

A selection of mineralized localities from the various zones containing different wallrock lithologies, were investigated to determine the chemical and mineralogical changes which have taken place as a result of wallrock alteration.

(i) Orchars vein

At present this is the only confirmed occurrence of a mineral vein wholly within the granite. As described previously (above) it contains a quartz, colloform silica and jasper gangue surrounding pyrite, chalcopyrite and fragments of altered granite.

Granite wallrocks show signs of alteration at least 2 metres away from the 5 metre thick vein, which may itself indicate moderate temperatures of intrusion. In thin section signs of crushing and granulation are apparent, and most quartz crystals exhibit undulose extinction in response to strain. Unaltered granite in the vicinity contains approximately equal quantities of biotite and muscovite, but during alteration biotite is removed and sericite formed from feldspars. Very obvious grains of grey-blue fluorapatite and pale yellow monazite are present and replace the normally colourless apatite.

Chemical trends mirror some of the mineralogical changes (Fig. 107, table 17). A measure of enrichment or depletion of elements or oxides is given by values of  $\Delta$ , which is the ratio of the composition of the altered over the unaltered rock (i.e.  $\Delta = x_1/x$  in tables 17-20).

$\text{SiO}_2$  is the only major oxide to be enriched (i.e.  $\Delta > 1$ ), and this may only be a relative enrichment due to removal of other oxides.  $\text{Al}^{3+}$  is one of the least mobile cations (Meyer and Hemley in Barnes, 1967) and therefore cation movements may be deduced relative to  $\text{Al}_2\text{O}_3$ , at constant volume of rock. The  $\Delta$  value of  $\text{Al}_2\text{O}_3$  is 0.64 (table 17); assuming the above statement to be correct, all values below this represent an actual depletion. The  $\Delta$  value of Zr is also 0.64, which endorses this concept because the bulk of Zr in the granite is contained within the very resistant mineral zircon.

Relative to  $\text{Al}_2\text{O}_3$  a much larger enrichment in  $\text{SiO}_2$  ( $\Delta = + 0.48$ ) is apparent and is a result of silicification. Depletion in  $\text{Fe}_2\text{O}_3$ , MnO, MgO, CaO,  $\text{Na}_2\text{O}$ , Sr and Zn is ascribed to removal of plagioclase, microcline and biotite during alteration.  $\text{K}_2\text{O}$  and Rb are enriched with respect to  $\text{Al}_2\text{O}_3$  and are accommodated in newly formed sericite. Y is concentrated by a factor of 14 in the wallrock and is undoubtedly held in the lattice of monazite, which may indicate that ore-forming fluids were rich in heavy rare-earth elements (Hermann, 1970). The distribution of Li (Fig. 107) is attributed to an initial depletion during alteration of biotite, followed by an enrichment as a result of a change in chemistry of the hydrothermal fluids.

From the relative enrichment of certain species the ore-bearing solutions probably contained Si, K, Li, Rb, Be and Y, and promoted silicification and sericitization (K-silicate alteration, Meyer and Hemley in Barnes, 1967) of wallrocks.

(ii) Culcronchie Vein

The upper vein at Culcronchie is one of the few localities in which wallrocks are pelitic. The vein infilling consists of brecciated black hornfelsed mudstone (Moffat Shale, see chapter 4, H), sphalerite, minor chalcopyrite and galena, and quartz. In thin section the altered wallrock has been observed to contain parallel orientated flakes of sericite, and quartz packed with inclusions of opaque carbonaceous material; biotite is absent.

Differences in the chemistry of this rock compared with an unaltered black hornfelsed mudstone along strike are given in table 18.  $\Delta$  values for  $Al_2O_3$  and Zr are again similar and amounts of these elements are assumed to have remained constant throughout alteration (above). Extreme enrichment of  $SiO_2$  (+ 0.96) has taken place as a result of silicification.  $TiO_2$ , MnO, MgO, CaO,  $Na_2O$ ,  $P_2O_5$ , Sr and Y are very depleted and  $Fe_2O_3$  rather less so, indicating removal of these elements in response to breakdown of biotite, feldspars and apatite.  $K_2O$  is slightly enriched relative to  $Al_2O_3$ , but Rb and Li have remained constant, and are all held in the lattice of sericite produced as a result of K-silicate alteration.

The chemistry of Culcronchie wallrock reflects a more intense silicification accompanied by less sericitization, compared with the Orchards vein above. The fluids responsible for alteration were probably not as enriched in Li, Rb, Be and Y.



(iii) Wood of Cree vein

This vein typically contains massive pyrite, sphalerite and galena ore, with very little gangue. Wallrocks are pale grey, bleached and obviously silicified.

Unaltered greywacke from the Wood of Cree area was not collected, therefore wallrock analyses are compared with the average of Silurian greywackes collected (table 19). Notable losses occur in Sr and  $\text{Na}_2\text{O}$ , and enrichment of  $\text{SiO}_2$ , CaO,  $\text{K}_2\text{O}$ , Li and Rb compared with  $\text{Al}_2\text{O}_3$ . Due to the absence of firm local control it is not possible to determine how much of these changes are the result of lithological variation. Nevertheless both silicification and sericitization have probably taken place, although not to the extent of the localities above.

(iv) Bargaly vein

The Bargaly vein is on the border between the zinc and lead zones, although the chemistry of the sulphides contained within it have more affinity with the former (see above). The gangue is mixed and contains both quartz and carbonates (calcite, dolomite and ankerite), surrounding sphalerite and galena. Biotite hornfels derived from greywacke, when altered adjacent to the vein is transformed into a quartz-sericite rock containing altered feldspars. Having replaced biotite, sericite retains the original lepidoblastic texture of the hornfels.

Geochemical variations between unaltered greywacke 500 metres from the vein, altered wallrock at the contact and a breccia fragment from within the vein are given on Figure 108 and table 20.  $\text{Al}_2\text{O}_3$  and  $\text{SiO}_2$  remain fairly

constant in response to decreased silicification, which may indicate a lower temperature of alteration.  $\text{Fe}_2\text{O}_3$ ,  $\text{MgO}$ ,  $\text{Na}_2\text{O}$ ,  $\text{CaO}$ ,  $\text{MnO}$ ,  $\text{P}_2\text{O}_5$  and  $\text{Sr}$  are, however, strongly depleted and replaced by  $\text{K}_2\text{O}$  and  $\text{Rb}$ , as a result of sericitization.

The degree of silicification appears to be proportional to the amount of quartz in the gangue, and where it is low it is replaced by sericitization.

(v) Dallash vein

The bulk of this vein consists of calcite and ankerite surrounding galena, sphalerite, chalcopyrite and brecciated wallrock. An initial phase of mineralization was quartz-rich and has resulted in slight silicification and chloritization of the purple-brown lepidoblastic biotite hornfels wallrock. Adjacent to the vein the altered rocks are pale green.

Chemical variations are slight (table 21) assuming  $\text{Al}_2\text{O}_3$  and  $\text{Zr}$  are constant, and include enrichment of  $\text{SiO}_2$  and depletion of  $\text{Fe}_2\text{O}_3$ ,  $\text{MgO}$ ,  $\text{CaO}$  and  $\text{Y}$ . More important losses of  $\text{K}_2\text{O}$  and  $\text{Rb}$ , and gains of  $\text{Na}_2\text{O}$  and  $\text{Sr}$  occur.

Wallrock alteration consisting mainly of chloritization associated with slight silicification and sericitization, is less severe than in the other localities investigated (above), and may be attributed to a lower temperature of formation.

(vi) Conclusions

Changes in the type and extent of wallrock alteration reflect changes in the mineralogy and chemistry of the vein deposits. There is a decrease in intensity of

wallrock alteration away from the copper zone which may be the result of decreasing temperature or increasing pH of the fluids responsible. In the zinc and copper zones adjacent to veins containing quartz gangue, silicification is dominant although accompanied by sericitization. Veins of the lead zone containing carbonate gangue are associated with wallrocks displaying more localised and less severe effects of chloritization, sericitization and silicification.

## CHAPTER 16

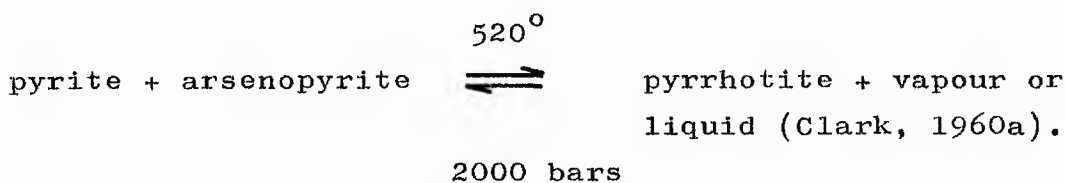
## CONCLUSIONS

A. Temperature of formation

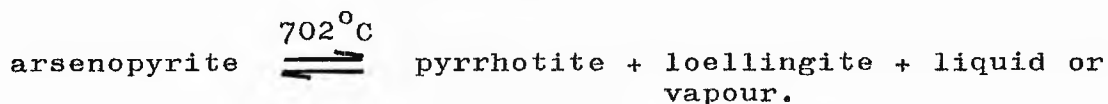
As a result of problems encountered in the application of geothermometers such as the Zn-Fe-S system (Kullerud, 1953) no attempt will be made at giving precise temperatures of formation. Some ideas have already been presented on the relative temperatures of formation of the vein deposits using Co and Ni concentrations and ratios in pyrites, and intensity of wallrock alteration, etc. Although the minerals were undoubtedly precipitated from hydrous systems, the data presented below are useful in restricting the physiochemical environment in terms of the most important variables, temperature and sulphur fugacity. (Barton and Skinner in Barnes, 1967).

The veins at Talnotry (see chapter 13, A) contain minerals of a typical high temperature assemblage. It has already been noted that arsenopyrite from the granite contact is enriched in S relative to As. This relationship is enhanced by high confining pressure during deposition (Clark, 1960a, 1960b). The upper limit of stability for coexisting pyrite and arsenopyrite is  $491^{\circ}\text{C}$  and increases to  $528^{\circ}\text{C}$  at 2,070 bars. It has already been proposed that the granite crystallized at confining pressures exceeding 2000 bars (see chapter 9, above), and if mineralization took place under the same conditions, it gives the assemblage at Glen of the Bar an upper temperature limit of approximately  $530^{\circ}\text{C}$ .

Above this temperature pyrrhotite is formed by the reaction:

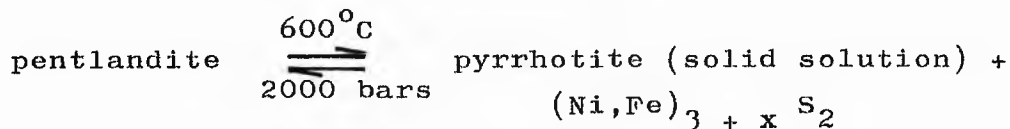


Assuming a simple system this equilibrium creates a minimum temperature of formation of  $530^\circ\text{C}$  for the Talnotry pyrrhotite deposit in the presence of As vapour. The Fe-As-S system is complicated to an unknown degree by the presence of chalcopyrite and Ni-Co arsenides. Pure arsenopyrite is more stable than that coexisting with pyrite and does not break down until  $702^\circ\text{C}$ :



Absence of loellingite in the pyrrhotite ore at Talnotry shows it is unlikely that this equilibrium has occurred, although the presence of Ni and Co may have favoured the formation of niccolite ( $\text{NiAs}$ ) and smaltite ( $\text{CoAs}_2$ ) rather than loellingite ( $\text{FeAs}_2$ ). It is therefore possible for the arsenopyrite at the granite contact to have formed at a higher temperature than the Glen of the Bar deposit.

Pentlandite, which occurs with pyrrhotite at Talnotry, breaks down at  $610^\circ\text{C}$ :



At 2000 bars the temperature of this equilibrium is about  $600^\circ\text{C}$  (Barton and Skinner in Barnes, 1967).

From this data it appears that the temperature of formation of the Talnotry pyrrhotite/pentlandite ore may have been of the order of  $600^\circ\text{C}$ , although the presence of

water would probably modify the equilibrium temperatures quoted above. The arsenopyrite deposit at the granite contact may have had a higher temperature of formation, but this is thought unlikely.

From the changes in mineralogy of the veins and the nature and extent of wallrock alteration it is proposed that mineralization took place under conditions of decreasing temperature away from the pluton. The Wood of Cree area is an exception to this simple concept, and may relate to a slightly different source, or differing conditions during formation.

#### B. Origin of the ores

From the geochemical, mineralogical and spatial data presented above it is clear that mineralization in the Fleet orefield is connected in some way to the Fleet pluton and the underlying batholith. Deposits with characteristics generally associated with higher temperatures of formation occur close to the outcrop of the granite.

Geochronological studies of ore minerals in the Southern Uplands were initiated by Moorbath (1962) using the common Pb method to date galena (Fig. 109). Each locality, including Silver Rig in this area (25, Fig. 91), gave ages of between 310 and 320 my, although errors are characteristically very large, i.e. of the order of 100 my. Recently work by Ineson and Mitchell (1974), using the K-Ar method on wallrock illites at Leadhills, has revealed continuous mineralization between 350 and 260 my, including errors (Fig. 109). It is very likely, although as yet

unconfirmed, that all the Fleet ores are of this age or older.

Ages for the plutonic igneous masses in the Southern Uplands have been presented in a number of works (Fig. 109). The Kirkmabreck granodiorite, the small dyke-like intrusion to the south of the Fleet pluton (map 8), gave an age of 396 my (Lambert and Mills, 1961). The marginal facies of the Cairnsmore of Fleet has been dated at 390 my. (Brown et al., 1968); both ages being determined by the K-Ar method. Further studies on the more central parts of the Fleet pluton, especially the later fine grained granite, are required to determine the age of the youngest phase of intrusion in this area.

Nevertheless it appears, from the available information, that there is a gap probably of at least 40 my between the crystallization of the Fleet pluton and its attendant mineralization. This relationship has been observed elsewhere, notably the northern Pennines (Dunham et al., 1964, 1965) where the Weardale granite (362 my) is overlain with obvious unconformity by sediments of Carboniferous age, and both contain a mineralization some 80 my younger than the granite. Dunham (*ibid*) proposes a genetical model invoking upwelling of juvenile waters, perhaps mixed with connate brines, from extreme depth. The already crystallized granite is envisaged as providing structural channelways opened up by Hercynian earth movements, locating the mineralization and bringing about the zoning pattern observed.

The model proposed for the genesis of the Fleet

ores is similar to this. However, from the geochemical characteristics of the Fleet pluton (see chapter 8, above) it is possible that some of the veins may be associated with late stage hydrothermal processes taking place in the granite (described above, see chapters 7 and 8). The fluids responsible for the mineralization may have therefore been derived either from a highly fractionated granite residuum or from greater depths (cf. Dunham, 1964, 1965). In both cases the Fleet pluton and/or the underlying batholith has acted as a channelway, and fracturing in the consolidated rock would allow upward passage of the low density fluids.

At levels where partial pressures of dissolved gases exceed the confining pressure, rapid exsolution of volatiles would take place. Increase in volume of gas in pore fluids might cause 'explosive brecciation' of wallrocks. Original wrench fault fractures in the surrounding sedimentary rocks may have opened up in response either to doming during intrusion of the batholith or to release of compressional stress. Ore bearing solutions would percolate upwards through the fractures, and might extend and further brecciate them by hydraulic fracturing (Phillips, 1972). The minerals would thereby be deposited in zones lying concentrically around the western margin of the pluton in response to decreasing temperatures or changes in fugacity of dissolved gases.



C. The area of study in relation to the rest of the Southern Uplands.

Sedimentation was initiated in the Southern Uplands during the Lower Ordovician. Data are scarce for the Arenig, only one outcrop being reasonably documented from the Southern Uplands proper (Walton and Weir, 1974), this being of graptolitic shales, laid down whilst the Ballantrae Igneous Complex and its associated cherts and mudstones were being intruded and deposited in the Girvan area, on the northwestern margin of the geosyncline. From the Llandeilo to the Llandovery, sedimentation was dominantly of graptolitic black shales and chert in the axial zone. Between these two areas a flysch succession formed in response to an influx of detritus, derived initially from the degradation of the uplifted Cockburnland and, after mid-Llandovery times, from the Highlands to the northwest and the uplifted marginal areas of the geosyncline (Dewey, 1969, 1971; Mitchell and McKerrow, 1975). Deposition was effected by turbidity currents (Walton, 1965).

Cockburnland contributed granitic and more basic igneous, often spilitic, detritus, the Ballantrae Igneous Complex being one likely source area (Kelling, 1962). Metamorphic and granitic fragments were probably contributed mainly by the Grampian Highlands (Dewey, 1971), though a Dalradian source within Cockburnland is also feasible (Walton, 1963; McGiven, 1967). Greywackes containing numerous basic igneous and ferromagnesian clasts appear to be restricted to the northern part of the trough (e.g. Kilfillan Formation, Gordon, 1962; Pyroxenous Group, Walton, 1955; Caignell Formation, basic facies, see above), whilst to the south, igneous detritus was more granitic in provenance, at least in

the Newton Stewart area (Craignell Formation, lithic facies, see above), and may have been derived in part from a southward-situated landmass, Solwayland (Walton, 1963). Some small contribution of detritus may also have been derived from a remnant of the Ordovician Cockburnland.

During the later Ordovician and early Silurian (Llandovery), turbidites to the north of the axial region overstepped the black shales and cherts in a southerly direction. There is evidence from the Newton Stewart area of a corresponding northwestward overstep by greywacke on the southern side of the axial region. Overstep was sustained until late in the Llandovery, after which flysch deposition dominated the entire trough.

As flysch sedimentation progressed, the greywackes became texturally and mineralogically more mature, reflected in an increasingly siliceous composition. Subduction along a northwestward dipping Benioff zone (Dewey, 1961) cropping out approximately along the line of the present Southern Uplands Fault may have caused uplift and accretion of Cockburnland by backthrusting of the pre-existing flysch successions (Mitchell and McKerrow, 1975). Erosion of these sediments would account for the increase in maturity of the greywackes through a process of recycling; an earlier proposition (Weir, 1974) that the Hawick Rocks succession of Gatehouse represents first-cycle derivatives is regarded only as tentative.

Closure of the Southern Uplands Trough, taking place in response to collision of the Eocaledonian and Anglo-Welsh cratonic blocks, in succession to an earlier phase of subduction down the Glen App Benioff zone (above) resulted in the production of structures within the sedimentary successions representing the successive, and separable, tectonic phases  $F_1$  to  $F_3$ . The major structures, monoclines and thrusts, were established during the

F<sub>2</sub> phase, which may be considered as the climax of the Caledonian orogeny (cf. Weir, in prep.). Post-Wenlock sediments are not known to exist within the Southern Uplands, and this tectonic climax was probably initiated during Ludlow times.

Increased thickening of the new continental crust so formed, coupled with melting of lower levels of the crust along a still active subduction zone, which may at this time have been in the course of southeastward migration (Mitchell and McKerrow, 1975), is considered to have brought about the production of magma of dioritic or granodioritic composition. As a result of a density contrast within the country rocks, this magma migrated upwards through the crust to be emplaced in a region embracing the Carsphairn, Doon, Fleet and Criffel plutons. Fractionation of this considerable batholith would have produced the large volume of granite deduced from gravity surveys to underlie large tracts of the Southern Uplands (Bott and Masson-Smith, 1960; Parslow and Randall, 1973; Batraukh, 1975).

Erosion of the irregular surface of the roof zone of this batholith has resulted in the exposure of several plutonic masses, having the status of stocks or cupolas. Amongst these the Loch Doon pluton has exposed at its southern end a shallow dipping roof zone, displaying granodiorite contaminated by contact hornfels to produce hypersthene diorite. Elsewhere within the domain of the batholith, diorite originating by this process may have been intruded into fractures above the roof of the batholith (produced as a result of doming) to produce minor intrusions such as the Talnotry sill.

The end product of fractionation within the batholith was a highly acidic granite, considerably less dense than the

parent granodiorite and thus displaying an even higher density contrast with the country rocks. As a consequence of this contrast, a mass of granite is deduced to have migrated upwards in a semi-solid state from the body of the batholith, forcing its way through the roof zone to form the Fleet pluton. Fractionation of this mass having taken place at depth, compositional zoning is not as evident at the present erosional level, nor is such zoning disposed with such regular concentricity, as in the Criffel and Loch Doon plutons. Forceful emplacement of semi-solid magma is indicated by sharp contacts, by granulation and dilation of the country rocks and by lack of extensive marginal contamination and of xenoliths.

Later, and whilst the bulk of the granite was cooling, a second intrusion was emplaced in the centre of the Fleet pluton, producing a fine-grained and even more highly fractionated granite. Compositional zoning is regularly disposed and concentric with the contact of this mass and therefore it is deduced that fractionation took place in situ. This intrusion is considered to have been preceded by a hydrothermal event which altered biotites in the previous granite to chlorite, and produced large quantities of secondary muscovite. In the later stages of the crystallization of the fine grained granite a second hydrothermal event took place, forming a localized area of granite containing large quantities of secondary muscovite.

The extensive areas of contact metamorphism in the southwest and northeast of the Fleet pluton are ascribed to the presence of granite (Parslow and Randall, 1973) or granodiorite at shallow depths, related to a sub-surface extension of the pluton and a gently dipping roof in these directions. This geometry is also partly held to account for localized high grade contact metamorphism, related to an

increased thermal gradient, in addition to forceful emplacement into the country rock under conditions of high stress, resulting in intense though again localized dynamothermal metamorphism. The narrower aureole adjacent to the northern and southern contacts reflects metamorphic effects produced solely as a result of intrusion of the semi-solid granite, and also steeply-inclined contacts.

Hydrothermal activity associated with the end phases of intrusion of the Fleet pluton probably accounts for the albitization of the lamprophyre and porphyritic microdiorite dyke rocks (Phillips, 1956). Much of the ore emplacement in and around the pluton is considered to have been related to this late hydrothermal activity, the mineral zoning originating through lowering of the temperature of the ore solutions away from the granite. Certain of the lead-zinc deposits may, however, have formed synchronously with the Leadhills-Wanlockhead ores, that is during the Hercynian orogeny (Ineson and Mitchell, 1974).

Intrusion of the base metal veins along sinistral and dextral wrench faults of Caledonian age may have been facilitated by the opening of these structures in response to doming during the intrusion of the batholith. The positions of some of the major occurrences of ores in the Southern Uplands appear to have been influenced by the distribution of the major thrusts. For instance, the Leadhills-Wanlockhead deposits are intimately associated with the Leadhills Thrust, the dominant structure in this sector of the Southern Uplands. Likewise the Woodhead deposit is associated with the Leadhills Thrust. The veins of the Fleet orefield are connected with two major structures, the Talnostry Thrust (again the dominant structure of the sector) and the Pibble Thrust, correlated

with the Ettrick Valley Thrust and a definitive structure within the orogen. Several thrusts of lesser magnitude are also associated.

Although it is not feasible to invoke a definite source for the metals in the ores, several modes of origin may reasonably be contemplated. Firstly, the base metals may have been derived directly from the batholith. Secondly, they may have been leached from the country rocks by hot aqueous solutions emanating from the batholith, which would also have provided a heat source to create a hot, aqueous, convective system of pore water within the host rocks. Thirdly, they may have had a joint origin involving both processes. Fourthly, the granite may have furnished a structural channelway for ore solutions derived from greater depths (cf. Dunham et al., 1965).

Later deformation took place during the Hercynian orogeny, producing the  $F_4$  structures and causing the movement of the Loch Ken Fault. Hercynian mineralization of lead-zinc type would be related to this phase. Weathering during the Permo-Triassic promoted deep oxidation along the line of this fault. The last earth movements to affect the Southern Uplands probably took place during the Tertiary (Rust, 1965) causing the development of the  $F_5$  structures.